الجمهورية الجزائرية الديمقراطية الشعبية

République Algérienne Démocratique et Populaire

Ministère de L'Enseignement Supérieur et de la Recherche Scientifique

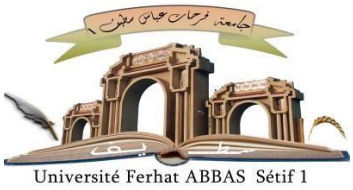

UNIVERSITÉ FERHAT ABBAS - SETIF1

FACULTÉ DE TECHNOLOGIE

THÈSE

Présentée au Département de Génie des Procèdes

Pour l'obtention du diplôme de

DOCTORAT

Domaine: Sciences et Technologie

Filière: Génie des Procédés **Option: Génie des Polymères**

Par

BENAYACHE Walid

THÈME

Étude théorique et expérimentale de la compatibilisation et de la fissuration sous contrainte environnementale dans les mélanges de polypropylène et de polyéthylène basse densité

Soutenue le 19/05/2024 devant le Jury :

NEKKAA Sorya	**Professeur**	**Univ. Ferhat Abbas Sétif 1**	**Présidente**
BENANIBA Mohamed Tahar	**Professeur**	**Univ. Ferhat Abbas Sétif 1**	**Directeur de thèse**
HELLATI Abdelhak	**Professeur**	**Univ. Mohamed El Bachir El Ibrahimi BBA**	**Examinateur**
GUESSOUM Melia	**Professeur**	**Univ. Ferhat Abbas Sétif 1**	**Examinatrice**
BENACHOUR Djafer	**Professeur**	**Univ. Ferhat Abbas Sétif 1**	**Membre invité**

الجمهورية الجزائرية الديمقراطية الشعبية

Democratic and Popular Republic of Algeria

Ministry of Higher Education and Scientific Research

FERHAT ABBAS SETIF 1 UNIVERSITY

FACULTY OF TECHNOLOGY

THESE

Presented to the Process Engineering Department

For obtaining of the diploma of

DOCTORAT

Domain: Science and technology

Sector: Process Engineering **Option: Polymer Engineering**

By

BENAYACHE Walid

THEME

Theoretical and experimental investigation of the compatibilization and Environmental Stress Cracking in Polypropylene/Low Density Polyethylene blends

Defended on 19/05/2024 Front of the Jury:

NEKKAA Sorya	**Professor**	**Univ. Ferhat Abbas Setif 1**	**President**
BENANIBA Mohamed Tahar	**Professor**	**Univ. Ferhat Abbas Setif 1**	**Supervisor**
HELLATI Abdelhak	**Professor**	**Univ. Mohamed El Bachir El Ibrahimi BBA**	**Examiner**
GUESSOUM Melia	**Professor**	**Univ. Ferhat Abbas Setif 1**	**Examiner**
BENACHOUR Djafer	**Professor**	**Univ. Ferhat Abbas Setif 1**	**Invited**

Dedications

To my dearest mother, who has waited patiently for the fruit of her good education. May she receive the testimony of my deep affection.

My sincere gratitude to my brother (Mounir), who showed me the right way by reminding me that will power always makes great men, and who helped, supported and encouraged me throughout my studies.

To my brothers

To my sisters

To my best friends Benghanem Mustapha, Aouissi Taher

I also dedicate this dissertation to everyone who has supported me in one way or the other.

W. BENAYACHE

Acknowledgments

First and foremost, I would like to express my deep and sincere gratitude to my supervisor Prof. **BENANIBA Mohamed Tahar** for his continuous support during my Ph.D. study and research, as well as for his patience, motivation, and immense knowledge. He was an exceptional supervisor, providing precious guidance, patience, and enthusiasm. Whenever I had questions or problems, he was always there to provide effective assistance.

I am very thankful to him for giving me such an interesting project that opened up a whole new world of science to me. His intelligence and rich knowledge always inspired and encouraged me.

My special acknowledgments go to Pr. **LARADJI Mohamed**, Pr. **BENACHOUR Djafer,** Pr. **BENGUERBA Yacine** and Dr. **ZERRIOUH Ali** for his precious help and services, as well as to all the professors and staff of Department of Process Engineering.

I express my sincere gratitude to all members at the Laboratory of **LMPMP**, as well as to all the other members of the lab for their technical and administrative assistance.

I would also like to thank all members of my jury committee for taking the time to read, assess, and judge my thesis. Your suggestions have made this work even better and more valuable.

Of course, I am infinitely grateful to my **family** and **friends** for their support and encouragement, which enabled me to comfortably focus on my studies.

Last but not least, I would like to thank my fellow lab mates, **Tahar**, **Mustapha**, **Ali**, **Faycal**, **Billal**, and **Mosaab**, for the unforgettable time we spent together.

I thank the committee members, Pr. **GUESSOUM Melia**, Pr. **NEKKAA Sorya**, and Pr. **HELLATI Abdelhak** for their valuable time and insightful comments throughout the examination of this thesis.

I want to thank Pr. **CAVALLO Dario** for agreeing to help me with my current and future research and for including me in his research laboratory.

W. BENAYACHE

Table of contents

Literature review

Structural study by theoretical calculation

Experimental study

List of figures

Chapter I

Chapter II

Chapter III

Chapter IV

Chapter V

List of tables

Chapter III

Chapter IV

Chapter V

List of Acronyms and abbreviations

PEHD:	High density polyethylene
LDPE:	Low density polyethylene
PP:	Polypropylene
SEBS:	Styrene-ethylene-butylene-styrene
SEBS-g-MA:	Maleic anhydride grafted styrene-ethylene-butylene-styrene
ZN :	Ziegler- Natta
IFT	interfacial tension
ΔG_m :	Gibb's free energy of mixing
ΔH_m :	Enthalpy of mixing
ΔS_m :	Entropy of mixing
IGEPAL CA 630:	Octylphenoxy poly(ethyleneoxy)ethanol
ESC:	Environmental stress cracking
COMPASS:	Condensed-phase Optimized Molecular Potentials for Atomistic Simulation Studies
VdW:	Van der Waals forces
NPT:	Constant temperature, constant pressure thermodynamic ensemble
NVT:	Constant temperature, constant volume thermodynamic ensemble
$E_{non-bond}$:	Energy of non-bond
E_{VdW}:	Energy of van der Waals
$E_{electrostatic}$:	Electrostatic energy
DFT:	Density functional theory
MDS:	Molecular dynamic Simulation
SEM:	Scanner electron microscopy
DSC:	Differential Scanning Calorimetry
FTIR:	Fourier Transform Infrared
XRD:	X-ray Diffraction
TGA:	Thermogravimetric Analysis
ESCR:	Environmental stress cracking resistance

General introduction

General introduction

For many years, polymers have been widely employed in industrial applications because of their vast range of characteristics and the relative simplicity of their production [1,2]**.** Their properties can be further improved and tuned by blending two or more polymers [3–5]. However, most polymers are thermodynamically incompatible due to their low entropy of mixing (Polymer mixing entropy is negatively correlated with molecular weight) [6]. Compatibilizers are often included in different immiscible thermoplastic blends to enhance their processing and characteristics. The choice of compatibilizer depends on the specific thermoplastic blend being used and the properties that need to be improved [7–9].

Low-density polyethylene (LDPE) and polypropylene (PP) are two of the most commonly used polymers due to their benefits of low density, high stiffness, high softening temperature, and outstanding chemical inertness. The fact that they are inexpensive and simple to process is also crucial[10]**.** A substantial amount of research has been done on the creation and evaluation of PP/PE mixes. Based on mechanical qualities, Bertin and Robin [11] It was shown in this research that adding compatibilizers, such as PE-g-(2-methyl-1,3 butadiene) graft copolymer, ethylene-propylene-diene monomer, or ethylene-propylene monomer, may boost impact strength and elongation at break for all blends. Similarly, Graziano et al [12]. examined the compatibilizing effects of grafted polyethylene (MAPE) with and without maleic anhydride on PP and PE blends. Microscopic examination demonstrated that MAPE results in an astonishingly fine PE/PP/MAPE morphology and provided evidence that MAPE may significantly enhance the miscibility of PE and PP. Mechanical and rheological testing revealed improvements in mechanical characteristics of 14 to 20% and reductions in interfacial tension and PE/PP viscosity shift of 10 to 20%, respectively. Recently, it was showed their PP/LDPE blends exhibit a combination of mechanical and material qualities necessary for flexible packaging applications [13].

Recent developments in theory and simulations of polymeric systems have allowed for accurate modelling of a wide range of polymeric systems both at the molecular and long wavelength scales. In particular, various computational techniques have proven to be powerful tools in obtaining atomic and molecular scale structural properties that complement experimental data. In general, utilising experimental techniques, intermolecular bonding in a polymer blend is relatively challenging to resolve. Molecular dynamics simulations have proven to be a reliable, cost-effective, and fast tool that can supplement experimental results or help overcome major

experimental limitations. Atomic scale simulations are also often used to predict the impact of compatibilizers on the structure and physical characteristics of polymer mixes [14-16].

For several decades, many groups have investigated environmental stress cracking (ESC), which refers to thermoplastic brittle failure, particularly PE [12-17]. PP can withstand ESC but is less sensitive than PE [18]. Unfortunately, there is a lack of information on ESC on two-component PE/PP blends [19]. Despite their ductility, polymer blends fracture brittlely when stressed after exposure to a surface-active chemical [20]. Although numerous factors influence polymers' environmental stress crack resistance (ESCR), shape and molecular weight significantly impact that resistance [21]. Increased tensile strength and a greater susceptibility to stress cracking over time are associated with higher density or crystallinity. As a result, ESCR often rises as density declines [22]. A narrower molecular weight distribution (MWD) also improves ESCR [22], although an overall higher molecular weight should result in a higher ESCR [23].

This work examined the impact of 5% (SEBS and SEBS-g-MA) as compatibilizers of PP/LDPE (80/20, 50/50, 20/80) blends using various analytical techniques, including FTIR, TGA, XRD and SEM. Furthermore, a molecular dynamics simulation was utilized to assess the relationships between chain mobility, glass transition temperature (Tg), and free volume of the mix. To learn more about the structural, electrical, and energetic aspects of LDPE-PP blends, researchers are investigating quantum chemistry calculations using density functional theory (DFT). By employing DFT calculations, we aim to understand the impact of compatibilizer agent SEBS-g-MA on the intermolecular interactions, phase behavior, and compatibility of LDPE and PP in the blend.

We performed to investigate the interactions between SEBS-g-MA, PP, and LDPE at the atomic-scale level. The principal objective of this study is to investigate the fracture behavior (ESCR) of this blend without and with the incorporation of compatibilizing agents. Characterization methods, including morphological and ESCR characteristics of the effect of IGEPAL CA 630 on the blend.

The literature review is divided into **two chapters** (**I** and **II**), the first dealing with polyolefin blends. It includes a general discussion on the thermodynamics of blends and some notions on miscibility and compatibility. The second chapter presents available information on the effect of environmental stress cracking.

Chapter III uses theoretical calculations to present the structural study of compatibilized PP/LDPE blends.

Chapters IV and **V** are devoted to the experimental study.

Chapter IV describes the materials, preparation methods, and techniques used during characterization.

Chapter V presents the study of blends (PP/LDPE) incorporating SEBS and SEBS-g-MA as compatibilising agents.

Finally, the thesis concludes with a general conclusion and recommendations for future work.

References

[1] A. Graziano, O A. Titton Dias, O. Petel. High-strain-rate mechanical performance of particle- and fiber-reinforced polymer composites measured with split Hopkinson bar: A review, Polym. Compos, 2021.

[2] Jeong, S H. Hwang, Y H. Yi, S C. Antibacterial properties of padded PP/PE nonwovens incorporating nano-sized silver colloids, J. Mater. Sci, 2005.

[3] Castejón, P. Antunes, M. Arencón, D. Development of inorganic particle-filled polypropylene/high density polyethylene membranes via multilayer co-extrusion and stretching, Polymers (Basel), 2021.

[4] Lin, J H. Pan, Y J. Liu, C F. Huang, C L. Hsieh, C T. Chen, C K. Lin, Z I. Lou, CW. Preparation and compatibility evaluation of polypropylene/high density polyethylene polyblends, Materials (Basel), 2015.

[5] Mofokeng, T.G. Ray, S S. Ojijo, V. Influence of selectively localised nanoclay particles on non-isothermal crystallisation and degradation behaviour of PP/LDPE blend composites, Polymers (Basel), 2018.

[6] Zhu, N. Gao, X. Liang, J. Wang, Y. Hou, R. Ni, Z. Finely Modulated LDPE/PS Blends via Synergistic Compatibilization with SEBS-g-MAH and OMMT, Symmetry (Basel), 2022.

[7] Rosales, C. Aranburu, N. Otaegi, I. Pettarin, V. Bernal, C. Muller, A J. Guerrica-Echevarria, G. Improving the Mechanical Performance of LDPE/PP Blends through Microfibrillation. ACS Applied Polymer Materials, 2022.

[8] Jamaludin, N A. Inuwa, I M. Hassan, A. Othman, N. Jawaid, M. Mechanical and thermal properties of SEBS-g-MA compatibilised halloysite nanotubes reinforced polyethylene terephthalate/polycarbonate/nanocomposites, J. Appl. Polym. Sci, 2015.

[9] Mengual, A. Juárez, D. Balart, R. Ferrándiz, S. PE-g-MA, PP-g-MA and SEBS-g-MA compatibilisers used in material blends, Procedia Manuf, 2017.

[10] Su, B. Zhou, Y G. Wu, H H. Influence of mechanical properties of polypropylene/low-density polyethylene nanocomposites: Compatibility and crystallization. Nanomaterials and Nanotechnology, 2017.

[11] Bertin, S. Robin, J J. Study and characterization of virgin and recycled LDPE/PP blends. European Polymer Journal, 2002.

[12] Graziano, A. Titton Dias, O A. Sena Maia, B. Li, J. Enhancing the mechanical, morphological, and rheological behavior of polyethylene/polypropylene blends with maleic anhydride-grafted polyethylene. Polymer Engineering and Science, 2021.

[13] Mofokeng, T G. Ojijo, V. Ray, S S. The influence of blend ratio on the morphology, mechanical, thermal, and rheological properties of PP/LDPE blends. Macromolecular Materials and Engineering, 2016.

[14] Deghiche, A. Haddaoui, N. Zerriouh, A. Fenni, S E. Cavallo, D. Erto, A. Benguerba, Y. Effect of the stearic acid-modified TiO2 on PLA nanocomposites: Morphological and thermal properties at the microscopic scale. Journal of Environmental Chemical Engineering, 2021.

[15] Otmani, L. Doufnoune, R. Benguerba, Y. Erto, A. Experimental and theoretical investigation of the interaction of sulfonated graphene oxide with polyvinylalcohol/poly (4-styrenesulfonic) complex. Journal of Molecular Liquids, 2019.

[16] Wei, Q. Zhang, Y. Wang, Y. Yang, M. A molecular dynamic simulation method to elucidate the interaction mechanism of nano-SiO2 in polymer blends. Journal of Materials Science, 2017.

[17] Soares, J B. Abbott, R F. Kim, J D. Environmental stress cracking resistance of polyethylene: The use of CRYSTAF and SEC to establish structure–property relationships. Journal of Polymer Science Part B: Polymer Physics, 2000.

[18] Harper C. Baker A, Mead J Modern plastics handbook. McGraw-Hill, 1999.

[19] Morris, B A. The Science and Technology of Flexible Packaging. Elsevier, 2017.

[20] Raman, A. Farris, R J. Lesser, A J. Effect of stress state and polymer morphology on environmental stress cracking in polycarbonate. J Appl Polym Sci, 2003.

[21] Scheirs, J. Compositional and failure analysis of polymer: a practical approach. John Wiley & Sons, 2000.

[22] Lustiger, A. Understanding environmental stress cracking in polyethylene. Med Plast Biomater, 1996.

[23] Wypych, G. Handbook of material weathering. ChemLK- Tec, 2003.

Chapter I. Polyolefin blends

I. Polyolefin blends

I.1. Introduction

Polypropylene/polyethylene blends have been studied for many years. Researchers from academia and industry have focused mostly on polypropylene matrix blends because to the commercial interest in enhancing this polymer's impact resistance at low temperatures. Polypropylene combined with a substance with a lower glass transition temperature or more ductility (elastomers, PE, etc.) has been extensively investigated to achieve this.

Despite having very similar chemical structures, polypropylene and polyethylene are immiscible and incompatible in most cases. The mechanical properties of their blends are often unattractive and unpredictable due to the influence of numerous parameters such as morphology and crystallinity. Compatibilization methods have been developed to improve the properties of blends.

I.2. Polyolefins

The most popular and widely utilized industrial polymer in the world, polyolefins (PO) make various goods used in almost every facet of our everyday life, including packaging films, pipelines, home bottles, and car components [1]. How the atoms in the chain molecules are arranged or entangled gives PO its physical characteristics. Both the molecular distribution and the physical characteristics are impacted by branching brought on by radical transfer [2]. Since they are based on inexpensive petrochemicals or natural gas and the necessary monomers are made by refining or breaking crude oil, resource depletion may become a deciding issue in PO manufacturing in the future [3]. Therefore, it is very desirable that PO material neither during its transformation into goods or components nor during service has any adverse effects on the environment [4]. After PO's life cycle, preventing any negative impacts is critical (see **Figure I.1**). PO are saturated hydrocarbon polymers based on ethylene, which include combinations of these monomers or high-density, low-density, and linear low-density polyethylene (LLDPE), propylene, and higher α-olefins. In addition, PO benefits greatly from its unique chemical makeup it consists only of carbon and hydrogen in comparison to other polymers including poly (vinyl chloride) (PVC), polyamides, and polyurethanes [5]. PO defined as ethylene and propylene copolymers and polymers, account for about 40% of the annual production of plastics and are clearly on the rise. The quantity of waste released into the environment increases with the breadth of the material's usage [5]. PO so have a significant

part in environmental issues, and whatever advancement they make significantly advances the cause as a whole [6]. The polyolefins' chemical and biological inertness was once seen as a benefit. These chemicals' excellent stability and resistance to degradation have caused them to accumulate in the environment, resulting in several issues, including a noticeable increase in visual pollution and a contribution to drain obstruction after heavy rains [7–10]. How polyolefins seem in the environment is a significant element affecting their market position; thus, the raw ingredients and manufacturing procedures used to create these materials determine how they look. In addition, products must consider using renewable resources and their capacity to be recycled or biodegraded.

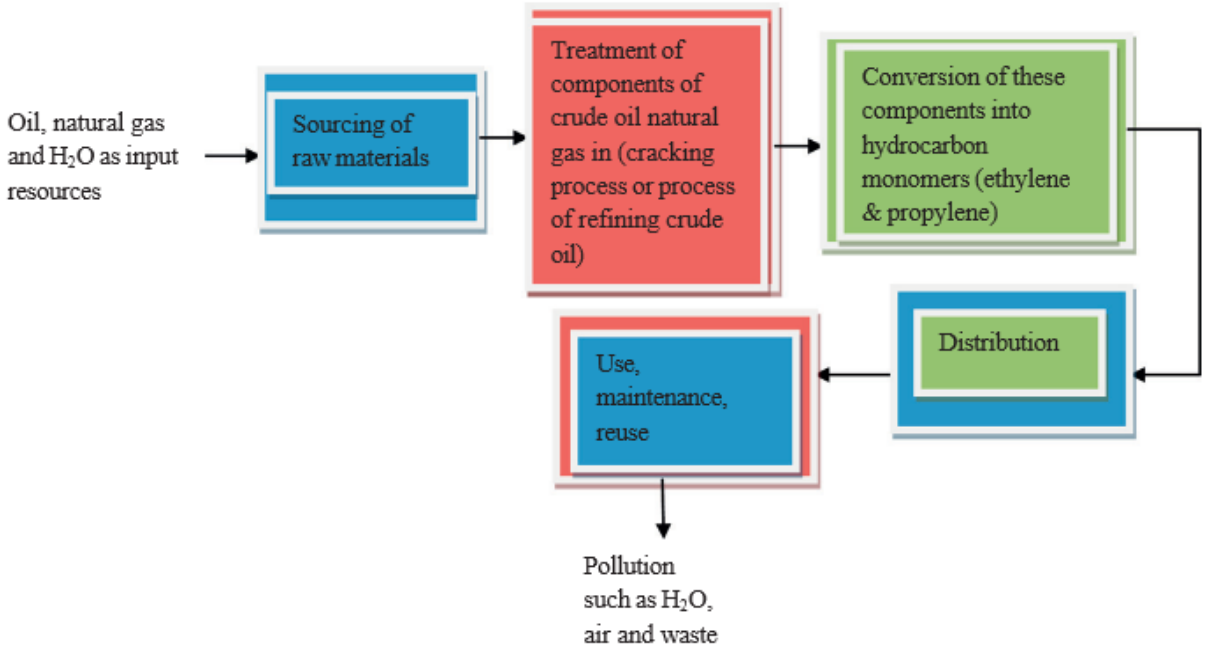

Figure I.1. Polyolefins product life cycle [3].

I.2.1. Polyethylene

On the globe, polyethylene (PE), the most extensively used plastic, belongs to the significant polyolefin resin family. Ethylene is catalyzed into polymers to prepare them [11]. It is a thermoplastic polymer made of lengthy chains created by combining ethylene monomer molecules. Three fundamental PE kinds are often employed, depending on the polymerization process: linear HDPE, branching LDPE, and LLDPE [12]. PEs are crystalline thermoplastics with a low coefficient of friction, near-zero moisture absorption, superior electrical insulating properties, durability, and simplicity of production. Their temperatures of heat deflection are acceptable but not very high. Compared to LDPE and LLDPE, HDPE has higher stiffness, rigidity, enhanced heat resistance, and increased resistance to permeability. HDPE has higher

intermolecular forces and tensile strength due to its low degree of branching. It may be generated via metallocene, Ziegler-Natta, or chromium/silica catalysts [13]. Molecular weights (MWs) of 10,000 to several million are used to produce HDPE. In addition to having a high density and melting point [14], it contains a linear polymeric chain (see **Figure I.2**). Milk jugs, water pipes, water pipes, toys, waste containers, soap bottles, margarine tubs, and packaging are all made of HDPE. Using peroxide initiators, low-density PE is produced at elevated pressure and temperature. Conversely, low pressure is used during the LLDPE manufacturing process. A little quantity of long-chain olefin is copolymerized with short branching to create LLDPE. Though many branches are added by utilizing comonomers, such as butene-1 or octene-1, it is linear (see **Figure I.3**). At a density of 920 g cm^{-3}, the typical comonomer content ranges from 8% to 10%. Strength comes from linearity and toughness from branching. Compared to branching LDPE, LLDPE has much better modulus and ultimate tensile qualities [14]. The density and crystallinity of LDPE and LLDPE are reduced by branching [15]. The LDPE or LLDPE form is recommended for film packaging and electrical insulation.

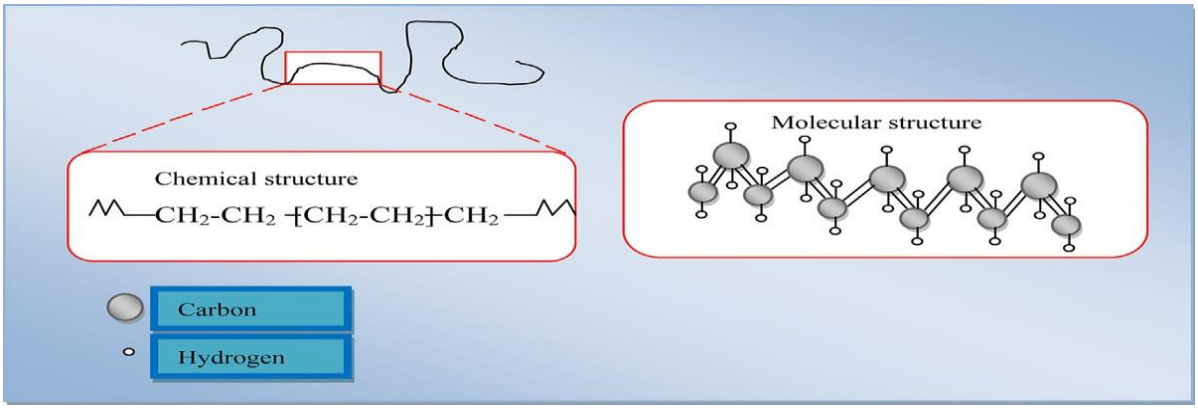

Figure I.2. High-density polyethylene [14].

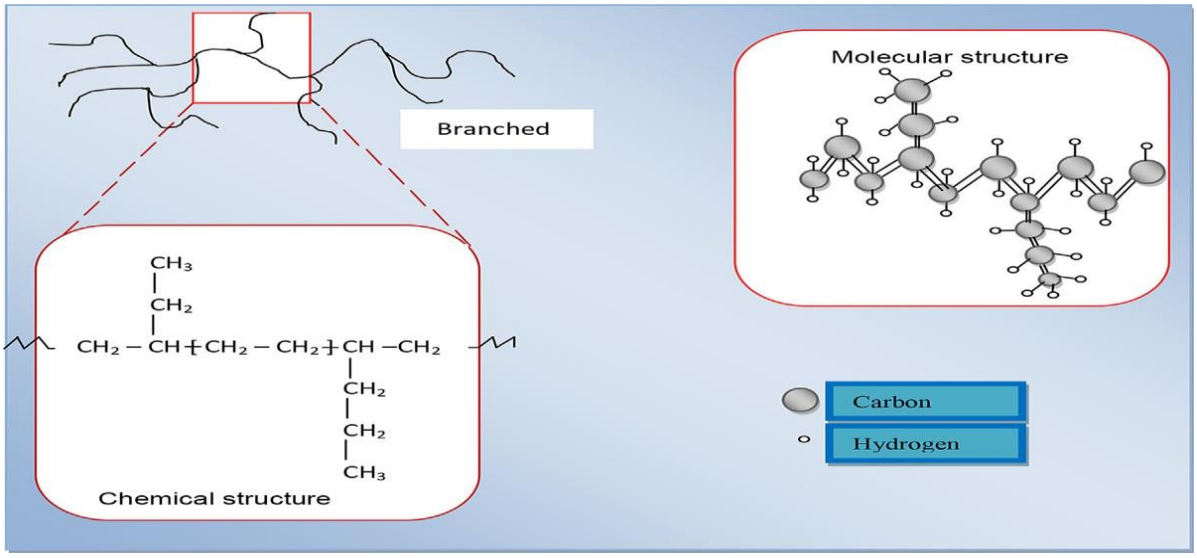

Figure I.3. Low-density polyethylene [15].

I.2.2. Polypropylene

Propylene undergoes polymerization to create the synthetic resin known as polypropylene. PP films have many uses in packaging, textiles, stationery, and other fields because of their high potential in aspects like dimensional stability, brilliance, barrier characteristics, and processability. PP and PE are comparable in many ways, particularly regarding their electrical characteristics and dissolution patterns. The molecular weight distribution (MWD), crystallinity, type, and amount of comonomer (if any) all affect the characteristics of polypropylene (PP). The degree to which PP is crystallinity-dependent determines its mechanical characteristics. While toughness and impact strength decline with increasing crystallinity, stiffness, yield stress, and flexural strength are all improved [13]. The steps in making PP include raw material preparation, polymerization, post treatment, and granulation. Another way to create an elastic ethylene-propylene copolymer is to polymerize propylene with ethylene. The manufacture of PP is mostly made of melt-spun fibers. PP fiber plays a significant role in home furnishings, such as carpets for indoor and outdoor use and upholstery [16]. **Figure I.4** shows the asymmetry of the propene molecule.

Depending on the location of the methyl groups, polymerization may result in one of three fundamental chain structures: two are stereo-regular (isotactic and syndiotactic), and the third, which lacks a regular structure and is referred to as atactic, is seen in **Figure I.5** [17].

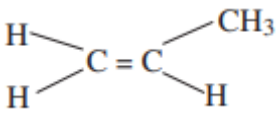

Figure I.4. Propene molecule.

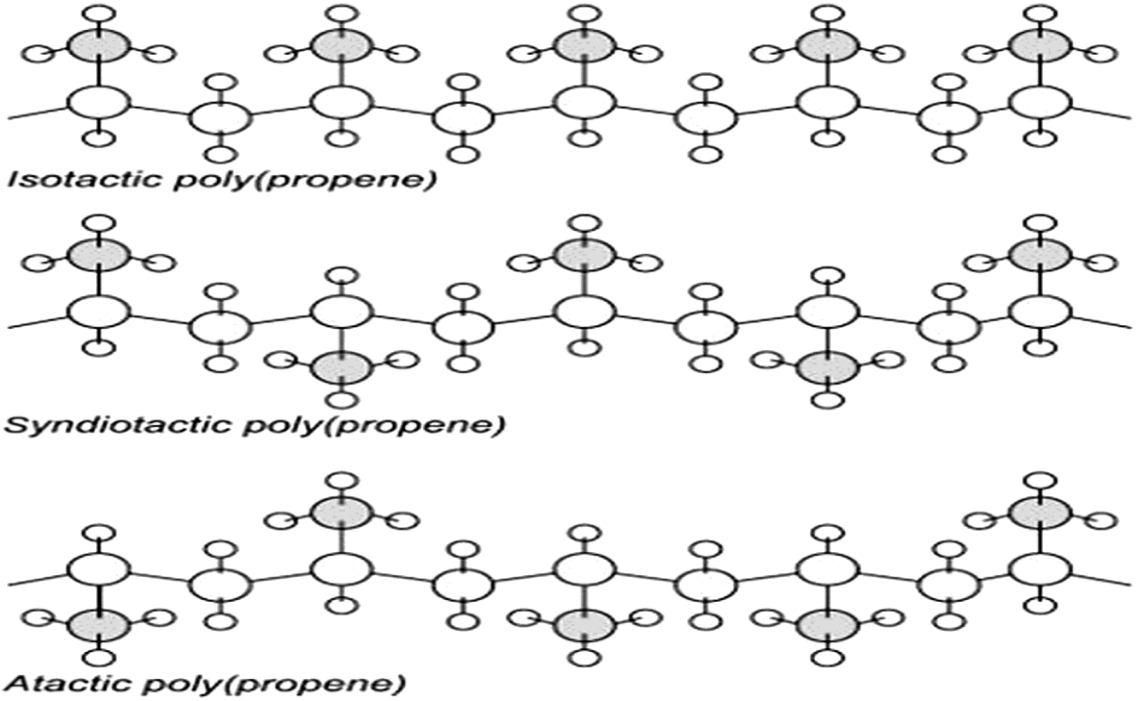

Figure I.5. Molecular structures of polypropylene [17].

I.2.3. Other Polyolefins

Polybutene-1 may also be produced with a Ziegler-Natta catalyst when required for a particular use. It was first developed to be a pipe material for water movement. Although it exhibits superior creep resistance compared to PE and PP, it eventually could not gain traction in the market since the pipes had significant failure due to their accelerated deformation during use [18].

I.G. Farben created polyisobutylene (PIB), a homopolymer of isobutylene, using cationic catalytic polymerization in the 1920s. Because of its poor permeability, it is used as a binding agent in medical sealants and explosives. While PIB's higher molecular weight variants are employed as toughening agents in polymers, the lower molecular weight version may be used in sealing applications [18].

Ethylene propylene diene (EPDM) is a saturated elastomeric thermoplastic material created by copolymerizing ethylene/propylene and unsaturated diene, typically used in the automotive, electrical, coatings, and construction sectors. Dienes are often added at a weight percentage of 2 to 5 weight percent. The most widely used dienes are ethylidene norbornene (ENB), 1,4 hexadiene, and dicyclopentadiene (DCPD). The ratio of ethylene to propylene will ultimately determine the overall qualities; a larger propylene concentration helps with low-temperature stability, while a higher ethylene content offers superior strength [19, 20]. Additionally, the kind and quantity of the third monomer unit (ENB), the molecular weight and distribution, the additions (oil and stabilizers), and the final microstructure differ between the commercially available grades of EPDM. The key advantages of EPDM over conventional diene rubbers are its low specific gravity [19], strong heat aging resistance, good chemical resistance, high resilience to ozone and temperature, and significant abrasion and tear resistance. Traditionally, alkyl-aluminum compounds catalyze the production of EPDM using vanadium-based catalysts; however, soluble metallocene catalysts have been studied in the last several decades. Metallocene catalysts, such as Ziegler catalysts, have many advantages over poisonous vanadium, such as the capacity to influence the random distribution of monomers and control the molecular weight distribution of the material [20].

I.3. Properties of Polyolefins

PO resins have low melting and crystallization temperatures due to weak Van Der Waals forces. This makes them unsuitable for applications needing more significant pressures and temperatures without further modification [18]. Crude oil is broken down into simpler hydrocarbon molecules, known as olefins, by breaking the carbon-carbon double or pi-bonds in complex organic alkanes.

The crystallinity, molecular weight, distribution, and kind of co-monomer used all affect the characteristics of polypropylene. While qualities like yield stress, flexural strength, and stiffness are improved by a rise in crystallinity, impact strength [21] and other toughness are decreased. Because of its better qualities, PP is more adaptable than other polyolefins (i.e., chemically resistant to numerous chemicals and having greater abrasion resistance). The characteristics mentioned above of polypropylene may be varied throughout the polymerization process, and its internal structure, which confers additional capabilities (such as mechanical and thermal properties), determines its crystallinity. Its tacticity produces three sub-classes of PP: isotactic (all substitution groups aligned on the same side of the molecule), syndiotactic

(substitution groups alternate along the molecule), and atactic (substitution groups are randomly arranged along the molecule).

Because of its superior mechanical and thermal properties, isotactic polypropylene (iPP) is used more frequently than its other stereoisomer configurations (such as syndiotactic polypropylene (sPP) and atactic polypropylene (aPP). Atactic PP is used in adhesives and certain low-cost applications. Due to its stereoregularity, iPP has a melting point of 165 °C, while non-stereospecific PP has a melting temperature window of 160–170 °C. Numerous industries, including but not limited to the textile and automotive sectors, use polypropylene. Automobile bumpers, gas cans, and interior parts (such as dashboards) are among the products made using PP [22]. In the textile business, PP is effectively used to make carpets, upholstery, and ropes when spun into fibers with a high molecular weight. It is used in the food business in the form of thermoforming-produced disposable food containers.

Comparable to polypropylene, polyethylene is a thermoplastic polymer with exceptional insulating qualities, hardness, low coefficient of friction, and strong chemical resistance [23]. The way that polyethylene branches varies throughout its many forms [22].

Differentiated by their degree of crystallinity and related physical features, the numerous varieties of polyolefins are used to make a broad variety of commercial items, including food containers, disposable diapers, packaging films, home bottles, pipelines, and car components [18]. The primary drivers of polyolefin manufacturing success are the availability of monomer units, the price of petroleum and other raw materials, current developments in polymerization reactor technology, and chemistry. **Figure I.6** illustrates the PO market share represented by polypropylene in 2018. This represents a 24% rise from 2010 (56 Mt) to 19.3% (69 Mt) in applications such as food packaging, snack wrappers, hinged caps, microwaveable containers, thermoplastic pipes, interior automobile components, banknotes, etc [24]. Conversely, in 2018 [25], the worldwide market shares of HDPE and LDPE were 12.2% (44 Mt) and 17.5% (63 Mt), respectively. The output of HDPE has risen by 23% in goods such as toys, milk and shampoo bottles, thermoplastic pipes, household appliances, etc. since 2010 [24, 25]. Since 2010, the quantity of LDPE that is transformed into completed consumer items like as cling wrap, food trays and containers, agricultural films, and reusable bags has grown by 25%.2,26. Last but not least, the total amount of all other polymers (such as EPS, ABS, PC, PMMA, PTFE, PET, PVC, and PS) has increased significantly year over year as well. These polymers also make up a significant portion of the debris that ecosystems discard annually [26]. This is because of its great stability and resistance to deterioration, which causes pollution and landfills

to rise globally. The material poses a bigger harm to the environment not only during the article's manufacture but also after it has completed its cycle of chemical and biological inertness [23]. Recyclability of the product is now accorded equal weight with the production process.

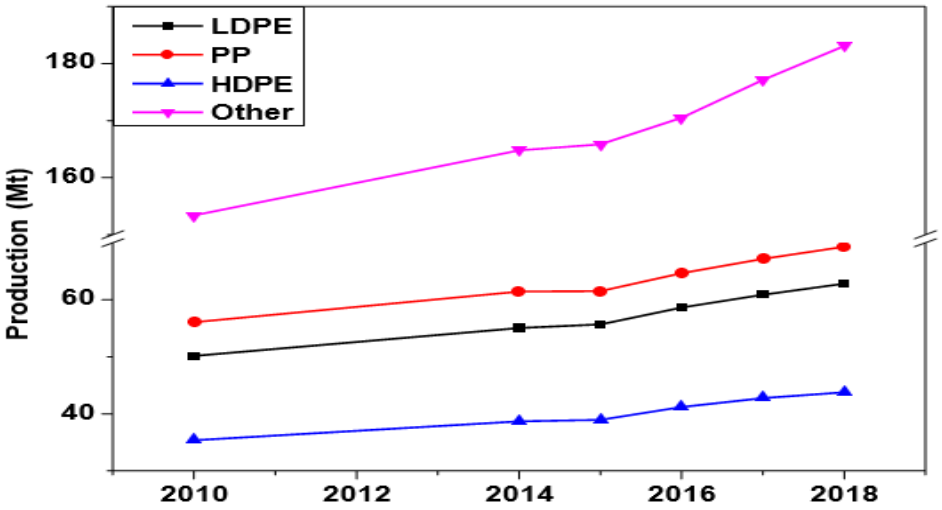

Figure I.6. Polyolefin production breakdown [24, 25, 27-31].

I.4. Polyolefin blends based on polyethylene and polypropylene

The thermoplastic polymers PP and LDPE are extensively used in diverse plastic sectors. Blends of PP and LDPE increase the processability and impact strength of PP as well as the heat resistance and environmental stress cracking resistance of LDPE [32]. Liang et al. investigated the mechanical and melt properties of a PP/LDPE blend system at varying LDPE concentrations (from 0 to 100 weight percent). It was determined that the blend system's melt flow rate was larger than that of the individual components and reached its maximum at a 50:50 ratio when the melt viscosities of the components, PP and LDPE, were closest to one another in value [32]. Salih et al. [33] examined the mechanical performance of blends made of PP/HDPE and PP/LDPE. It was noted that the tensile strength and Young's modulus dropped when the LDPE content rose from 0% to 80% weight percent. Impact strength results [33] showed a similar pattern of observation. Based on SEM data, the same investigation demonstrated that the PP/LDPE (80/20) was immiscible. A compatibilizer, or third component, may be added to an immiscible thermoplastic binary system to improve its characteristics and increase its compatibility. Ethylene-propylene rubber (EPR) is often utilized for compatibilization in PP/PE mix systems [34]. To increase compatibility, the propylene and ethylene units of EPR are introduced into PP and LDPE, respectively. Reactive compatibilizers

include maleic anhydride-grafted polypropylene (PP-g-MA) and maleic anhydride-grafted polyethylene (PE-g-MA) [34]. Using an in-situ process, Tselios et al. combined PP/LDPE with PP-g-MA and poly (ethylene-co-vinyl alcohol) (EVAL) in their study [35]. Compatibilizers enhanced mechanical qualities such impact strength, tensile strength, and elongation at break [35]. Unmodified 75/25 wt.% (PP/LDPE) was shown to exhibit 44% increase in impact strength and 47% increase in elongation at break when compared to 10 wt.% compatibilizers in the same 75/25 wt.% sample. Su et al. investigated the effects of a 75/25 weight percent (PP/LDPE) mix with compatibilizer and antioxidant agent in their article [36]. PP-g-MA served as the compatibilizer, while hindered phenolic served as the antioxidant. Tensile strength, percentage strain at break, and modulus were all greatest in the sample containing 9 weight percent and 0.15% compatibilizer and antioxidant agent, respectively. Nevertheless, no compatibilizer or antioxidant was added to the PP/LDPE blends in this thesis. The purpose of this was to comprehend how shear and temperature affected PP/LDPE blends throughout the repeated extrusion process.

I.4.1. Blending techniques

The structure of polymer blends is very closely dependent on the technique used to prepare them:

I.4.1.1. Mechanical blending

In this method, the transformation temperature must be higher than the glass transition temperature (and even the melting temperature if one of the constituents is semi-crystalline or crystalline). For dispersion to be effective, the shear forces generated by mixing may cause partial degradation of the mixtures.

I.4.1.2. Solution blending

Blending can be achieved by dissolving the two polymers in the same solvent. If the two solutions are miscible, mixing takes place under ideal conditions. The mixture can be recovered from the solution by evaporation of the solvent or by co-precipitation.

I.4.2. Advantages and inconvenient of the two methods

The mechanical mixing technique appears to be the most widely used industrially. This method allows good dispersion of one phase in the other thanks to the shearing forces generated by

mixing, but the second method appears to be more expensive.

I.4.3. Using blends in industry

- Originally, the aim of blends was to improve a given property of the matrix, most often its impact resistance. Today, new challenges are emerging, such as Cost reduction (dilution of an expensive technical polymer);
- Responding to a given specification with the best properties/cost ratio;
- Reducing the number of grades to be produced and stock levels;
- Improving a property (processability, heat resistance, mechanical and chemical resistance).

I.5. Immiscibility of PP/PE blends

The goal of blending PP and PE is to combine their advantageous qualities to create a final product that can be used to highly demanding applications. Furthermore, the majority of the global plastic market is made up of PE and PP, which provide significant recycling challenges due to their nonbiodegradable nature. [37] As a result, mixing PP and PE is also seen to be a helpful method of recycling them, making them suitable for highly demanding applications and promoting the growth of a sustainable global plastic market while also enhancing the recycling of commodity plastics. Though PP and PE are comparable, they are not interchangeable, which means that combining the two will reduce the final product's qualities. This often occurs when one polymer, in the form of spheres with various diameters, is neither evenly nor homogeneously spread into the other. The two polymers have a high interfacial tension (IFT), which promotes the dispersion phase's coalescence. Consequently, limited interfacial adhesion and inadequate stress transmission at the contact result in subpar end characteristics. It is important to note, however, that there are methods for arranging PE and PP in more intricate ways that combine the components' favorable qualities to create a new material that may be used again in industrial settings. This helps address the previously noted issue of recycling PE and PP. A notable example is the research conducted by Jordan et al [38], which examined the effects of using various catalyzed PEs and PPs and processing conditions (cooling rate of the processed PE/PP bilayers) on the interfacial adhesion of PE/PP bilayers. These variables have a significant influence on interfacial adhesion because they alter the polymer's crystallization and the chain alignments at the PE/PP bilayer contact.

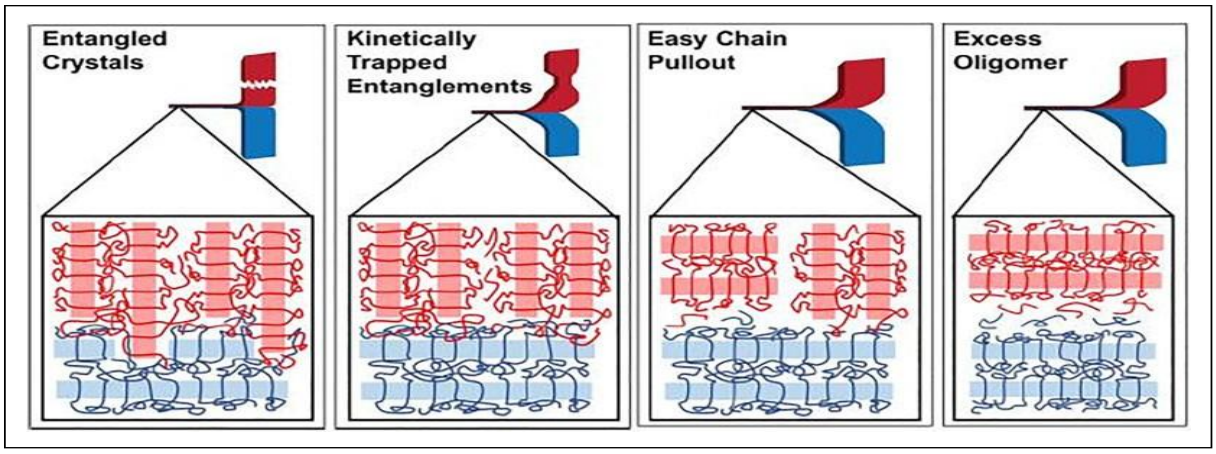

Figure I.7. Schematic representation of the four classes of POE interfaces [38].

Figure I.7 shows the four kinds of interfaces that were found. The ZN-based PE and PP represent the excess oligomer class; they exhibit a weak interface and poor interfacial adhesion as a result. This occurs as a result of the vast amorphous, non-crystalllizable property of ZN polymers. As a result, when mixing ZN PE and ZN PP, the extra amorphous oligomer at the interface weakens the contact and reduces interfacial adhesion by preventing cross-interfacial crystallization, which is the formation of strong chain entanglements between the crystalline domains of the two polymers. On the other extreme is the class of entangled crystals, which are nearly entirely amorphous and are represented by pairings of M-based PE and PP. As a result, interfacial interlocking is preferred in this situation, and the two polymers' crystals are so strongly anchored that interfacial adhesion rises dramatically it is 40 times greater than that of the excess oligomer class. In contrast to the excess oligomer class, the applied cooling rate of the produced PE/PP bilayers was much greater, which is another advantage for the entangled crystals class. The adoption of a PE with a greater amorphous character in comparison to the excess oligomer case and a lower cooling rate are linked to the two intermediate classes of kinetically trapped entanglements and facile chain pullout, respectively. This research proposes that a more sustainable usage of mixed recycled streams might be implemented by comprehending and managing the nature of the polymer and the processing conditions. Mauri et al [39]. work on improving the characteristics of PE/PP binary systems by organizing them in nanoscale multilayered films is another intriguing study on this topic. They were able to create a PE/PP nanolayered system with hundreds of layers and a thickness of less than 100 nm by using the layer multiplying co-extrusion approach. In this manner, a significant amount of interfacial space is created between PP and PE, which helps to promote the surface nucleation effects. In fact, the presence of one component influences the crystallization of the other during

the melt processing of a polymeric binary system. According to their research, the high interfacial area of the PE phase promoted the PP phase's crystal rearrangement by providing a large number of nucleating sites. This resulted in a notable increase in the mechanical properties of the nanolayered PE/PP system, especially the tensile modulus (TM). Furthermore, because PE's nucleating impact on PP's positive crystal rearrangement was effective right away after the creation of the multilayered system, annealing was not necessary. More precisely, in comparison to the system with 3 layers (thickness of 7.2 mm each), the system with 257 layers (thickness of 50 nm each) increased in Young's modulus, TS, and elongation at break (EB) by 87%, 21%, and 7%, respectively. These findings may promote the large-scale production of high-performance materials, which would save costs by combining the high TS and heat resistance of PP with the high flexibility and toughness of PE in an efficient manner without the requirement for annealing or the use of additives. Packaging is one application that benefits from this strategy, as The Compound Company, for instance, has already established it effectively with their brand Y parex. Packaging applications, on the other hand, have a limited lifespan, which makes recycling difficult when pure components from these multilayered polymeric systems—which include petroleum-based thermoplastic POEs—need to be entirely recovered. There are methods for separating PP and PE from streams of mixed plastic trash, such the delamination process or the dissolution-reprecipitation method for recycling post-industrial multilayer waste [40]. The first involves the chemical breakdown of an interlayer, whilst the second may be created by successively dissolving the mixture's various polymers at a certain temperature. These two methods, however, are exceedingly challenging and sophisticated, require a lot of energy and time, and do not ensure 100% component separation. Consequently, the development of a sustainable global plastics market often favors the recycling and mixing of mixed plastic waste streams. Compatibilization can improve the characteristics of immiscible binary mixes, both recycled and virgin.

I.6. Thermodynamic considerations

The miscibility of a mixture is governed by the thermodynamics of the system [41, 42]. It must be possible to create interactions within the mixture that allow the different components to mix intimately at the molecular level. This characteristic can be described by the free energy of mixing, which is expressed by the Gibbs relation according to equation 1:

$$\Delta G_m = \Delta H_m - T.\Delta S_m \qquad (1)$$

with: ΔG_m: free energy ΔS_m: entropy of mixing

ΔH_m : enthalpy of mixing T : temperature (Kelvin)

For a mixture to be miscible in the thermodynamic sense, the free energy ΔGm must be negative. In the case of polymer mixtures, the change in entropy of the mixture is considered to be almost zero between the state before and after mixing. Because of the high molar masses of the constituents, the conformation of the molecules does not change significantly so that they can be considered in two different states after mixing. The second term in equation 1 can be neglected. The enthalpy of mixing ΔHm represents the affinity between the different constituents. The three scenarios for polymers are as follows:

ΔHm < 0 : the mixture is miscible. The attractive interactions that can take place are of the donor-acceptor type, i.e. dipole ion, dipole-dipole or hydrogen bonds. The material has an arithmetic mean of those of its components. Few polymer pairs are miscible. The materials in our study do not fit this case.

ΔHm ≈ 0 : there are few positive or negative interactions between the different components. At least two distinct phases are formed in the mixture. The surface tension remains low between the phases, the intra-component forces are slightly stronger and do not allow intimate mixing at the molecular level throughout the domain of the different phases. Nevertheless, fine morphology remains possible. On the other hand, it is possible to compatibilized them [43-46], the materials used in our study correspond to this case.

ΔHm > 0 : the interactions between the various constituents are far too great. The interfacial tension is then far too high. There is therefore very little mixing between the components. A coarse morphology can be observed in this case [47-49]. The interface is clean, with little adhesion between the components. The mixture is very fragile mechanically. Equation 1 is not sufficient on its own to characterize the morphology of a mixture between two immiscible components. Indeed, it characterizes a state of equilibrium. However, as the mixture is produced during a processing operation, it will be subjected to various stresses such as shearing, elongational flow or temperature gradients which will impact the thermodynamic equilibrium, and therefore the morphology of the mixture.

I.7. Improving the miscibility of PP/PE blends

There are three principal strategies for increasing the miscibility of a blend of immiscible phases while improving certain properties. Firstly, a compound called a copolymer can be added to the

formulation, which migrates selectively to the interface between the phases and improves adhesion between them, lowers surface tension and therefore increases their miscibility [50, 51]. This is known as pre-formed compatibilization. This strategy is often used in competition with another strategy, which is the in-situ formation of a copolymer.

In a second phase, it is possible to form the copolymer during the preparation of the mixture. Chemical bonds are created between different phases by grafting or introducing specific chemical groups. Depending on the coupling agent chosen, reactions can take place between the different phases, giving rise either to strong interactions such as covalent bonds or weaker interactions such as hydrogen or Van der Waals bonds [52, 53]. However, this strategy can be difficult to implement. In-situ copolymer formation must be possible in highly viscous reaction media (around 103 Pa.s), at fairly high temperatures (above 200°C) and for residence times of the order of one minute for mixing in the process. Finally, it is possible to use fillers, and in particular nanofillers, to either screen the repulsive interactions between components or create specific interactions between the different phases [54, 55].

I.7.1. Compatibilization using copolymers

Numerous studies have treated the compatibility of PP/PE blends through the use of preformed copolymers. Among the most widely used copolymers are those based on ethylene (ethylene-octene copolymers, known as EO, and ethylene-propylene copolymers, known as EP). It is difficult to choose a copolymer a priori because the nature and viscosity of the matrix and the dispersed phase have to be taken into account. PP can be found in the form of a homopolymer [56] or a blend of PP and copolymer [43, 57], known as impact polypropylene (mainly used in the manufacture of car bumpers). PE can be polymerised in different ways. PEs with different structures are obtained, either low-density polyethylene, LDPE, with a high level of branching along the PE carbon chain [58, 59], or high-density polyethylene, HDPE, with a much lower level of branching [43, 56]. In addition, there are other grades of PE with higher or lower branching rates than the two PEs mentioned above. Koning and Utracki give a non-exhaustive list of the different types of polyolefin blends and copolymers used [42].

Lin et al [56] studied the impact of the structure of EO-type copolymers in a PP/HDPE blend. They found that a multiblock copolymer gave better mechanical properties, particularly in terms of Charpy impact strength over a wide temperature range (from -40°C to 40°C), than a linear copolymer.

All the studies agree that the addition of a well-chosen copolymer creates an interphase between immiscible phases through the selective migration of the copolymer at the interfaces of the mixed phases, as shown in **Figure I.8**. This is referred to as a "core-crown" morphology between the compatibilizer and the dispersed phase. The molecular weight and structure of the copolymer can act as a brake on its effectiveness, due to potential problems with copolymer migration kinetics. There is no empirical law to guide the choice of one copolymer over another. Changing the matrix or the choice of forming process can have an impact on the mechanical properties of a blend. For a PP/HDPE blend (75/25) compatibilized with a blend of EP and EO copolymers, replacing the PP matrix with an impact PP matrix with the same level of EO does not give the same improvements in elongation at break, dropping from nearly 700% to 150% [43].So, to validate the choice of a type of copolymer, a preliminary study of the mechanical properties is essential, in order to target the requirements of a specification as effectively as possible.

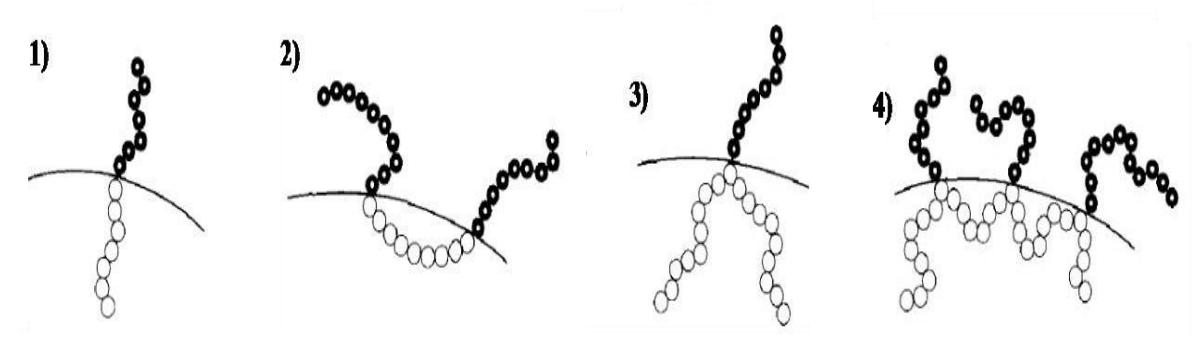

Figure I.8. Diagram of the different types of block copolymers that can be found: 1) Diblock, 2) Triblock, 3) Single graft and 4) Multigraft [42].

However, the addition of copolymers remains an effective way of compatibles polyolefin blends. The most judicious choice would be to opt for a block copolymer that is miscible with the different phases and has an "optimized" molar mass to ensure good migration at the interface. This technique therefore requires the ability to synthesize copolymers with fairly specific structures, and can involve fairly high costs. This is why another alternative strategy is to produce these copolymers in-situ, i.e. during the preparation of the mixture.

I.7.2. Compatibilization using copolymers synthesized in-situ

In-situ compatibilization offers the advantage of being able to synthesize copolymers with original structures. The reactions involved are mainly grafting reactions, which are considered to be rapid. There are three main ways of synthesizing these copolymers: so-called living copolymerization, chemical substitution after polymerization or chemical coupling between

chemical functions specific to the polymers under study. The first two routes are referred to as "grafting from" and the last as "grafting onto". The structure of the polymers studied, PP and PE, does not allow chemical coupling to be carried out easily. A grafting step must first be carried out. This involves introducing a reactive species onto the PP or PE, so that radicals can be generated for grafting. **Figure I.9** shows the example of grafting maleic anhydride onto PP using a peroxide [53].

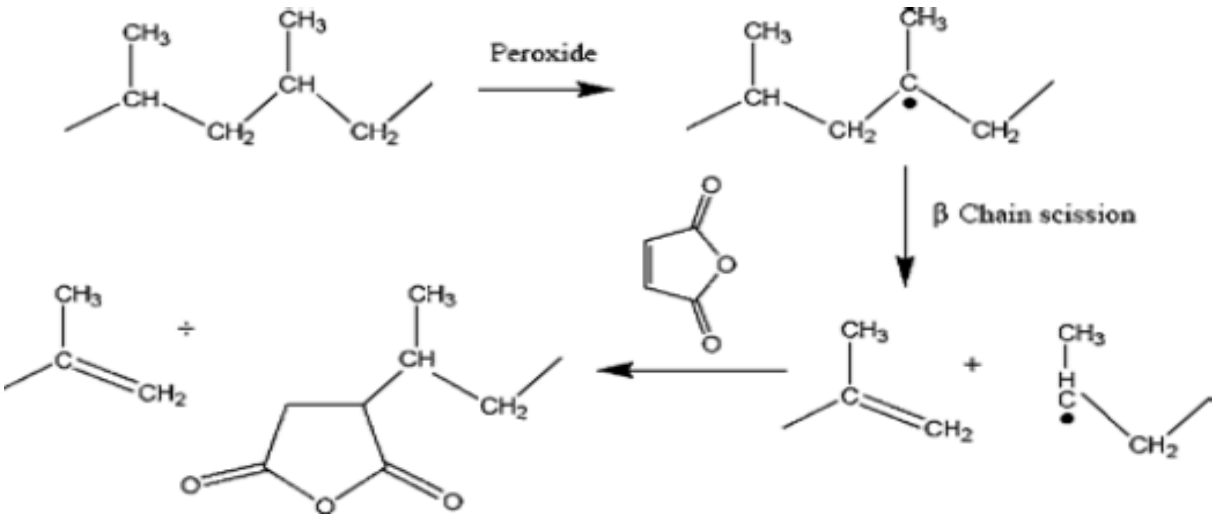

Figure I.9. Grafting maleic anhydride onto PP using a peroxide [53].

However, this grafting step needs to be well controlled as secondary reactions can occur. As can be seen, peroxide tends to cut the chains of PP macromolecules, degrading the PP [60]. On PE, cross-linking reactions can take place, making it more viscous and therefore less easy to handle [61]. Once grafting has been carried out on PP and PE macromolecules, chemical coupling reactions can take place. Colbeaux et al [62] studied the impact of the choice of coupling agents between grafted polyolefins in a PP/PE blend. In their studies, they used PP and PE grafted with maleic anhydride, PP-g-MA and PE-g-MA, and two types of coupling agent: an organic compound, 1,12 diamine dodecane, and two organic salts, zinc acetate and sodium bicarbonate. The special feature of these coupling agents is that they are bifunctional. This study shows that, to obtain good mechanical properties and good morphological refinement, a minimum of 30% by weight of grafted polyolefins must be introduced. The choice of coupling agent depends on the mechanical property to be improved: organic compounds tend to improve elongation at break and salts increase Charpy impact strength. However, they were unable to determine the chemical reactions involved between the different grafted polyolefins, i.e. inter- or intra-chemical coupling between the grafts introduced on the PP and PE chains and the coupling agents. Nevertheless, it is possible to form copolymers between PP-g-MA and PE-

g-MA using diamine coupling agents. It is then possible to graft reactive functions onto the macromolecules of our PP and PE, generally anhydrides, alcohols or amines, using various techniques, radical reactions or irradiation. The latter enable different types of interactions (hydrogen bonds or Van der Waals interactions) or covalent bonds to be formed between the grafts introduced and coupling agents such as amines, anhydrides, epoxies, etc. One of the most commonly used coupling reactions is that between an anhydride and an amine, because it is very fast [63]. A recent approach to compatibles PP/PE blends is to introduce reactive fillers. This strategy is similar to in-situ compatibilization, in that polyolefins that have also undergone grafting reactions are used to react with fillers that have undergone specific chemical treatments. This strategy simply involves trying to replace the coupling agents with fillers, and mechanically reinforcing the blend.

I.7.3. Compatibility with use of charges

Compatibilization of PP/PE blends is strongly motivated by an increase in mechanical properties such as elongation at break or Charpy impact strength, but this increase is generally accompanied by a reduction in the blend's rigidity. In some cases, the addition of fillers can mechanically reinforce the mix. There are several types of filler, the most commonly used in polyolefin blends being talc [43] and montmorillonite [64]. Due to their chemical structures, the presence of silanol functions (Si-OH) in talc and the presence of siloxane functions (Si-O-Si) on the surface of montmorillonites, the latter are widely used as is or grafted, in blends with polar polyolefins such as polyamides. In the literature, other fillers can be used, such as sodium carbonate [65], silica [44]**,** carbon black [66] or alumina or titanium nanoparticles [67]. Moreover, the use of these fillers in nanoparticle form is becoming increasingly widespread.

One example is the use of calcium carbonate, $CaCO_3$, as a reinforcing filler in a PP/HDPE blend in the study by Gonzalez et al [55]. They used two different particle sizes of $CaCO_3$, 3 and 1.8 µm in mean diameter, and four types of coupling agent, three of which were titanium oxides and one zirconium oxide. Irrespective of the particle size used, they were able to show that, without the addition of a coupling agent, an increase in crystallinity and losses in mechanical properties were obtained, whereas, when the coupling agent was added to the formulation, a decrease in crystallinity, combined with an increase in certain mechanical properties, was observed. Depending on the coupling agent used, it is possible to modulate the desired mechanical properties, as in the study by Colbeaux et al [62]. An increase in Young's modulus and elongation at break was observed when titanium-based coupling agents were used, whereas

zirconium oxide only had an impact on Young's modulus. In addition, synergistic effects were observed when mixtures of coupling agents were used. When a mixture of two titanium oxides was added, the Charpy impact strength increased significantly, from 12 $J.m^{-1}$ for the PP/HDPE/$CaCO_3$ mixture without a coupling agent, to nearly 16 J.m-1, whereas with a single coupling agent, the increase in impact strength was around 13 $J.m^{-1}$. In conclusion, the use of fillers to reinforce the final mechanical properties of the mix is growing rapidly. However, depending on the processing conditions, unexpected changes in the properties of blends using fillers can be observed, unlike blends using copolymers. The latter form an entangled system quite easily, whatever the orientation of the copolymer. Depending on the shape of the filler considered, the orientation of the filler in the mix is preferentially based on the flow of the mix during processing and will have a crucial importance depending on the direction of the stress (σ) applied [43, 54]. An example is given of the appearance of cavities and the deformation of montmorillonite sheets in a PA6 matrix, **Figure I.10** When the laminae are perpendicular or at an angle to the direction of the applied stress, cavities appear in the filler, causing early failure, **Figure I.10.a** and **b**, whereas when the laminae and the stress have the same orientation, slippage of the laminae relative to each other can occur without causing early failure, **Figure I.10.c.**

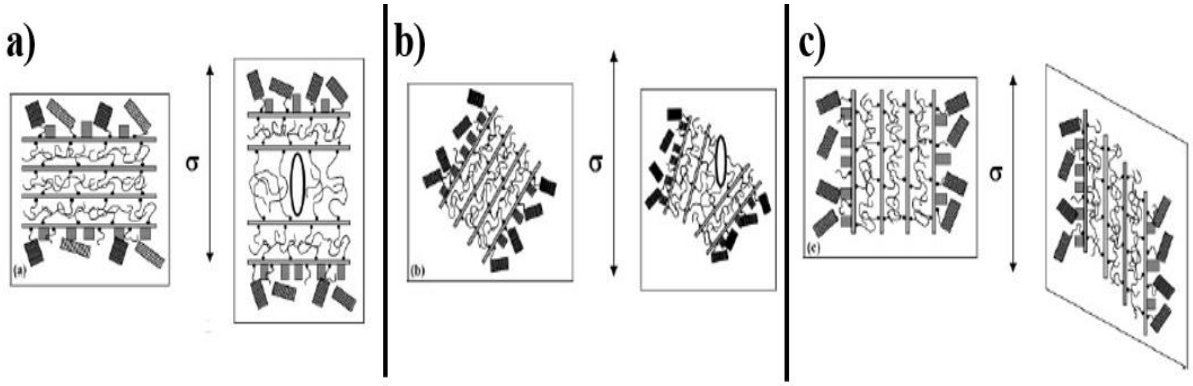

Figure I.10. Schematic representation of the fracture/deformation mechanisms around modified montmorillonite sheets in a PA6 matrix as a function of their orientation and the direction of the applied stress [54].

Controlling the orientation of the fillers during compounding is an important parameter for compatibilization by addition of fillers. We will now look at how to characterize compatibilization in the case of a preformed copolymer. In fact, we have to deal with the modulation of the properties of PP/PE blends using a continuous twin-screw extrusion process. In view of the results obtained in the first chapter, this process has an average residence time of around one minute, and the distribution of residence times is asymmetrical when high screw

rotation speeds are used. Therefore, the development of in-situ compatibilities and the use of fillers can suffer from problems of efficiency and reproducibility.

References

[1] Ulrich H. Introduction to industrial polymers. 2nd Ed. Munich: Carl, Hanser Verlag, 1993.

[2] Barlow A. The chemistry of polyethylene insulation. IEEE Electr Insul Mag, 1991.

[3] Harding KG, Dennis JS, Von Blottnitz H, Harrison STL. Environmental analysis of plastic production processes: comparing petroleum-based polypropylene and polyethylene with biologically-based poly-β-hydroxybutyric acid using life cycle analysis. J Biotechnol, 2007.

[4] Ramano U, Garbassi F. The environmental issues: a challenge for new generation polyolefins. Pure Appl Chem, 2000.

[5] Majumda J, Cser F, Jollands MC, Shanks RA. Thermal properties of polypropylene post-consumer waste (PP PCW). J Ther Anal Calorimet, 2004.

[6] Karpukhin ON, Siobodetskaya EM. Kinetics of the photochemical oxidation of polyolefins. Russ Chem Rev, 1973.

[7] Scott G. Polymers and the environment. Cambridge: RSC Paperbacks, 1999.

[8] Swift G, Wiles DM. Biodegradable and degradable polymers and plastics in landfill sites. In: Kroschwitz JI, editor. Encyclopedia of polymer science and technology. Hoboken, NJ: John Wiley & Sons, 2004.

[9] Sudhakar M, Doble M, Murthy PS, Venkatesan R. Marine microbe-mediated biodegradation of low- and high-density polyethylenes. Int Biodeterior Biodegrad, 2008.

[10] Ojeda T, Freitas A, Birck K, Dalmolin E, Jacques R, Bento F, Camargo. Degradability of linear polyolefins under natural weathering. Polym Degrad Stab, 2011.

[11] Zhu X, Guo Z, Cen W, Mao B. Ethylene polymerization using improved polyethylene catalyst. Chin J Chem Eng, 2011.

[12] Kutz M. Hand book of materials selection. New York: John Wiley and Sons, 2002.

[13] Francis V. Modification of low linear polyethylene for improved photo and biodegradation. Ph.D. Thesis, Faculty of Technology, Department of Polymer Science and Rubber Technology, Kerala, India, 2012.

[14] Lundba¨ck M. Doctoral thesis, environments including chlorinated water: antioxidant consumption, migration, and polymer degradation. School of Chemical Science and Engineering KTH Fibre and Polymer Technology, Germany, 2005.

[15] Edward N, Peters. Thermoplastics, thermosets and elastomers—descriptions and properties. In: Kutz M, editor. Mechanical engineers' handbook, fourth edition, vol. 1: materials and engineering mechanics. USA: John Wiley & Sons, 2015.

[16] Agboola, O. Sadiku, R. Mokrani, T., Amer, I., & Imoru, O. Polyolefins and the environment. In Polyolefin Fibres, 2017.

[17] Agboola, O. Sadiku, R. & Mokrani, T. Ismael Amer and Odunayo Imoru 3 1University of South Africa, Johannesburg, South Africa, 2Tshwane University of Technology, Pretoria, South Africa, 3Federal University of Technology, Minna, Nigeria. Polyolefin Fibres, 2017.

[18] Lohse, D J. polyolefins. appl. polym. sci. 21st century, 2000.

[19] Keklikcioğlu çakmak, N. engin, Y E. synthesis and characterization ofethylene propylene diene monomer (epdm) rubber mixture. ömer halisdemir üniversitesi mühendislik bilim. derg, 2019.

[20] Bavarian, N. Baird, M C. Parent, J S. EPDM Synthesis by the Ziegler Catalyst Cp*TiMe3/B(C6F5)3. Macromol. Chem. Phys, 2001.

[21] Jordan, A M. Kim, K. Soetrisno, D. Hannah, J. Bates, F S. Jaffer, S A. Lhost, O. Macosko, C W. Role of Crystallization on Polyolefin Interfaces: An Improved Outlook forPolyolefin Blends. Macromolecules, 2018.

[22] Ojijo, V. Sadiku, E R. Improving Wear Resistance of Polyolefins. Elsevier Ltd, 2017.

[23] Agboola, O. Sadiku, R. Mokrani, T. Amer, I. Imoru, O. Polyolefins and the Environment. Polyolefin Fibres, 2017.

[24] Plastics Europe - The Facts 2011. Plastics - the Facts 2010: An Analysis of European PlasticsProduction, Demand and Recovery for 2009. Plastics Europe, 2010.

[25] Manufacturers, P.-A. of P. Plastics – the Facts 2019. Plastics Europe, 2019.

[26] Posch, D W. Polyolefins for Polyolefin Production. Appl. Plast. Eng. Handb, 2017.

[27] Manufacturers, P. Plastics – the Facts 2017. Plastics Europe, 2017.

[28] The European Plastics Industry. Plastics – the Facts 2013 An Analysis of European Latest Plastics Production, Demand and Waste Data. Plast. (Association Plast. Manuf, 2013.

[29] Europe, P. Plastics the facts 2014/2015: an analysis of European plastics production, demand and waste data. Plastic Europe, 2015.

[30] Plastics Europe; EPRO. Plastics – the Facts 2016. Plast. – Facts 2016 2016, zu finden unter www.plasticseurope.de/informations.

[31] Sonam, C. Prasad, Y B. Anwar, S N. Kumar, C S. Mathematical Modelling and Analysisof Plastic Waste Pollution and Its Impact on the Ocean Surface. J. Ocean Eng. Sci, 2019.

[32] Liang, J Z. Ness, J N. The Melt Die-Swell Behaviour during Capillary Extrusion of LDPE/PP Blends. Polym. Test, 1998.

[33] Salih, S E. Hamood, A F. Abd Alsalam, A H. Comparison of the Characteristics of LDPE: PP and HDPE: PP Polymer Blends. Mod. Appl. Sci, 2013.

[34] Graziano, A. Jaffer, S. Sain, M. Review on Modification Strategies of Polyethylene/Polypropylene Immiscible Thermoplastic Polymer Blends for Enhancing Their Mechanical Behavior, 2019.

[35] Tselios, C. Bikiaris, D. Maslis, V. Panayiotou, C. In Situ Compatibilization of Polypropylene – Polyethylene Blends: A Thermomechanical and Spectroscopic Study, 1998.

[36] Su, B. Zhou, Y. Wu, H. Influence of Mechanical Properties of Polypropylene / Low-Density Polyethylene Nanocomposites: Compatibility and Crystallization, 2017.

[37] Kumar S, Panda A K, Singh R K. A review on tertiary recycling of high-density poly-

ethylene to fuel. Resour Conserv Recycl, 2011.

[38] Jordan A M, Kim K, Soetrisno D, et al. Role of crystallization on polyolefin interfaces: an improved outlook for polyolefin blends. Macromolecules, 2018.

[39] Mauri M, Ponting M, Causin V, et al. Morphological reorganization and mechanical enhancement in multilayered polyethylene/polypropylene films by layer multiplication or mild annealing. J Polym Sci B Polym Phys, 2018.

[40] Kaiser K, Schmid M, and Schlummer M. Recycling of polymer-based multilayer packaging: a review. Recycling, 2017.

[41] Barlow, J W. Paul, D R., Polymer belds and alloys – A review of selected considerations, Polym. Eng, 1981.

[42] Koning, C. van Duin, M. Pagnoulle, C. Jerome, R. Strategies for compatibilization of polymer blends, Prog. Polym. Sci, 1998.

[43] Abgrall, F. Elaboration de mléanges ternaires a matrice polypropylene renforcés par les contributions combinées de dispersions indépendantes de polyéthylène et polyamide, Lyon : INSA de Lyon, 2013.

[44] Louisi, M. Formulation de mélanges de polyoléfines à l'aide d'une extrudeuse à très haute vitess. Application à la dispersion de particules de traceurs, détectables par fluorescence X ou UV, en vue du tri de déchets polymères post-consommation, Lyon : INSA de Lyon, 2013a.

[45] Louizi, M. Massardier, V. Cassagnau, P h. Contribution of high-shear processing to the compatibilization of (PP/EPR)/PE ternary blends, Macromolecular Materials and Engineering 2013b.

[46] Souza, A M C. Demarquette, N R. Influence of composition on the linear viscoelastic behavior and morphology of PP/PE blends, Polym, 2002.

[47] Palmer, G. Demarquette, R. Evaluation of imbedded fiber retraction phenomenological models for determining tension between molten polymers. Polymer, 2005.

[48] Lee, J K. Han, C D. Evolution of polymer blend morphology during compounding in a twin- screw extruder. Polymer, 2000.

[49] Schoolenberg, G E. During, F. Coalescence and interfacial tension measurments for polymer melts: A technique using the spinning drop apparatus. Polym, 1998.

[50] Kim, G M. Michler, G H. Gahleitner, M. Fiebig, J. Relationship between morphology and micromechanical toughening mechanisms in modified polypropylenes, J. Appl. Polym. Sci, 1996.

[51] Lyatskaya, Y. Gersappe, D. Balazs, A C. Effetc of copolymer architecture on the efficiency of compatibilizers. Macromol, 1995.

[52] Gao, H. Xie, Y. Ou, R. Wang. Grafting effects of polypropylene/polyethylene blends with maleic anhydride on the properties of the resulting wood-plastic composites, Comp.: Part A, 2012.

[53] Cassagnau, P. Fenouillot, F. Bounor-Legaré, V. “Reactive processing of thermoplastic polymers: A review of the fundamental aspects”, Int. Polym. Proc, 2007.

[54] Kim, G M. Goerlitz, S. Michler, G H. Deformation mechanism of Nylon6/layered silicate nanocomposites: role of the layered silicate, J. Appli., Polym. Sci, 2007.

[55] Gonzalez, J. Albano, C. Ichazo, M. Diaz, B. Effects of coupling agents on mechanical and morphological behaviour of the PP/HDPE blend with two different CaCO3, Europ. Polym, 2002.

[56] Lin, Y. Yakovlena, V. Chen, H. Hiltner, A. Baer. Comparaison of olefin coplymers as compatibilizers for polypropylene and high-density polyethylene, J. Appl. Polym. Sci, 2009.

[57] Zhang, C. Shangguan, Y. Chen, R. Wu, Y. Chen, F. Zheng, Q. Hu, G. Morphology structure and compatibility of impact polypropylene copolymer, Polym, 2010.

[58] Kock, C. Gahleitner, M. Schausberger, A. Ingolic, E. Polypropylene/polyethylene blends as models for high impact propylene-ethylene copolymers, Part I: interaction between rheology and morphology, J. Appl. Polym. Sci, 2013.

[59] Kock, C. Aust, N. Grein, C. Gahleitner, M. Polypropylene/Polyethylene blends as maodels for high-impact popylene-ethylene copolymlers, Part 2: Relation between composition and mechanical performance, J. Appl. Polym. Sci., 2013.

[60] Azizi, H. Ghasemi, I. Reactive extrusion of polypropylene: production of controlled-rheology polypropylene (CRPP) by peroxide-promoted degradation, Polym. Test, 2004.

[61] Do, I H. Yoon, L K. Kim, B K. Jeong, H M. Effect of viscosity ration and peroxide/coagent treatment in PP/EPR/PE ternary blends, Eur. Polym, J, 1996.

[62] Colbeaux, A. Fenouillot, F. Gerard, J-F. Taha, M. Wautier, H. Compatibilization of polyolefin blend through covalent and ionic coupling of grafted polypropylene and polyethylene. II. Morphology, J. Appl. Polym. Sci, 2004.

[63] Macosko, C W. Jeon, H K. Hoye, T R. Reactions at polymer-polymer interfaces for blend compatibilization, Prog. Polym. Sci, 2005.

[64] Labaume, I. Huitric, J. Mederic, P. Aubry, T. Structural and rheological properties of different polyamide/polyethylene blends filled with clay nanoparticles: A comparative study, Polym, 2013.

[65] Cheraghi, H. Ghaseli, F A. Payganeh, G. Morphology and mechanical properties of PP/LLDPE blends and ternary PP/LLDPE/Nano-CaCO3 composites, Stren. Mat, 2013.

[66] Huang, S. Liu, Z. Zheng, S. Yang, M. Enhacing the conductivity of isotactic polypropylene/polyethylene/carbon black composites by oscillatory shear, Colloid. Polym. Sci, 2013.

[67] Fan, Z. Deng, J. Zuo, Y M. Fu, Z S. Influence of copolymerization conditions on the structure and properties of polyethylene/polpropylene/poly(ethylen-co-polymers) in reactor alloys synthesized in gas-phase with spherical Ziegler-Natta catalyst, J. APpl. Polym. Sci, 2006.

Chapter II. Environmental stress cracking

II. Environmental stress cracking

II.1. Introduction

Using materials has been fraught with failure from the dawn of recorded history. Developments in material science and engineering were fueled by these sometimes-disastrous failures. Any alteration in a material's or component's qualities that renders it unsatisfactory in terms of function, structure, or aesthetics is referred to as failure. Engineering polymers have successfully replaced metals in many demanding applications over the past several decades, and failures of this kind will become more significant. In order to take action to stop polymer failure from happening again, it is often essential to determine the cause of the failure. When in storage, transit, or use, polymeric materials are susceptible to processing and are impacted by temperature, time, and the surrounding environment. Long-term characteristics in particular are usually "unpredictable" [1]. Failure in polymer components may be caused by liquid substances (environmental stress cracking), cyclic stressors (fatigue failure), or long-term stress (creep rupture) at relatively low stress levels (sometimes far below the tensile strength). After a while, stress cracking may happen to a polymer that has been strained in air to a degree that is slightly below its yield point. On the other hand, the time to failure will be drastically shortened when stress and a chemical media are applied at the same time. Environmental stress cracking is the term used to describe this kind of failure (ESC). ESC has been the focus of in-depth research for about 50 years. Since ESC is responsible for 15–25% of all plastic component failures that occur while they are in operation, it has garnered a great deal of attention [2]. Furthermore, since it deals with stress-enhanced absorption, permeation, the thermodynamics of mixtures, local yielding, cavitation, fibrillation, and fracture, the phenomena of ESC is very intriguing to chemists and physicists [3].

When polyethylene first began to be used commercially, it was generally believed to be inert to all liquids. Since the new material was supposedly stable, new uses appeared very once. For example, concentrated hydrofluoric acid was packaged in polyethylene bottles for the first time [4]. The industry was now faced with a plethora of reports about polyethylene failure. According to reports, polyethylene is not suitable for use in cables because, at room temperature, it rapidly cracks when it comes into contact with methanol [5]. J. B. Howard, who had led the way in studying this phenomenon, provided the formal definition of the word ESC. Polyethylene has an excellent profile of properties, and it may be used in a wide variety of ways

with the right treatment and/or additions. The packaging industry (bottles, containers, foils, films, etc.), the electric industry and electronics (wire and cable insulation), the medical field (labware, caps, implant components, etc.), the automotive industry (tanks, pipes, coatings, etc.), and many other industries depend heavily on the solution to the ESC problem.

II.2. Definition of environmental stress cracking (ESC)

When plastics fail at room temperature as a result of continuously occurring external and/or internal stresses in the presence of surface-active substances (also referred to as stress cracking agents), such as alcohols, soaps, dyes, and agents containing moisture, the phenomenon is known as environmental stress cracking (ESC) [1, 2, 6, 7]. ESC is not a chemical reaction between the polymer and the active environment, even if it arises from the polymer's interaction with certain molecules. The stress cracking agents speed up the production of macroscopic brittle-cracks but do not chemically degrade the polymer. One of the main issues with plastic items' long-term service behavior is ESC. When ESC malfunctions after manufacture for instance, during shipping, point of sale, warehouse storage, or long-term applications quite costly failures may result. The stress corrosion issue in metals may be compared to ESC in polymers [8, 9]. In the presence of surfactants and under stress, a similar mechanism was seen in the metals. Macroscopically, ESC is defined by the slow, brittle decomposition of organic compounds in polymers. A certain amount of time passes before ESC occurs; the longer the durability, the lower the stress [10]. There are two origins of the time factor. Two things happen: first, plastic deformation happens gradually; and second, it takes time for the stress cracking agent to enter the tiny fractures that serve as the starting point for the final fracture. Stress cracking tends to happen at loads well below the yield point and becomes more likely as temperature rises [11].

II.3. Characteristics of environmental stress cracking

The ESC phenomenon is characterized by the acceleration of the cracking process in materials due to several factors such as temperature, stress, age, and chemical activity. Before the material approaches the yield point, brittle fracture and elastic area fractures appear in the material undergoing ESC. In other words, the stress exerted at this moment is less than the material's stress at the yield point. Chemicals that are utilized with materials after they are manufactured that is, secondary chemicals are often the ones that induce ESC in materials [12].

Another feature of ESC is that when exposed to chemicals, the polymeric material does not

experience chemical changes such as the production of new bonds or morphological alterations. The sole thing that causes material fracture is the breakdown of secondary bonds, or interlinkages. Additionally, since amorphous polymers have a larger free volume than crystalline polymers, they are more prone to ESC. As a result, the degree of crystallinity and environmental stress cracking resistance (ESCR) are closely correlated. Because a bigger chemical makes it more difficult for it to access the free volume of the material, ESCR is also strongly correlated with the molecular weight of the chemical attacking the polymer [12].

Generally speaking, the material's tensile stress causes molecular disentanglements, which result in ESC. As a result, when compressive load is applied, the material will not undergo ESC [12]. In terms of the chemicals that cause ESC, due to the compounds' solubility compatibility with the materials, fluids with moderate hydrogen bonding, such as organic fluids (aromatic hydrocarbons, halogenated hydrocarbons, ethers, ketones, aldehydes, esters, etc.), are more likely to be severe stress cracking agents than non-hydrogen bonded fluids, such as aliphatic hydrocarbons, and highly hydrogen bonded compounds, such as water or alcohol [12]. Liquid nitrogen, which has a boiling point of -196 °C, is a stress cracking fluid for many polymers because fluids are most aggressive at temperatures close to their boiling points [12].

The stress vs strain curve (Hooke's law) for polymers is seen in **figure II.1** below, with the elastic area being represented by the first straight diagonal line. In this area, the amount of stress placed on the material is equal to the amount of strain it is under. When the tension is relieved in this instance, the material returns to its initial state when no stress was applied. The material eventually reaches a point after a certain amount of stress when it becomes permanently stretched and is unable to return to its previous shape when the tension relaxes. We refer to this as the yield point. As the tension is increased further, the material is under more strain, which continues until the material ultimately fractures and cracks. That is the fracture stress point, when necking occurs. Therefore, the stress applied to the material should be below the yield point and ideally in the lower or middle portion of the elastic area, according to the ESC theory.

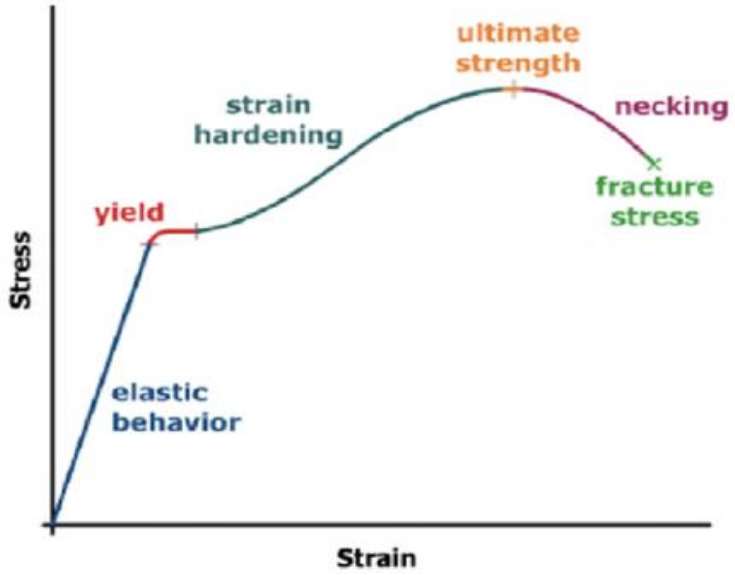

Figure II.1. Hooke's Law (stress vs. strain curve) for polymers.

II.4. Stress cracking agents

Any liquid that under basic immersion circumstances is rapidly absorbed by a plastic with a high absorption rate has a great potential to be a severe stress cracking agent for that specific plastic. These liquid/plastic combinations are readily obtained via basic chemical compatibility testing. When choosing polymers and designing systems, it is best to steer clear of these pairings. Strong or moderate stress cracking agents are often found in most liquids with poor hydrogen bonding. These consist of organic liquids such as ethers, ketones, aldehydes, sulphur- and nitrogen-containing chemicals, halogenated hydrocarbons, aromatic hydrocarbons, and esters [2]. This makes alcohols and water, as well as other liquids with strong hydrogen bonds, such as alpha-hydroxycarbons, less aggressive agents. The temperature at which many liquids become more aggressive is close to their boiling point. High molar volume liquids are not as likely to be strong stress cracking agents. These liquids often boil at high temperatures and have high viscosities. For the majority of amorphous polymers, typical solvents that induce stress cracking include petroleum ether, carbon tetrachloride, toluene, acetone, ethanol, and chloroform. Components of plastic medical devices are often exposed to substances like lipid solutions and isopropanol, which may cause ESC [1].

Surface-active environments are often liquids that have the ability to reduce the surface energy of polymers without dissolving or swelling them. The yield point and shrinkage are inversely correlated with the liquid environment's capacity to reduce the polymer surface energy [13].

The driving power by which the stress cracking liquid travels through the crazy fibril structure determines the ability of a stress cracking chemical to produce stress cracking of the polymer. The liquid starts to plasticize the polymer as soon as it reaches the craze tip, which permits the craze to spread. The solubility characteristics of the liquid and the polymer determine how much of a solvent is absorbed by the polymer. Three forms of cohesive forces are included in Hansen's definition of the solubility parameter: dispersive, polar, and hydrogen bonding [1, 14]. The overall cohesive attraction between the fluid molecules is measured by a stress cracking agent's solubility characteristic. If the polymer's solubility parameter and the fluid's match, diffusion of the agent will take place, increasing the likelihood of ESC. The relationship between the solvent's solubility parameter and the critical strain for solvent-induced stress cracking and craze onset was initially shown by Kambour et al. [15]. Examining the solubility properties of both the polymer and the stress cracking agent may help anticipate the degree of stress cracking in situations when the stress cracking agent is an organic solvent [16]. The cause of ESC is the stress cracking agent's selective absorption into a micro-yielded or stress-dilated zone. This process causes fracture and locally lowers the polymer's yield strength. The kind of fracture may vary between ductile and brittle based on factors like load and duration. Stress-induced detergent molecule diffusion into the polymer may increase chain mobility, which in turn lowers the activation energy (plasticizing effect) of the deformation process [7]. By reducing the cohesive forces that hold the tie molecules in the crystallites, stress-cracking chemicals let the molecules "pull-out" and detangle from the lamellae [1].

II.5. Failure mechanism of environmental stress cracking

A visual inspection of the semi-crystalline polymer deformation process is helpful in providing a molecular description of ESC. Then, ductile behavior and brittle behavior may be contrasted using this paradigm. It is crucial to take into account the intercrystalline or amorphous polymer chains while explaining the failure process. **Figure II.2a** displays three forms of intercrystalline material: Chains hung from the end of a crystalline chain are known as cilia; loose loops are chains that start and finish in the same lamella; and tie molecules are chains that start and finish in neighboring lamellae.

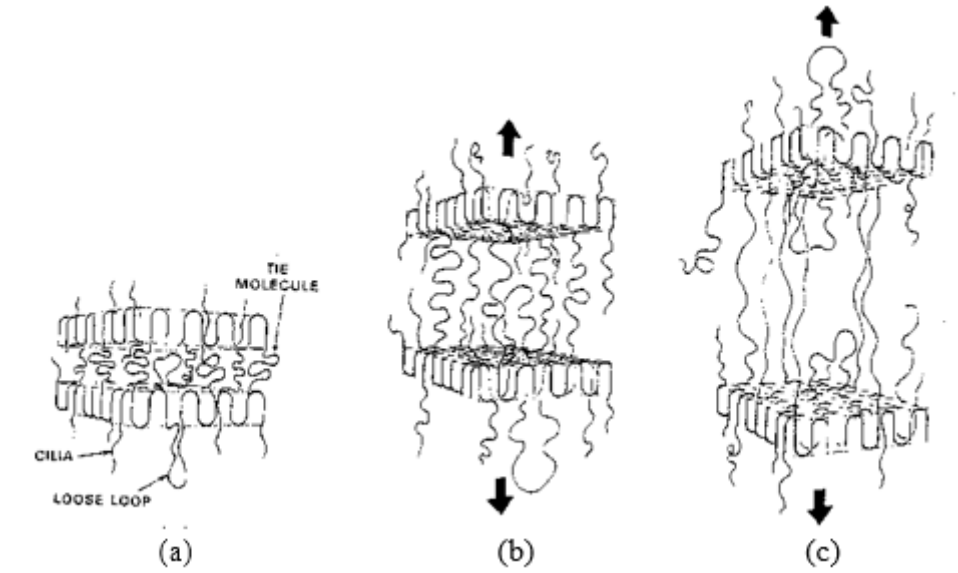

Figure II.2. Initial steps in the deformation of polyethylene [4].

The failure mode may be either brittle or ductile, based on the amount of stress and the time factor. The tie molecules expand as shown in **figure II.2b** when a tensile stress is applied normally to the face of lamellae. The knot molecules can only be dragged out so far before breaking (**figure II.2c**). The lamellae now fragment into tiny units (**figure II.3a**). These so-called "mosaic blocks" are immediately integrated into a new fiber shape, as per this concept [17] (**figure II.3b**). The integrity of the tie molecules is essential for ductile-type action to take place because they keep the lamellae "bricks" together [4].

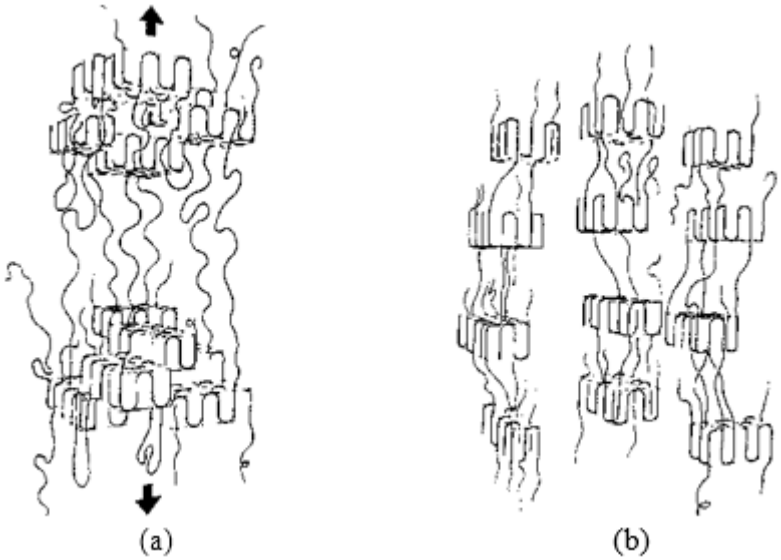

Figure II.3. Steps in the ductile deformation of polyethylene [4].

The long-term brittle-type plastic failure occurs at lower stress levels than the ductile process previously outlined [18]. The low stress level of the material prevents it from achieving the requisite tension for large-scale fiber pullout. As a result, for a considerable amount of time, the loading scenario as shown in **figure II.2** is projected to persist. The material breaks in a brittle way when, after a certain amount of time, the majority of the tie molecules detangle and the load can no longer be maintained by the few tie molecules that remain (**figure II.4**).

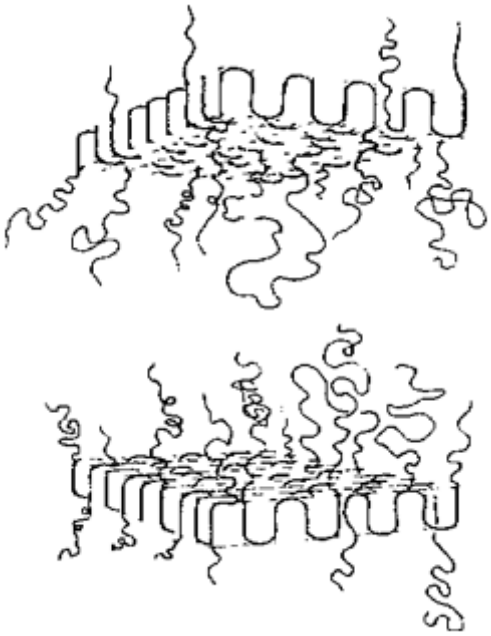

Figure II.4. Final step in the brittle failure of polyethylene [4].

The brittle-failure process is accelerated by the stress cracking agents, as was previously described. Any substance that causes stress cracking will lubricate the tie molecules, making it easier for them to separate from the lamellae. Each semicrystalline polymer's deformation behavior is complexly influenced by a number of parameters, including shape, molecular orientation, degree of crystallinity, molar mass, and drawing circumstances. Polyethylene goes through a number of distinct structural states when it is distorted in the solid state up to fracture. Based on measurements of real stress-strain curves, elastic-recovery characteristics, and texture changes at various phases of the deformation process, Strobl et al. [19–21] investigated the deformation behavior of several polyethylenes under an applied tensile load. The findings of their study indicate the existence of a common general scheme for the behavior of deformation, which can be linked to four distinct events: (1) the initiation of isolated slip processes; (2) a shift in the slips' activity towards collective activity; (3) the initiation of fibril formation following the fragmentation of lamellar crystals; and (4) chain disentanglement leading to a

finite truly irreversible deformation. The stresses at which these points occur don't change at different temperatures throughout the drawing and crystallization processes. Conversely, there are significant differences in the associated stresses. The bulk orientation variations of crystalline and amorphous chain segments may be characterized using Raman spectroscopy and polarized vibrational spectroscopy [22–23]. The backbones of chains often align in the direction of a polymer's stretch. Pezolet [24] observed that, in particular, for polyethylene, the high mobility of the flexible amorphous regions causes the amorphous chains to exhibit greater alignment in the strain direction than the crystalline chains at draw ratios of 7. At higher draw ratios, the crystalline chains align with the direction of stress as the initial crystalline lamellae disintegrate. X-ray scattering measurements for high density polyethylene show that the flexible amorphous areas' facilitation of lamellae block rotation is the main deformation mechanism [25]. The chain-slip process within the lamellae is the deformation mechanism that occurs beyond the yield point. Kip et al.'s [26] comprehensive morphological analysis of cold-drawn polyethylene materials was conducted using wide-angle X-ray scattering and Raman spectroscopy. Their findings indicate that molecules are most likely drawn through the crystals to generate the crystalline structure with dislocations and ruptured crystals that are formed by cold drawing. Using atomic force microscopy, Somorjai et al. [27] described the surfaces of low- and high-density polyethylene while the polymers were stretched. Stretching the polymers causes the surfaces to become rougher. When the strain increases, the nodular domains on the surface expand in the direction of the stretch, and compress when the strain decreases. The yielding and fracture of polyethylenes are significantly influenced by the degree of crystallinity. Nonetheless, the temperature of deformation affects how much crystallinity there is. The yield point rises with crystallinity degree in the temperature range where yielding is the mechanism of failure [28]. For linear polyethylenes, the fracture toughness typically rises with lowering the degree of crystallinity in the low-temperature zone, where the brittle fracture is the failure mode.

II.6. Factors influencing the ESC-behavior

The concentration of the stress-cracking agent, exposure temperature, exposure duration, and most importantly, the degree of strain on or inside the polymer, all have a significant impact on the ESC behavior of a polymer. Stress concentrations, dilational stress, cyclic loading, and rising temperatures all hasten the shift to brittle behavior [2]. Temperature has a complicated influence. Physical aging results from small-scale relaxation processes that occur in amorphous portions of glassy polymers, which compress the sample's volume and cause it to become denser

[29]. The local chain packing changes, but the polymer structure stays the same. As a result, physical characteristics including tensile strength, glass transition temperature, and brittleness are altered and their dimensions vary. The material's enthalpy, specific volume, and fracture toughness all drop as physical aging progresses, while the yield stress, tensile modulus, glass transition temperature, and other properties may all rise. Stress will rise and the nature of the stress field will change owing to localized concentration of stress caused by local geometrical features such as voids, inclusions, and notches. Stress fields with significant dilational stress speed up the start of a craze, whereas hydrostatic pressure slows it down [2]. Important polymer characteristics and factors influence ESCR. Longer polymer chains produce more tie molecules and an increase in ESCR when the molar mass is larger [30]. As the degree of crystallinity increases, ESCR decreases [6, 30]. Better ESCR of LLDPE is provided by longer comonomer short chain branching (more α-olefins) and greater comonomer content [4, 31]. The ESCR typically decreases with increased pigment concentration [32, 33]. The material's thermal history and the processing circumstances have a significant impact on the polymers' ESCR behavior [34–37].

II.7. Environmental stress cracking resistance (ESCR)

The capacity of the materials to withstand fracture or a cracking process is known as environmental stress cracking resistance. If these materials fail, ESCR can guarantee a decrease in the costs associated with manufacturing, waste, and product repair [38].

There are several strategies that may be used to lower ESC. Here are a few of them:

1. By selecting the proper polymeric material according on the application's environment, ESC may be decreased. This entails selecting a material that is resistant to the chemicals that will be used as well as other elements like temperature and stress.

2. The distribution, molecular weight, and shape of the polymer all have a significant impact on ESC resistance. The ESCR may rise when the polymer's molecular weight increases [39]. Additionally, as a general rule of thumb, the polymer's ESCR increases as the polymer's branching increases. Consequently, ESCR rises as density falls [40]. The explanation for this is that polymers with higher chain entanglements are more resistant to ESC. Chain length affects the quantity of chain entanglements. There is greater entanglement in larger chains (higher molecular weight) than in shorter chains. Less mobile chains would also need more time to untangle. greater molecular weight polymers have greater ESCR, which is further supported by

polymers with longer chains having superior ESCR [41].

3. Selecting a chemical during material assembly or production that won't start the material's cracking process is an additional strategy. This may also be measured to determine if the chemical and the material are compatible using Hansen's solubility parameter calculation, which is explained later. ESCR will rise in proportion to the difference in the solubility parameter between the polymer and the chemical. An additional approach to verify the compatibility of fluids with the polymer would be to use different conventional testing techniques. We'll talk about these test techniques later. In addition, the material's susceptibility to stress cracking may be influenced by chemical concentration. Because of the chemical's increased aggressiveness on the material, chemical concentration may generally be directly correlated with the rate of stress cracking [40].

4. Research also demonstrates that ESC rate increases with test environment temperature, hence lower temperatures are preferable for ESCR [40].

5. Reducing the amount of stress that is applied to the material lowers its ESC rate. [40]

6. Because of increased secondary bond interlocking and cross-linking, crystalline or crosslinked polymers have a lower void volume accessible for chemical entry, making them more resistant to ESC than glassy or amorphous polymers.

7. The use of polymer mixes may raise ESCR. An appropriate ratio of crystalline to amorphous polymers may raise the ESCR. L. M. Robeson [38] reported that when a miscible combination of amorphous PEI and crystalline PEEK was used instead of pure PEI, the ESCR rose. Similarly, adding crystalline and miscible PVF to amorphous PMMA resulted in an improvement in ESCR. Polymer blends used in automotive applications have shown enhanced resistance to cracking when subjected to lubricants such as gasoline and oil. Noryl GTX (PPO/nylon 6,6), Xenoy (PC/PBT), Germax (PPO/PBT), Triax (ABS/nylon 6), Elemid (ABS/nylon 6,6), and fiberglass reinforced PSF/PET are a few examples of polymer blends utilized in the automobile industry.

8. Using fiber reinforcement in the materials is another method for raising ESCR. Fiber reinforcements may assist stop the simple development of fractures and crazes that can form on surfaces by bridging them. An example of this was seen in fiber-reinforced polystyrene (PS), which, according to L. M. Robeson [42], required more tension in the presence of acetone to

shatter than PS without fiber reinforcement. Another example is the superiority of fiber reinforced PSF over other materials in the automobile sector for spring-loaded safety interlock devices. Additionally, when glass fibers are included in the materials, a lower cooling rate will result in fibers free of the amorphous phase and greater crystallinity, according to M. N. Bureau et al. [42].

9. Impact modification, particularly with rubber, may raise the material's ESCR since the material can tolerate more chemicals and greater stress. Nonetheless, the material's ESCR is significantly impacted by the size of the rubber particles. L. M. Robeson states that materials with bigger rubber particles have stronger ESCR qualities than those with smaller rubber particles, but only to a certain degree [38]. After that, the ESCR decreases as the size of the rubber particles increases. The size limit that was noted was six micrometers. In comparison to materials without rubber modification, there is a drop in modulus and thus a decrease in surface stress at constant strain as a result of rubber modification. Rubber modification further aids in stabilizing any surface crazing that may have happened. Evidence of rubber modification raising ESCR in PC, ABS, and polystyrene (PS) has been found. Enhancing PC's ESCR and impact strength has also been seen by the use of thermoplastic polyurethanes or hydrogenated styrene-butadiene-styrene block copolymer [38].

10. The material's ESCR may be affected differently by a variety of manufacturing process characteristics. A few factors affecting the material's ESCR include its design, injection molding, sharpness of the material's edges, manufacturing process temperature, injection molding cycle duration, quenching rate, etc. For instance, a material with sharp edges has a greater chance of exhibiting fractures because those edges may help cracks start and spread more quickly. The ESCR of the material may also be impacted by molding pressure and processing temperature. These factors may alter surface flaws and crystal shape, which may have an impact on ESC [43].

II.8. Test methods for evaluation of ESCR of plastics

Checking ESCR performance for quality control, competitive product assessments, and research and development activities is a regular laboratory requirement for ESC-prone polymers. The ESCR of thermoplastics may be measured using a range of test techniques, which are categorized into two groups: tests at constant strain and testing at constant load (stress). Remember that since the strain is not kept constant during the test, any test that applies

a constant strain is less harsh than the seemingly similar test that applies a constant load [2]. The ESC conditions will get less severe over time as a result of stress relaxation, which causes the tension in the sample caused by continuous strain to diminish.

II.8.1. Tests at constant strain

Constant strain methods are the most widely used because they are inexpensive to conduct and require little equipment investment. The main drawback of using constant strain tests with plastics is that the stress will decay over time due to stress relaxation. It is crucial for the accuracy of the ESC tests to choose the most appropriate strain applied on the sample because high strain will cause cracking to occur too quickly to observe, and lower strain will result in long-term experiments. Wang et al. [44] conducted research to establish the appropriate values of strain to be exerted in the ESC test of various types of plastics. They discovered that the strain should be selected in the elastic region of the stress-strain curve for brittle plastics, while the plastic region.

II.8.1.1. Three-point bending test

In order to achieve a maximal surface strain, a mid-point deflection □ is often used. The exam has two main variations, which are shown in **Figure II.5** [2, 45]. Samples are inserted into the test apparatus, and the screw is adjusted to provide the necessary strain. The stress cracking agent is submerged in the deformed samples, or strips. The samples are taken out after the prearranged test duration, cleaned with distilled water, and left to dry for a full day at room temperature. After that, the samples' tensile characteristics are examined and they are checked for crazing.

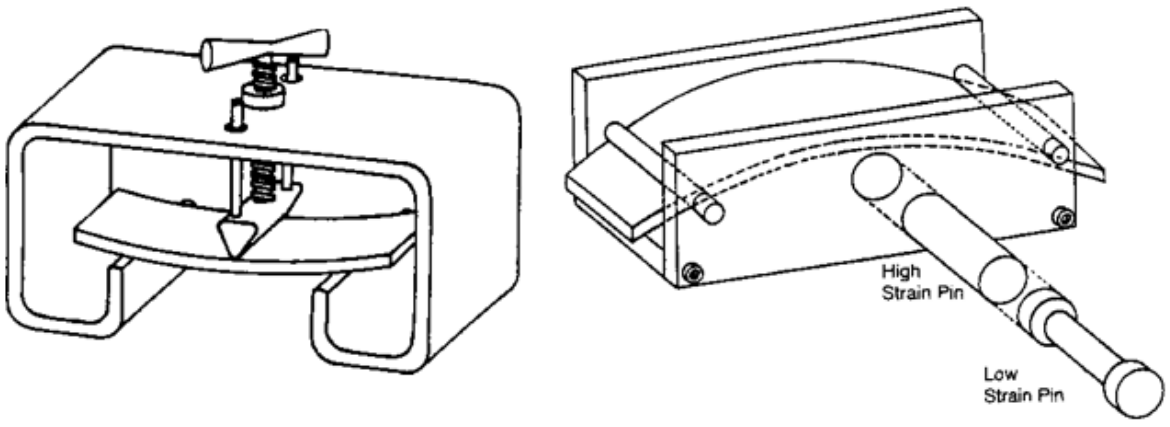

Figure II.5. Three-point bending apparatus for testing the ESCR under constant strain.

II.8.1.2. Bell telephone test (BTT)

Bell Laboratories in the USA developed this test to evaluate the ESCR efficacy of polyethylene cable insulation [1, 2]. The test specimens (38 x 13 x 3 mm3) are placed in a metal U-shaped specimen holder after being bent and notched (at around 180°C) with the notch facing downwards (Figure II.6).

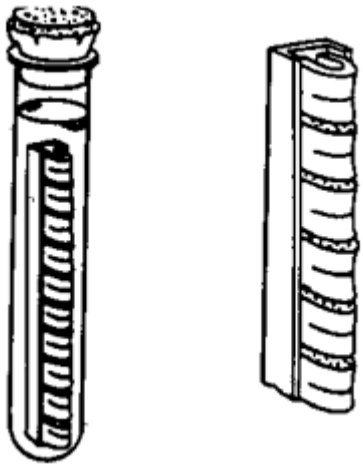

Figure II.6. Bent-strip test for flexible materials (Bell telephone test).

The maximum surface strain is calculated by using the following equation:

$$\varepsilon_{max.} = \frac{t}{w - t} \times 100\ [\%] \qquad (1)$$

where t is the thickness of the sample and w is the width of the holder.

The holder is put within a glass tube that has a water solution containing 10% Igepal CO-630. After being sealed, the tubes are submerged in 50°C water. A function of time is used to record the quantity of samples exhibiting cracking. The emergence of any crack that is apparent to the unaided eye is used to assess failure. Duration of the test should be at least 48 h. Every sample must pass the examination. The test should be deemed unsuccessful if even one test specimen fails.

The BTT approach has become the accepted standard technique. On the other hand, automating this process is difficult. The only method used to identify the presence of cracks or fractures in the test pieces is visual inspection carried out at predetermined intervals. As a result, the procedure might result in a mistake. An almost entirely human error-free technique for measuring the ESC at constant strain was presented by Saeda and Suzaka [46]. Because it was

invented at Oita Research Laboratory, Showa Denko, Japan, this approach is known as the ORL method. **Figure II.7** depicts the device's longitudinal sectioned view.

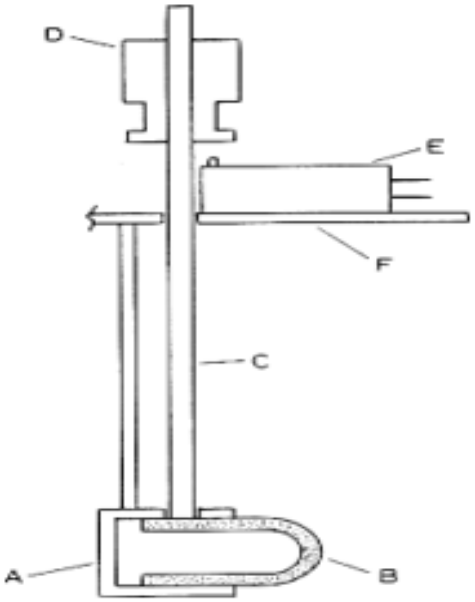

Figure II.7. Oita Research Laboratory (ORL) ESCR test device. A – sample holder, B – bent strips, C – shaft, D – load, E – electric switch, F – supporting plate [46].

The sample holder is the same size as the ASTM-D1693 sample holder (Bell telephone test), which has the capacity to retain 10 bent test strips in place while they are being tested. The ORL technique can accurately and human error-free identify the time to failure by automated methods (by employing an electric device), while the BTT detects the time when a tiny fracture occurs in the specimen.

II.8.2. Tests at constant load (Stress)

II.8.2.1. Constant tensile load test

Lu and Brown [47, 48] created the test to gauge the slow fracture development characteristic of polyethylenes. A single edge notched specimen is subjected to a continual load test in air or a stress cracking agent at different temperatures while simple strain requirements are fulfilled. The device arrangement utilized for the test under constant load is shown in **figure II.8**. The failure time is captured using a basic timer. When the specimen fractures, the timer stops. By plotting the crack opening displacement against time, one may use a microscope to observe the pace of slow crack development.

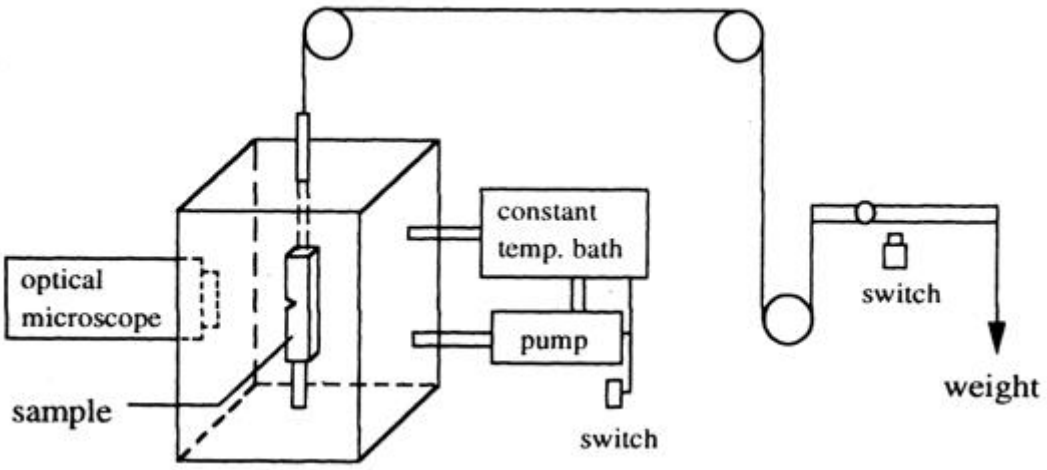

Figure II.8. Apparatus for the test at constant load [49].

The testing temperature affects the applied stress value. The value that results in brittle failure as quickly as feasible is the one that is advised. Based on in-depth research on many polyethylenes conducted by Lu and Brown [50, 51], the constant load test is typically performed in a 10% Igepal solution at a temperature of 50°C and a load of 4.2 MPa.

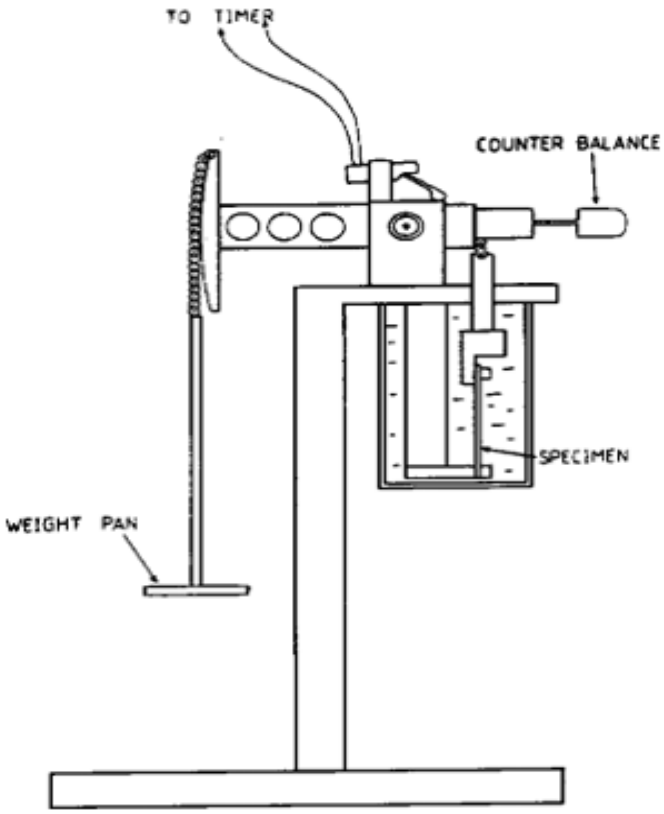

Figure II.9. Rapra high temperature tensile creep rupture set-up [2].

The Rapra high temperature tensile creep rupture testing apparatus, which is very comparable to the standard test under constant load, is shown in **figure II.9**. The process involves applying a tensile tension and timing the rupture.

II.8.2.2. Monotonic creep test

A monotonic creep testing apparatus was created by Hough and Wright [3] to evaluate the ESC of amorphous thermoplastics. This is comparable to the long-used slow strain rate testing method that the metals industry used to evaluate hydrogen embrittlement and stress corrosion cracking [52]. Here, however, the strain reaction to a steady stress rate is seen. The procedure shown in **figure II.10** uses a tensile creep machine in which a blow-molded vessel is used in lieu of the weight pan. **figure II.11** shows the Moirè fringe extensometer used to assess specimen strain.

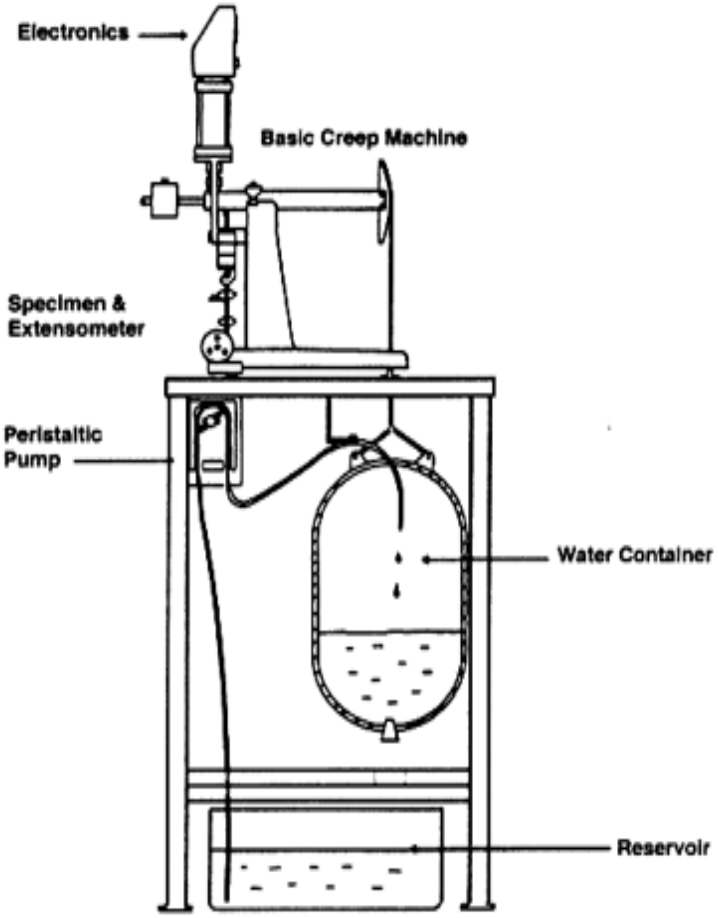

Figure II.10. Monotonic creep testing machine [3].

High resolution and discrimination may be achieved using the monotonic creep approach. The method's ability to produce critical time, critical stress, and critical strain suggests using it to

look into the criteria for the ESC phenomenon's starting [2].

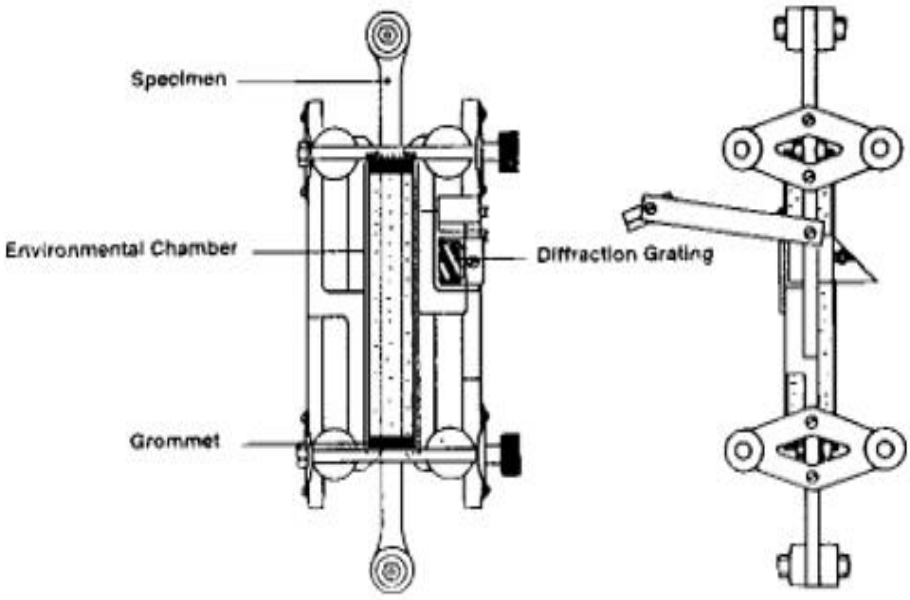

Figure II.11. Rapra Moirè fringe extensometer with environmental chamber attached to the specimen [3].

II.8.2.3. Test method for determining ESCR of polyethylene plastics

The most widely used technique in the industry to gauge the ESCR of polyethylene polymers is BTT. Even while BTT seems appealing when considering simplicity, there are a number of issues with it. A few factors may influence how easily the test findings can be repeated: The stiffness of the polymer material determines the bent specimen's curvature; the strain is not kept constant throughout the test; therefore it is challenging to guarantee a sharp notch that is consistent from specimen to specimen. A novel technique for calculating the ESCR of ethylene polymers at various strains and temperatures was created by Crissman [53] (**Figure II.12**). A metal cylindrical shape with a predetermined radius of curvature is bent around a strip specimen. This guarantees that during the test, every specimen will adhere to the same geometry. The specimens are usually strips without notches. A ten percent Igepal solution in water serves as the stress-cracking agent. The behavior of several polyethylenes under continuous applied stress and in the temperature range of 23 to 90°C is examined for stress-cracking behavior. It was found that a set of parameters may be used for polyethylenes with molar masses and densities that vary greatly. A notional specimen thickness of 1 to 1.25 mm, a bend radius of 5.5 mm, an applied stress of 5 MPa, and a temperature of 75°C are the ideal test

parameters.

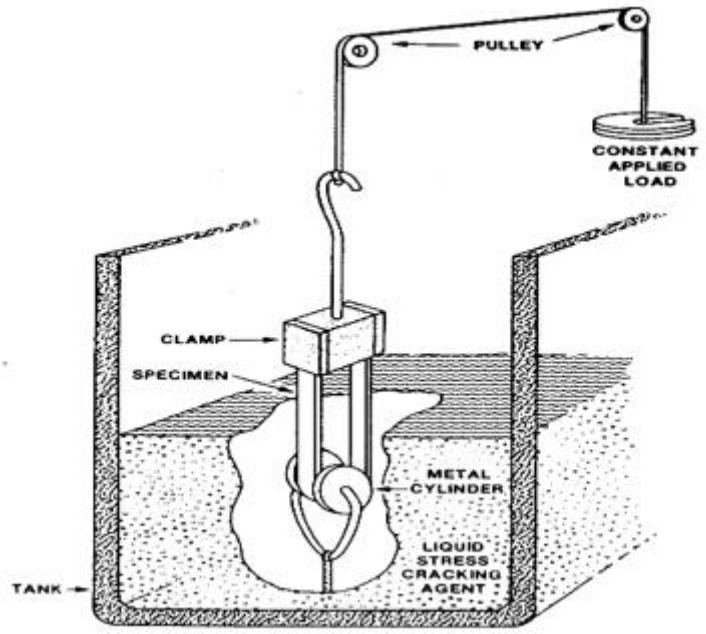

Figure II.12. View of the device for testing ESCR of polyethylene plastics [53].

II.8.3. Bottle ESCR test

Regretfully, findings obtained for bottles constructed of the same material may not always match with data collected using bent strip techniques. To evaluate the ESCR of plastic bottles, a bottle ESCR test has been created. Using this method, ten volume percent of the bottles are filled with a stress cracking solution. After that, the sealed bottles are heated to 60°C in an oven, which causes a rise in internal pressure [1]. Bottles that hold up after seven days are deemed sufficient. It may be inferred that because of their ease of use and low cost of testing equipment, constant strain techniques are often used to investigate the ESCR of plastics. However, the findings are not as repeatable due to human mistake (visual failing), the test specimen's curvature depending on the polymer material's stiffness, and the test's inability to sustain consistent strain. Because tension relaxes with time, the stress will gradually lessen. Because the notch opening and crack opening displacement are often detected using an optical microscope, tests conducted under continuous load have higher accuracy levels. In the early stages of the slow crack development process, time to failure may be predicted since the time to full failure is exactly related to the time for fracture initiation. As a result, the testing process is quicker than it would be under constant strain [53].

II.9. Importance of study of ESC

These days, ESC of materials is a prominent subject because to the many companies that are dealing with this issue. ESC may reduce material durability, which might have an adverse effect on the brand's reputation and the economy. For this reason, a lot of effort is put into this field. Fifteen to twenty-five percent of plastic failures have been attributed to stress cracking [54]. It seems like 40 or 50 years have passed since the issue of ESC of polymers was first studied. Due to the infinite variety of materials and chemicals that can be combined with different environmental conditions to create a seemingly endless research topic, it is impossible to draw conclusions from the data that has been collected thus far because each combination of chemical, material, and environmental condition will produce a unique effect. Different materials may be utilized in different sectors to create a wide range of goods, each with its own set of uses. Different chemical agents may be used at unknown circumstances throughout the production process of these items or even during the usage of these materials by consumers, which might fracture the material. As a result, it's critical to understand which fluids may be utilized in both the production process and by consumers once they've received the knowledge about additional circumstances under which the material won't fail. The packaging, automotive, and aerospace sectors are just a few that are impacted by polymeric material cracking. Due to the extensive use of amorphous polymers in their products, several sectors are particularly significant in this regard. Several additional businesses that may be impacted by this polymeric material breaking include the toy, sports, FMCG, and medical sectors, among others. The following is a discussion on ESC in the automotive sector, since the thesis focuses on ESC of interior polymers, notably ABS and PC/ABS used in cars.

II.10. Analysis techniques of ESC

Environmental stress cracking may be examined utilizing a variety of methods after ESC testing. The simplest method of analyzing ESC of materials is to simply look for crazes and cracks in the materials' morphology using an optical microscope. Then, compare the materials based on how many crazes and cracks they have after a given test time, or compare them based on which material fractures the fastest. If distinguishing between materials using an optical microscope proves to be challenging, a Scanning Electron Microscope (SEM) may be used as an additional means of material observation. Because SEM has a better resolution power than an optical microscope, it can identify materials down to very fine details. These techniques are qualitative analysis; quantitative data for comparison cannot be provided.

References

[1] Scheirs,Compositional, J. and Failure Analysis of Polymers. J. Wiley & Sons, 2000.

[2] Wright, D. Environmental Stress Cracking of Plastics. RAPRA Technology Ltd, 1996.

[3] Hough, M C. Wright, D C. Two new test methods for assessing environmental stress cracking of amorphous thermoplastics. Polymer Testing, 1996.

[4] Lustiger, A. Understanding environmental stress cracking in polyethylene. Medical plastics: degradation resistance and failure analysis, 1998.

[5] Pinsky, J. Plast. Tech, 1959.

[6] Lagarón, J M. Dixon, N M. Gerrard, D L. Reed, W. Kip, B J. Cold-drawn material as model material for the environmental stress cracking (ESC) phenomenon in polyethylene. A Raman spectroscopy study of molecular stress induced by macroscopic strain in drawn polyethylenes and their relation to environmental stress cracking. Macromolecules, 1998.

[7] Lagarón, J M. Pastor, J M. Kip, B J. Role of an active environment of use in an environmental stress crack resistance (ESCR) test in stretched polyethylene: A vibrational spectroscopy and a SEM study. Polymer, 1999.

[8] Schmiedel, H. Handbuch der Kunststoffprüffung. Carl Hanser Verlag, 1992.

[9] Felbeck, D. Atkins, A. Strength and Fracture of Engineering Solids. 2nd edition. Prentice Hall, 1996.

[10] Hittmair, P. Ullman, R. Environmental stress cracking of polyethylene. Journal of Applied Polymer Science, 1962.

[11] Lustiger, A. Corneliussen, R D. The role of crazes in the crack growth of polyethylene. Journal of materials Science, 1987.

[12] Wright, D C. Environmental stress cracking of plastics. iSmithers Rapra Publishing, 1996.

[13] Volynskii, A L. Aleskerov, A G. Bakeev, N F. on mechanical-properties of high-disperse oriented polyethylene terephthalate. vysokomolekulyarnye soedineniya seriya a, 1982.

[14] Hansen, C M. Just, L. Prediction of environmental stress cracking in plastics with Hansen solubility parameters. Industrial & engineering chemistry research, 2001.

[15] Kambour, R P. Gruner, C L. Romagosa, E D. Solvent crazing of “dry” polystyrene and “dry” crazing of plasticized polystyrene. Journal of Polymer Science: Polymer Physics Edition, 1973.

[16] Kambour, R P. Yee, A F. Influence of viscosity and capillary force on the relationship between crack toughness and crack velocity for an acrylonitrile-butadiene-styrene plastic in environmental stress cracking liquids. Polymer Engineering & Science, 1981.

[17] Friedrich, K. Crazes and Shear Bands in Semi-Crystalline Thermoplastics. Advances in Polymer Science, 1983.

[18] Lu, X. Brown, N. The ductile-brittle transition in a polyethylene copolymer. Journal of materials science, 1990.

[19] Hiss, R. Hobeika, S. Lynn, C. Strobl, G. Network stretching, slip processes, and fragmentation of crystallites during uniaxial drawing of polyethylene and related copolymers. A comparative study. Macromolecules, 1999.

[20] Hobeika, S. Men, Y. Strobl, G. Temperature and strain rate independence of critical strains in polyethylene and poly (ethylene-co-vinyl acetate). Macromolecules, 2000.

[21] Al-Hussein, M. Strobl, G. Strain-controlled tensile deformation behavior of isotactic poly (1-butene) and its ethylene copolymers. Macromolecules, 2002.

[22] Lafrance, C P. Chabot, P. Pigeon, M. Prud'homme, R E. Pézolet, M. Study of the distribution of the molecular orientation in thick polyethylene samples by X-ray diffraction, infra-red dichroism and Raman spectroscopy. Polymer, 1993.

[23] Rodriguez-Cabello, J C. Merino, J C. Jawhari, T. Pastor, J M. Rheo-optical Raman study of chain deformation in uniaxially stretched bulk polyethylene. Polymer, 1995.

[24] Pigeon, M. Prud'Homme, R E. Pezolet, M. Characterization of molecular orientation in polyethylene by Raman spectroscopy. Macromolecules, 1991.

[25] Brooks, N W J. Unwin, A P. Duckett, R A. Ward, I M. Double yield points in polyethylene: Structural changes under tensile deformation. Journal of Macromolecular Science, Part B: Physics, 1995.

[26] Lagaron, J M., Dixon, N M. Reed, W. Pastor, J M. Kip, B J. Morphological characterization of the crystalline structure of cold-drawn HDPE used as a model material for the environmental stress cracking (ESC) phenomenon. Polymer, 40(10), 1999.

[27] Opdahl, A. Somorjai, G A. Stretched polymer surfaces: Atomic force microscopy measurement of the surface deformation and surface elastic properties of stretched polyethylene. Journal of Polymer Science Part B: Polymer Physics, 2001.

[28] Lu, X. Qian, R. Brown, N. The effect of crystallinity on fracture and yielding of polyethylenes. Polymer, 1995.

[29] Cowie, J M G. McEwen, I J. McIntyre, R. Aging and degradation of polymer blends. Polymer blends handbook, 2003.

[30] Huang, Y L. Brown, N. The effect of molecular weight on slow crack growth in linear polyethylene homopolymers. Journal of materials science, 1988.

[31] Soares, J B. Abbott, R F. Kim, J D. Environmental stress cracking resistance of polyethylene: The use of CRYSTAF and SEC to establish structure–property relationships. Journal of Polymer Science Part B: Polymer Physics, 2000.

[32] Lustiger, A. Environmental stress cracking: the phenomenon and its utility. Carl Hanser Verlag, Failure of Plastics, 1986.

[33] Kendall, K. Sherliker, F R. Effect of polymer molecular weight on colloidal reinforcement. British Polymer Journal, 1980.

[34] Narisawa, I. Ishikawa, M. Crazing in semicrystalline thermoplastics. In Crazing in Polymers Vol. 2. Berlin, Heidelberg: Springer Berlin Heidelberg, 2005.

[35] Brown, N. Ward, I M. The influence of morphology and molecular weight on ductile-brittle transitions in linear polyethylene. Journal of materials science, 1983.

[36] Lu, X. Brown, N. Effect of thermal history on the initiation of slow crack growth in linear polyethylene. Polymer, 1987.

[37] Roe, R J. Gieniewski, C. Reproducibility of stress-cracking test results. Polymer Engineering and Science, 1975.

[38] Robeson, L M. Environmental stress cracking: A review. Polymer Engineering and Science, 2013.

[39] Brown, H R. A theory of the environmental stress cracking of polyethylene. polymer, 1978.

[40] Bhalla, A K. Environmental Stress Cracking of Interior Polymers used in the car. Master's thesis NTNU, 2018.

[41] Cheng, J J. Polak, M A. Penlidis, A. Influence of micromolecular structure on environmental stress cracking resistance of high-density polyethylene. Tunnelling and Underground Space Technology, 2011.

[42] Bureau, M N. Denault, J. Perrin, F. Dickson, I. Crack propagation in continuous glass fiber/polypropylene composites: matrix microstructure. Plastics Failure Analysis and Prevention, 2001.

[43] Soares, J B P. Abbott, R F. Kim, J D. Environmental Stress Cracking Resistance of Polyethylene: The Use of CRYSTAF and SEC to Establish Structure-Property Relationships. Journal of Polymer Science: Part B: Polymer Physics, 2000.

[44] Wang, H T. Pan, B R. Du, Q G. Li, Y Q. The strain in the test environmental stress cracking of plastics. Polymer testing, 2003.

[45] Arnold, J C. The use of flexural tests in the study of environmental stress cracking of polymers. Polymer Engineering & Science, 1994.

[46] Saeda, S. Suzaka, Y. The environmental stress cracking of linear ethylene copolymers. Polymers for advanced technologies, 1995.

[47] Lu, X. Brown, N. A test for slow crack growth failure in polyethylene under a constant load. Polymer Testing, 1992.

[48] Zhou, Z. Brown, N. A new automated method for recording and predicting failure by slow crack growth in polyethylene. Polymer testing, 1996.

[49] Yeh, J T. Chen, J H. Hong, H S. Environmental stress cracking behavior of short-chain branch polyethylenes in Igepal solution under a constant load. Journal of applied polymer science, 1994.

[50] Ward, A L. Lu, X. Brown, N. Accelerated test for evaluating slow crack growth of polyethylene copolymers in Igepal and air. Polymer Engineering and Science, 1990.

[51] Lu, X. Zhou, Z. Brown, N. A sensitive mechanical test for slow crack growth in polyethylene. Polymer Engineering and Science, 1997.

[52] Hay, J N. Kemmish, D J. Environmental stress crack resistance of and absorption of low-molecular-weight penetrants by poly (aryl ether ether ketone). Polymer, 1988).

[53] Crissman, J M. A new test method for determining environmental stress-crack resistance of polyethylene plastics. Journal of testing and evaluation, 1983.

[54] Jansen, J A. Environmental Stress Cracking - The Plastic Killer. Advanced Materials Processes, 2004.

Chapter III. Theoretical calculation

III. Theoretical calculation

III.1. Computational part

Recent developments in theory and simulations of polymeric systems have allowed for accurate modelling of a wide range of polymeric systems both at the molecular and long wavelength scales. In particular, various computational techniques have proven to be a powerful tool, in obtaining atomic and molecular scale structural properties, which complement experimental data. In general, utilizing experimental techniques, intermolecular bonding in a polymer blend is relatively challenging to resolve. Molecular dynamics simulations have proven to be a reliable, cost-effective and fast tool, that can supplement experimental results, or help in overcoming major experimental limitations. Atomic scale simulations are also often used to predict the impact of compatibilizers on the structure and physical characteristics of polymer mixes.

III.1.1. Molecular dynamic simulation (MDS)

Molecular Dynamic simulation is a useful tool for understanding how SEBS and SEBS-g-MAH compatibilizer interact with an LDPE/PP blend. It's used to assess their effects on compatibility. In the present work, chains of PP and LDPE with and without oxidation (the PP and LDPE oxidized chains are called PPO and PEO respectively) with 50 repeat units were constructed. The oxidized models are built on the basis of FTIR results, to approximate the actual behavior of the blend and to study the effect of oxidation on blend compatibility All MD simulations were carried out using the Materials Studio program from Accelrys Inc. In order to clarify the inter- and intramolecular interactions, the COMPASS force field was used. The velocity-Varlet method with a 1 fs integration timestep was used to integrate the motion equations. The van der Waals (VdW) interaction has an 8.5 cutoff. The Coulomb interactions were calculated using the Ewald summation technique. To execute the simulations, the NVT ensemble used the Anderson thermostat and Berendsen barostat was used for NPT [1]. The pressure was fixed at 1 atm, and the temperature at 483 K.

III.1.2. Quantum computational calculation

The Material Studio Software 7.0 numerical-based density-functional module (DMol3) was used to carry out the Density Functional Theory (DFT) investigation. It is used to estimate the

density of states (DOS) and the exchange-correlation function; it returns information related to the effect of SEBS-g-MA adsorption on the properties of the blended complex PP-PE, and how (E_{gab}) changes next to the interactions that take place, together with an all-electron double numerical basis set with polarized d-function (DNP). The GGA (Generalized Gradient Approximation) with PBE (Perdew-Burke-Ernzerhof) functional [2,3] was selected for calculating the exchange and functional correlation using the Grimme [4] method for DFT D corrections. A polarization d-function for all atoms is included in the DNP basis set, which contains a numerical function for each orbital that is occupied. The maximum force and maximum displacement thresholds have been set at 0.004 Ha/Å, and 0.005 Å, respectively, with the maximum energy change set at 2×10^{-5} Ha [5,6].

Frontier molecular orbitals (FMO) of PP-PE and their mixtures were studied to highlight the impact of contact on the electrical charge properties of the blends systems. We took into account both the Higher Occupied Molecular Orbital (HOMO) and the Lower Unoccupied Molecular Orbital (LUMO) while describing the electrical characteristics of the molecule [7]. The lowest unoccupied orbital is a good place for electrophilic action, according to the border orbital theory. The flexibility to participate in the reaction is greater for the electrons in the HOMO orbital. The electrophilicity indices (ω), chemical potential (μ), and global hardness (η) are electronic parameters which return information about the reactivity of molecules and help in interpreting their properties and understanding the nature of molecules in terms of their stability. The following equations were used to calculate them in both gaseous and solvent phases:

$$\omega = \mu^2/2\eta \tag{1}$$

$$\mu = \frac{E_{HOMO} + E_{LUMO}}{2} \tag{2}$$

$$\eta = \frac{E_{LUMO} - E_{HOMO}}{2} \tag{3}$$

Fukui functions f(r) were used to predict electrophilic and nucleophilic locations favored for covalent and noncovalent interactions created between PP-PE and SEBS-g-MA [8].

The Fukui function f(r) (Eq.4) [9] is a derivative of a molecular electronic density with a specific electronic potential (V(r)) and a fixed number of electrons (N) [10]:

$$f(r) = \left(\frac{\partial \rho r)}{\partial N}\right)_{V(r)} \quad (4)$$

Eq 5 and 6 discuss two Fukui formulations for cationic and anionic atoms based on a finite difference approximation of the Fukui function f(r) [10]:

$$f^{+}(r) = \left(\frac{\partial \rho(r)}{\partial N}\right)^{+}_{V(r)} = \rho_{N+1}(r) - \rho_{N}(r) \quad (5)$$

$$f^{-}(r) = \left(\frac{\partial \rho(r)}{\partial N}\right)^{-}_{V(r)} = \rho_{N}(r) - \rho_{N-1}(r) \quad (6)$$

Where $f^{+}(r)$ and $f^{-}(r)$ represent the cationic and anionic Fukui functions, respectively, and $\rho_{N+1}(r)$, $\rho_{N}(r)$, and $\rho_{N-1}(r)$represent the electronic density at distance in the system made up of $N + 1$, N, and $N - 1$electrons, respectively.

III.2. Computational analysis

The binding energy were explored from MD simulations. **Figure III.1** shows various structures obtained after equilibration and density stabilization.

III.2.1. Molecular dynamic simulation

a) Binding energy

We can completely comprehend the interaction process by computing and comparing the binding energies of the various equations. Equations 7 may be used to compute the binding energies of the PP-PE, PPO-PEO, and SEBS-g-MA interaction models.

$$Ebind = -Einter = -E\ total - E1 - E2 \quad (7)$$

Where Etotal, E1 and E2 are the energies of the blends studied. The binding energies of different blends are given in **Table III.1.**

Table III.1. Interaction energies for binding (kcal/mol).

N° Sys	System	E(Total)	E(PP) / E(PPO)	E(PE) / E(PEO)	E(SEBS-g-MA)	E(SEBS)	E(bind)	E(Inter)
1	**3PP-3PE**	-3213,34	-1415,84	-1357,03	---------	---------	440,47	-440,47
2	**3PP-3PE-1SEBS**	-3688,97	-1167,30	-1304,44	----------	-545,97	671,26	-671,26
3	**3PP-3PE-1SEBS-g-MA**	-3581,89	-1326,51	-1195,31	-179,98	---------	880,09	-880,09
4	**3PPO-3PEO**	-1740,73	-759,22	-691,24	----------	---------	290,27	-290,27
5	**3PPO-3PEO-1SEBS**	-3280,05	-940,56	-928,47	----------	-461,57	949,45	-949,45
6	**3PPO-3PEO-1SEBS-g-MA**	-2340,98	-743,97	-704,84	-524,35	---------	367,82	-367,82

The binding energy of PP/PE increases with the inclusion of the compatibilizer SEBS-g-MA, which indicates that the interaction strength between PP-SEBS-g-MA and PE-SEBS-g-MA is greater than that of PP-PE comparison between of 3PP-3PE-SEBS-g-MA and 3PP-3PE which are 440.47 and 880.09 kcal/mol. Comparing between the systems 3PP-3PE-SEBS-g-MA and 3PP-3PE- SEBS the presence of anhydride maleic in the compatibilizer agent enhance the binding interaction from 671.26 to 880 kcal/mol.

The patterns of their contact may also be seen after MD modeling to reach the same conclusion (**Figure III.1**). The molecular chains of PP or PE are wrapped on them showing in **Figure III.1**. The inclusion of SEBS-g-MA increases the compatibility between the two polymers in the matrix or we can say that the miscibility of the blend increases, which explains the experimental results. In the case of SEBS as a compatibilizer and as shown in **Figure III.1 e** and **f**, SEBS in the box favors interaction with the PEO or PE chain rather than PP or PPO due to the ethylene segment existing in the SEBS structure, and as it is clear that the PP chains overlap each other creating a separate phase in the system. This finding confirms the result obtained in the experimental results, i.e. that SEBS-g-MA is the best computerizing agent compared with SEBS-g-MA.

1- 3PP-3PE

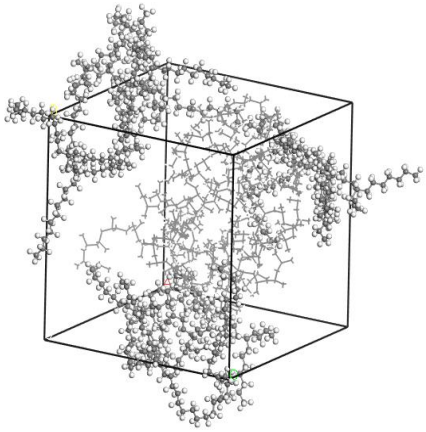

2- 3PP-3PE-1SEBS

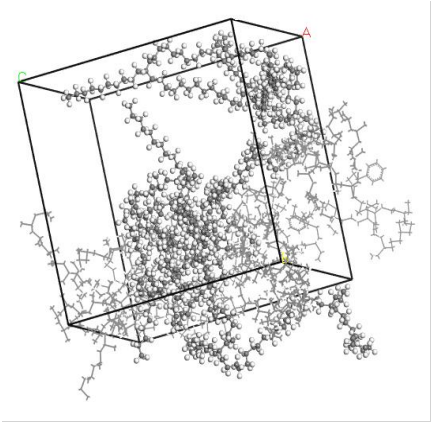

3- 3PP-3PE-1SEBS-g-MA

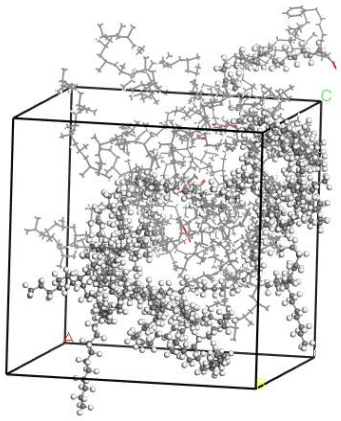

4- 3PPO-3PEO

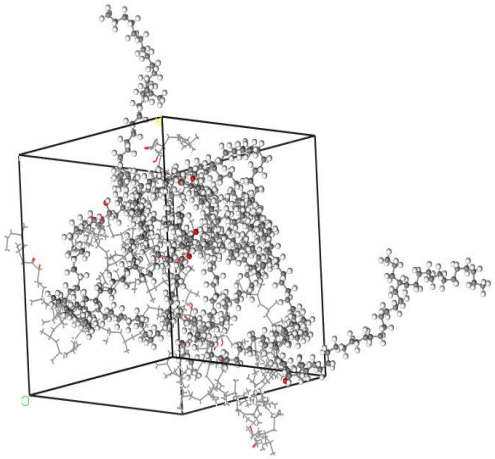

5- 3PPO-3PEO-1SEBS

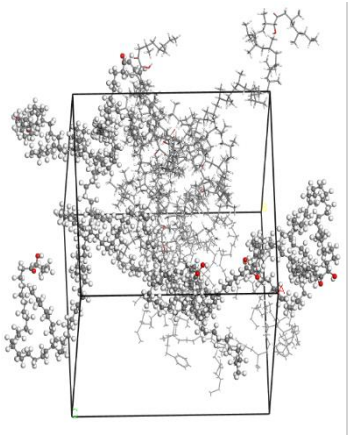

6- 3PPO-3PEO-1SEBS-g-MA

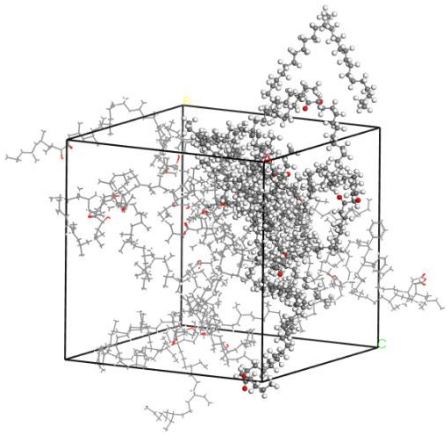

Figure III.1. The final structures, which were determined by dynamic simulations for the formulation of PP/PE and PPO/PEO blends, show the structures following equilibration and density stabilization.

b) Intermolecular interactions

In blended systems, the bonds between the PP-PE systems are insufficiently strong due to their saturated chemical nature. **Table III.2** highlights the corresponding binding energies, indicating that electrostatic binding predominates in this system. However, the mixture's binding strengths are strengthened by the addition of SEBS-g-MA. This rise is ascribed to SEBS-g-MA's impact on the mixes' characteristics. The unbound interaction energies E (Kcal/mol) for the different chemical systems are listed in **Table III.2**.

Table III.2. The energy of non-bonded interactions ΔE (Kcal/mol) for various chemical.

N° Sys	System	$\Delta E_{non\text{-}bond}$	ΔE_{VdW}	$\Delta E_{H\text{-}bond}$	$\Delta E_{electrostatic}$
1	**3PP-3PE**	-1318,667	-244,418	0,000	-1074,250
2	**3PP-3PE-1SEBS**	-1561,690	-251,800	0,000	-1309,890
3	**3PP-3PE-1SEBS-g-MA**	-1661,533	-72,844	0,000	-1588,689
4	**3PPO-3PEO**	-320,147	-314,675	-0,002	-5.470
5	**3PPO-3PEO-1SEBS**	-1486,600	-180,380	-0,320	-1306,540
6	**3PPO-3PEO-1SEBS-g-MA**	-582,607	-376,386	-0,001	-206,222

The energies E_(VdW), E_(H-bond), E_(electrostatic), and E_(non-bond), which, using the Dreiding Force Field, calculate the exact value of the hydrogen bond energy for each structure [11].

$$E\ (non\text{-}bond) = E\ (H\text{-}bond) + E\_VdW + E\_electrostatic \quad (8)$$

On the other hand, when maleic anhydride is present in SEBS-g-MA, the contact energies with oxidized PP-PE are similarly increased, leading to a strong interaction. The most important interaction in the case of SEBS in the blending system is electrostatic, as shown in **Figure III.1 (f)**, in the amorphous cells between the PE chain and the ethylene segments present in the compatibilizer, implying that SEBS-g-MA can function well as a compatibilizer for PP-PE blends.

III.2.2. Quantum molecular descriptors (QMDs)

Table III.3. Electrophilicity index (ω) global hardness (η), and chemical potential (μ) are all measures of the global reactivity of DFT.

System	E_{HOMO} (eV)	E_{LUMO} (eV)	E_{gap} (eV)	μ (eV)	η (eV)	ω (eV)
PP-PE	-4,675	-3,868	0,807	-4,2715	0,4035	22,61
PE-SEBS-g-MA	-4,432	-4,072	0,36	-4,252	0,18	50,22
PP-SEBS-g-MA	-4,434	-3,612	0,822	-4,023	0,411	19,69
PPO-PEO	-4,616	-4,399	0,217	-4,5075	0,1085	93,63
PEO-SEBS-g-MA	-5,079	-3,287	1,792	-4,183	0,896	9,76
PPO-SEBS-g-MA	-5,103	-3,245	1,858	-4,174	0,929	9,37
PEO-SEBS	-6,39	-0,15	6,54	-3,12	3,27	1,49
PPO-SEBS	-5,573	-0,73	4,84	-3,15	2,42	2,05

Frontier molecular orbitals (FMOs) are the most crucial molecular orbitals for assessing chemical reactivity and kinetic stability. The HOMO and LUMO orbitals are the boundary

molecular orbitals. It is well known that the transition from the ground state to the first excited state (electro-absorption) is brought about by a one-electron excitation from HOMO to LUMO. The kinetic stability of the system improves with increasing HOMO-LUMO separation. Therefore, more energy is needed to transfer electrons from HOMO to LUMO. Regarding this, **Table III.3** lists the orbital energies of PE-PP, PE-SEBS-g-MA, PP-SEBS-g-MA, PPO-PEO, PEO-SEBS-g-MA, and PPO-SEBS-g-MA along with other chemical properties.

Considering the findings in **Table III.3**, It is evident that PP-PE Blend is the most stable than PPO-PEO since the HOMO-LUMO gap is 0.807 eV, 0.217 eV respectively with a global hardness is equal to 22.61 eV and 93.63 respectively. In the case of PPO-PEO, η have the lowest values thus resulting the most reactive component. With the use of thermodynamic parameters, Deghiche et al [5] detailed in their study that the global electrophilicity index (ω), which quantifies the advantageous energy change that occurs as an electron-rich chemical system approaches saturation. As a result of the electrons moving from the donor (HOMO) to the acceptor (LUMO), there is an energy loss. **table III.2** shows the PPO-PEO blend is the largest electron acceptor, indicating the presence of oxygenated groups in the structure of the blends resulting from thermo-oxidation during the transformation, which supports the FTIR results. If we accept that the molecules' high EHOMO values tend to give electrons to the acceptor molecules with low EHOMO values. Therefore, the addition of the computerizing agent improves the chemical agreement between PPO and PEO as it is compatible with both polymers at the same time as it is clearly shown in **table III.3**.

Figure III.2 shown The DFT global reactivity of PPO-SEBS, PEO-SEBS, PPO-SEBS-g-MA, PEO-SEBS-g-MA and PPO-PEO blends. "-C-" atom of the CH3 group in the PP chain is where the PPO-PEO's HOMO is located, whereas the "-H" atom of the CH2 group in the PP chain is where the LUMO is located (see **figure 9**). The LUMO is located on the carbon atom connected to the "-H" atom of the CH group associated with the phenyl group of the SEBS-g-MA chain, while the HOMO of the PPO-SEBS-g-MA is found on the "-C-" atom of the CH3 of the PP chain. This conclusion was supported by the Fukui indices, f (+) and f (-), which showed that this functional group is in charge of electron-donating and electron-accepting, respectively. This result indicates a high degree of affinity between PPO and SEBS-g-MA.

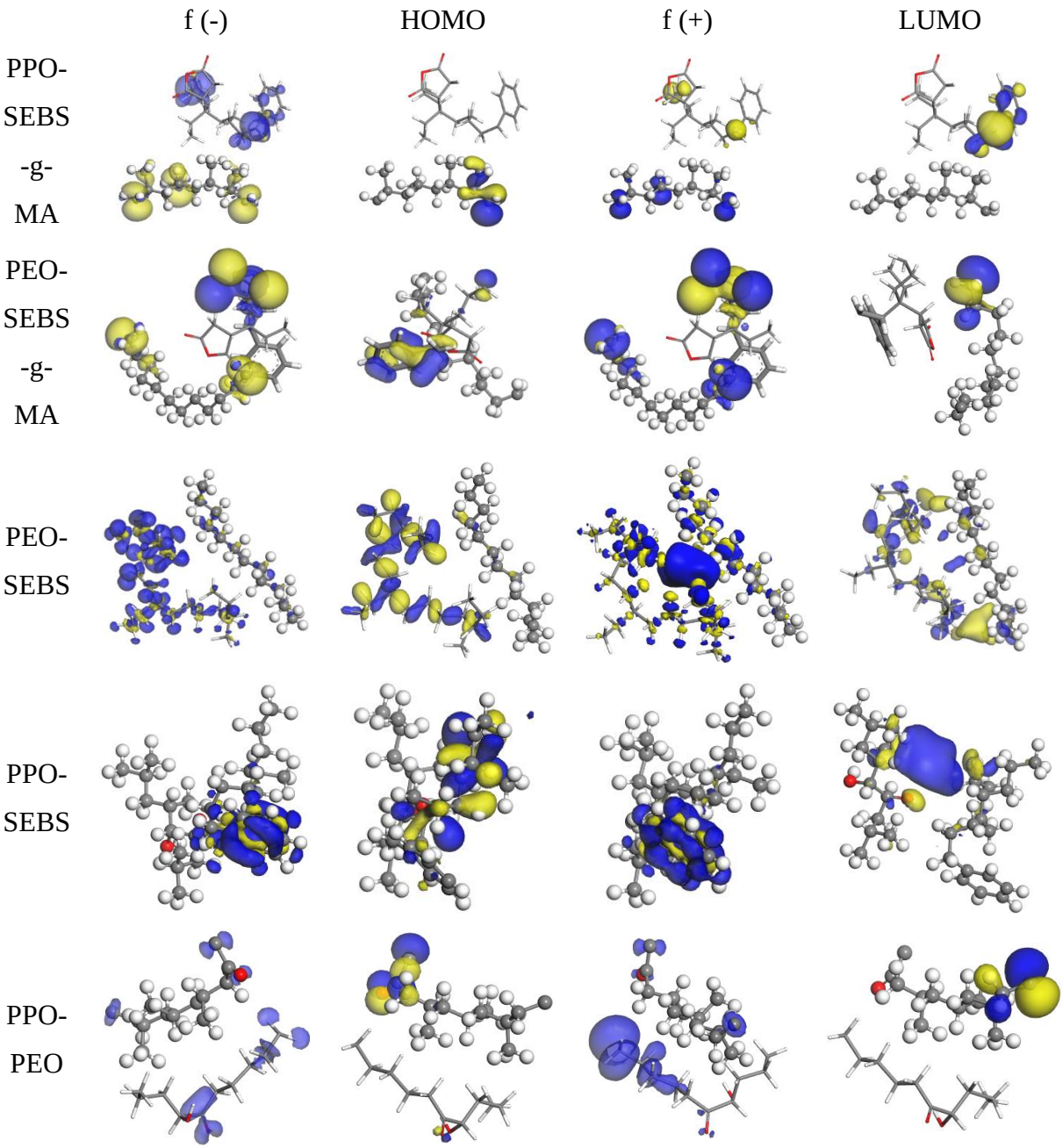

Figure III.2. DFT global reactivity of PPO-PEO blends with and without SEBS-g-MA/SEBS.

The same result for PEO-SEBS-g-MA, the HOMO of the PEO-SEBS-g-MA is found on the "-C-" atom of the CH_3 of the PE chain, whereas the LUMO is found on the carbon linked to the "-H" atom of CH group attached with phenyl group of SEBS-g-MA chain. In the case of SEBS used as a compatible's agent, the HOMO of PPO-SEBS was found between C=C in the aromatic groups present in the SEBS chain, whereas LUMO is found in the H atom of the CH3 group of PPO. In PEO-SEBS, the HOMO is clustered between the C-H of the PEO chain and the SEBS

ethylene segments, whereas the LUMO is located between the H atoms on either side of the SEBS ethylene and the PEO. This finding match with the morphological conclusion (XRD and SEM). The HOMO-LUMO study has provided us with valuable information on the underlying molecular mechanisms that govern the behavior of these materials. This sheds light on how the SEBS-g-MA molecule enhances the compatibility of the PP-PE blend.

III.2.3. Density of state

In order to determine how the compatibilizer will affect the final blend's properties, density of state (DOS) calculations was done on blends of PP-PE and PPO-PEO with and without SEBS-g-MA. **Figure III.3** displays the findings for the complexes of PP-PE and PPO-PEO. With matching HOMO-LUMO energy gaps of 4.90 and 4.33 eV, PP-PE and PPO-PEO are anticipated to be insulators, while the gap values of PE-SEBS-g-MA, PP-SEBS-g-MA, PEO-SEBS-g-MA, PPO-SEBS-g-MA, PEO-SEBS, and PPO-SEBS are 0.36, 0.822, 1.792, 1. 858, 4.382 and 5.973 eV. The presence of the phenyl group in the SEBS-g-MA structure is responsible for the clear decrease in gap energy in the presence of the compatibilizer. This impact validates the chemical composition of SEBS-g-MA with respect to each PP component. In the overall DFT reactivity picture, it is evident that, whether the PE is oxidized or not, the affinity between the components is located in the olefin part of the SEBS-g-MA compatibilizer due to the presence of the PE chain in the SEBS structure, which enhances the interaction, mainly of an electrostatic type, that favors the dispersion of the MDS cells. Maleic anhydride interacts more with the oxidation group of PP. In the case of SEBS without maleic anhydride, the Gap energy of PPO-SEBS is higher than that of PPO-SEBS-G-MA, the PPO chain favors interaction with them, indicating that there is no affinity between PP and SEBS, which in fact leads to phase separation and incompatibility and confirming also that the presence of MA is responsible for the compatibilization. Meanwhile, the same observation was made for PEO-SEBS with PEO-SEBS-g-MA, where the PEO chain interacts with the ethylene present in the SEBS structure.

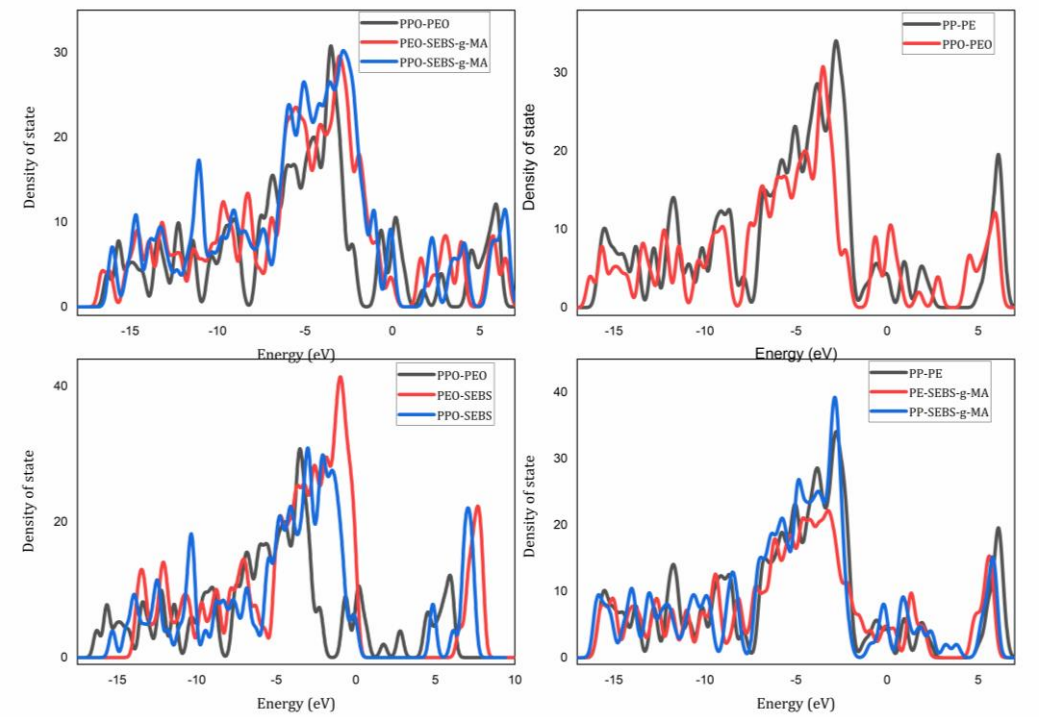

Figure III.3. DOS of PP-PE blends and PPO-PEO with and without SEBS-g-MA/SEBS.

Reference

[1] Wang Z, Lv Q, Chen S, Li C, Sun S, Hu S. Effect of Interfacial Bonding on Interphase Properties in SiO2/Epoxy Nanocomposite: A Molecular Dynamics Simulation Study. ACS Appl. Mater. Interfaces, 2016.

[2] Lee I.H, Martin R.M. Applications of the generalized-gradient approximation to atoms, clusters, and solids, Phys. Rev. B - Condens. Matter Mater. Phys, 1997.

[3] Smith J.M, Jones S.P, White L.D. Rapid Communication. Gastroenterology, 1977.

[4] Warrag S.E.E, Darwish A.S, Adeyemi I.A, Hadj-Kali M.K, Kroon M.C, AlNashef I.M. Extraction of pyridine from n-alkane mixtures using methyltriphenylphosphonium bromide-based deep eutectic solvents as extractive denitrogenation agents. Fluid Phase Equilib, 2020.

[5] Deghiche A, Haddaoui N, Zerriouh A, Fenni S.E, Cavallo D, Erto A, Benguerba Y. Effect of the stearic acid-modified TiO2 on PLA nanocomposites: Morphological and thermal properties at the microscopic scale. J. Environ. Chem. Eng, 2021.

[6] Basiuk V.A, Henao-Holguín L.V. Effects of orbital cutoff in DMol3 DFT calculations: A case study of meso-tetraphenylporphine-C60 complex. J. Comput. Theor. Nanosci, 2013.

[7] Bououden W, Benguerba Y, Darwish A.S, Attoui A, Lemaoui T, Balsamo M, Erto A, Alnashef I.M. Surface Adsorption of Crizotinib on Carbon and Boron Nitride Nanotubes as Anti-Cancer Drug Carriers: COSMO-RS and DFT Molecular Insights. J. Mol. Liq, 2021.

[8] Shojaeiarani J, Bajwa D.S, Stark N.M, Bajwa S.G. Rheological properties of cellulose nanocrystals engineered polylactic acid nanocomposites. Compos. Part B Eng, 2019.

[9] Kurnia K.A, Lima F, Cláudio A.F.M, Coutinho J.A.P, Freire M.G. Hydrogen-bond acidity of ionic liquids: an extended scale. Phys. Chem. Chem. Phys, 2015.

[10] Benabid S, Streit A.F.M, Benguerba Y, Dotto G.L, Erto A, Ernst B. Molecular modeling of anionic and cationic dyes adsorption on sludge derived activated carbon. J. Mol. Liq, 2019.

[11] Zerriouh A, Deghiche A, Bououden W, Cavallo D, Rainone F, Erto A, Haddaoui N. A computational and experimental investigation of TEOS-treated graphene oxide-PVA interaction : Molecular dynamics simulation and COSMO-RS insights Molecular dynamic Simulation. J. Mol. Liq, 2023.

Chapter IV. Materials used and experimental techniques

IV. Materials used and experimental techniques

IV.1. Materials

IV.1.1. Polypropylene (PP)

polypropylene (PP H 1045) was supplied by TASNEE, Saudi Arabia. The melt flow rate (230°C/2.16Kg) is 4.5 g/ 10 min, the density is 0.9 g/cm^3.

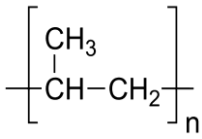

IV.1.2. Low-density polyethylene (LDPE)

Low-density polyethylene (FD0274) was supplied by LOTRÈNE, Qatar. The MFI is 2.4 g/ 10 min, the density is 0.932.

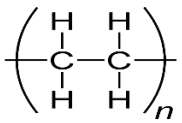

IV.1.3. Styrene ethylene butylene styrene (SEBS)

marketed as Kraton G1652, has a molecular weight of 7200 g/mol, and a block of poly (ethylene-co-butylene) medium (EB) with a molecular weight of 37500 g/mol, its density was 0.90.

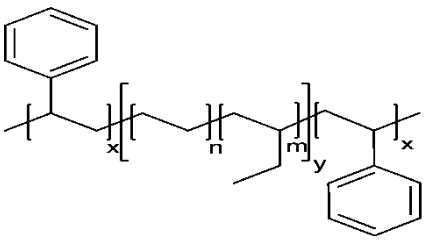

IV.1.4. Maleic anhydride grafted styrene-ethylene-butylene-styrene (SEBS-g-MA)

SEBS-g-MA sold under the trade name Kraton FG1924X is a three-block copolymer of type S-EB-S.

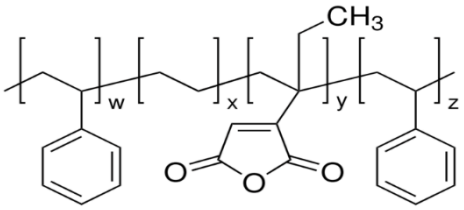

IV.1.5. Nonylphenyl-polyethylenglycol (igepal ca 630)

Nonidet P40 substitute detergents consist of nonyl-phenyl-polyethylene glycol, was supplied from Sigma-Aldrich.

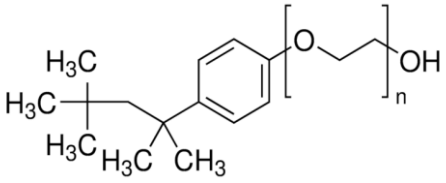

IV.2. Preparation of blends

An internal mixer (**Figure IV.1**), the PLASTI-CORDER Brabender, was used to mix a sample of plain polymers and PP/LDPE mixes with and without a compatibilizer for five minutes at 210°C and 80 rpm.

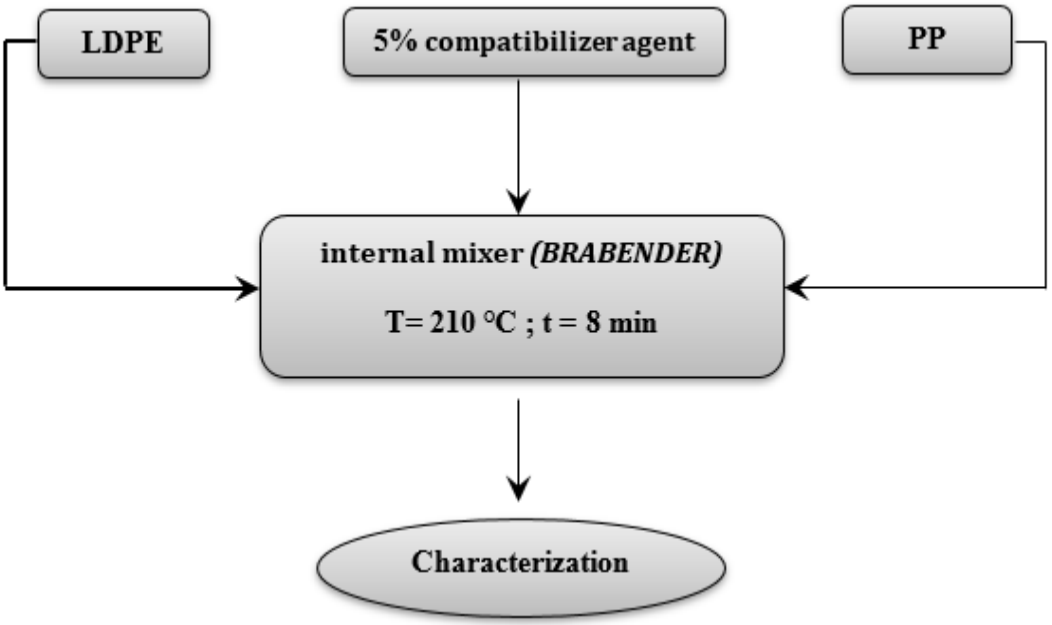

Figure IV.1. Blend preparation procedure flowchart.

Table IV.1. Formulations and compositions of the different blends.

Formulation	PP (%)	LDPE (%)	SEBS (%)	SEBS-g-MA (%)
M1	100	-	-	-
M2	-	100	-	-
M3	80	20	-	-
M4	50	50	-	-
M5	20	80	-	-
M6	77.5	17.5	5	-
M7	47.5	47.5	5	-
M8	17.5	77.5	5	-
M9	77.5	17.5	-	5
M10	47.5	47.5	-	5
M11	17.5	77.5	-	5

After its removal from the mixing chamber, the mixtures are cooled in ambient air and then crushed. The blend is eventually compressed with a hydraulic press POLYLAB at 210°C for 7 min plus 5 min degassing. The volume fraction of the compatibilizing agent (SEBS or SEBS-g-MA) was 5% with different weight fractions of PP and LDPE in the blend. **Table IV.1** lists the many formulations that were examined.

IV.3. Experimental techniques

IV.3.1. Fourier transform infrared spectroscopy (FTIR)

Fourier transform infrared (FTIR) spectroscopy analysis was performed using a spectrometer SHIMADZU IRSprit. was used to identify functional groups and evaluating the chemical changes in the materials. The spectra were determined in the wavenumber range from 4000 to 400 cm^{-1} at 64 scans and resolution at 4 cm^{-1}.

IV.3.2. Differential Scanning Calorimetry (DSC)

A Netzsch DSC 200 F3 Maia® thermal analyzer differential scanning calorimeter was used to analyze each blend's melting behavior. First, the apparatus was calibrated using indium as a reference material. A nitrogen atmosphere was used for the DSC analysis of the samples. The same scan rate was used for all experiments, which were conducted with sample mass of 10 mg. The samples were heated from 30 to 200 °C at a rate of 10°C/min. The crystallinity (χ) of the polymers in the blends was determined using the following equations: [1]

$$\%\chi pp = \frac{\Delta Hfm}{\varphi PP\ \Delta HPP_m^0} \times 100 \quad (1)$$

$$\%\chi LDPE = \frac{\Delta Him}{\varphi LDPE\ \Delta HLDPE_m^0} \times 100 \quad (2)$$

Where %χ PP is the percentage crystallinity of PP, %χ LDPE is the percentage crystallinity of LDPE, ΔH^f_m is the melting enthalpy of PP, ΔH^i_m is the melting enthalpy of LDPE, ΔH^0 m(LDPE) is the equilibrium melting enthalpy of LDPE = 288 $J \cdot g^{-1}$ [2], ΔH^0 m(PP) is the equilibrium melting enthalpy of PP = 207 $J \cdot g^{-1}$ [3], φ PP is the weight fraction of PP, and φ LDPE is the weight fraction of LDPE.

IV.3.3. Thermogravimetric analysis (TGA)

An analyser (Mettler Toledo, Stare system Mettler thermobalance) was used to examine the thermal degradation behaviour of PP/LDPE blends and their components. The samples, weighing 5-8 mg (film), were heated from 20 to 600 °C at a heating rate of 10 °C/min, under nitrogen atmosphere.

IV.3.4. X-ray diffraction (XRD)

The X-ray diffraction (XRD) pattern for LDPE, PP and their blends was recorded on the Rigaku miniflex Benchtop X-ray Diffractometer system operating at 30 kV and 15 mA current with Cu $K\alpha$ radiation (λ = 1.5418Å). The diffracted intensities were recorded in the 2θ angles from 10° to 40°.

IV.3.5. Scanning electron microscopy (SEM)

Using a field emission scanning electron microscope (model Supra 40 VP, Zeiss, Germany) set to an accelerating voltage of 1 KV, the morphology of the blend's fracture surface was investigated. The samples were cryogenically cracked after being submerged in liquid nitrogen. All surfaces were then covered in gold to enhance image quality and eliminate electrostatic discharge.

IV.3.6. Mechanical properties

The most fundamental of all mechanical tests are without a doubt the tensile test. It is employed to ascertain fundamental mechanical characteristics, such as the elastic modulus, strength at break, and elongation at break. A ZWICK Roell Z100 universal instrument was used to conduct tensile testing in accordance with ASTM D882. The samples were examined at a cross-head

speed of 3 mm/min under standard temperature and pressure conditions. We tested the tensile strength, Young's modulus, and elongation at break.

IV.3.7. Environmental stress cracking resistance (ESCR)

The ESCR was performed for LDPE/PP blends in a 10% aqueous solution of IGEPAL CA-630 according to ASTM D1693 using the following procedure **(In Figure IV.2)**:

1-Make a 3.15mm thick plate using a press.

2-Cut 10 specimens of (38.1 x 12.7mm) for each analysis.

3-Maintain the specimens at 23°C for 24h.

4-Gauge the surface of each specimen with a (19 x 0.5 x 0.5 mm^3) blade perfectly in the center.

5-Introduce the specimens in the U-shaped specimen holder so that the incision is facing outwards.

6-Immerse the specimen holders with the 10 specimens in the test tube containing the reagent (IGEPAL) previously maintained at 50°C by immersion in the thermostatic bath.

7-Monitor the moment at which each specimen breaks and note the results up to 50%.

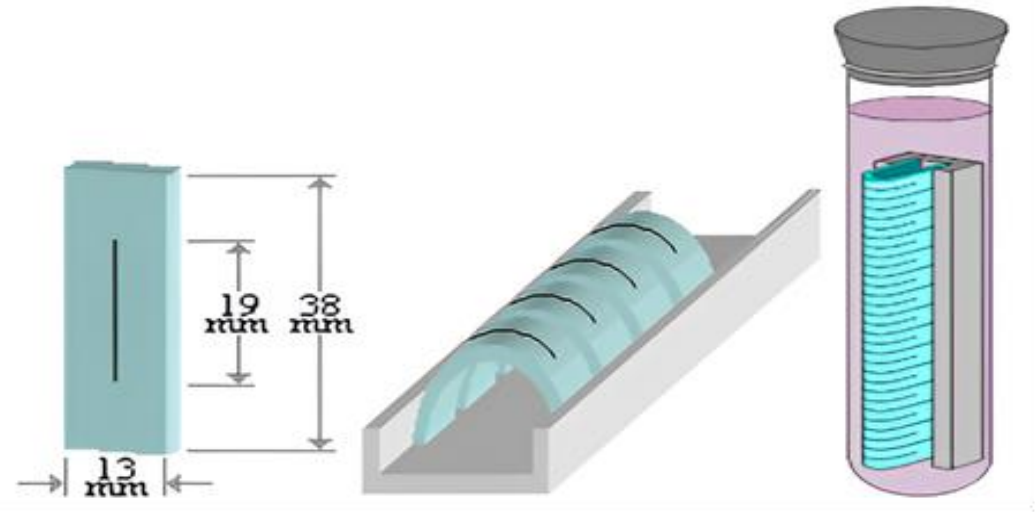

Figure IV.2. Strip bent test based on ASTM D1693.

IV.3.8. Scanning electron microscopy after ESCR tests

The samples microstructure was investigated using a NeoScope JCM-5000 scanning electron microscope and an accelerating voltage of 10 kV. The material surfaces of the observed samples were prepared by cryogenic fracturing in liquid nitrogen to prevent plastic deformation. surfaces were subsequently coated with gold to enhance picture resolution and prevent electrostatic charges. After ESCR tests, the failed samples were gathered for further scanning electron microscopy examination of the fracture surface (SEM). Sample morphologies were examined by (1) inspection of the fracture surface of the unsuccessful samples to determine the morphology of the crack surface, and (2) cross-sectional image of the ESCR using microtome sectioning in a direction parallel to the crack direction.

References

[1] Mofokeng TG, Ray SS, Ojijo V. Influence of selectively localised nanoclay particles on Appl Radiat Isot non-isothermal crystallisation and degradation behaviour of PP/LDPE blend composites. Polymers (Basel), 2018.

[2] Bioki, H. A., Mirbagheri, Z. A., Tabbakh, F., & Mirjalili, G. Effect of crystallinity and irradiation on thermal properties and specific heat capacity of LDPE & LDPE/EVA. Applied Radiation and Isotopes, 2012.

[3] Na B, Wang K, Zhang Q, et al. Tensile properties in the oriented blends of high-density polyethylene and isotactic polypropylene obtained by dynamic packing injection molding. Polymer (Guildf), 2005 .

Chapter V. Results and discussions

V. Results and discussions

V.1 Fourier transform infrared spectroscopy (FTIR)

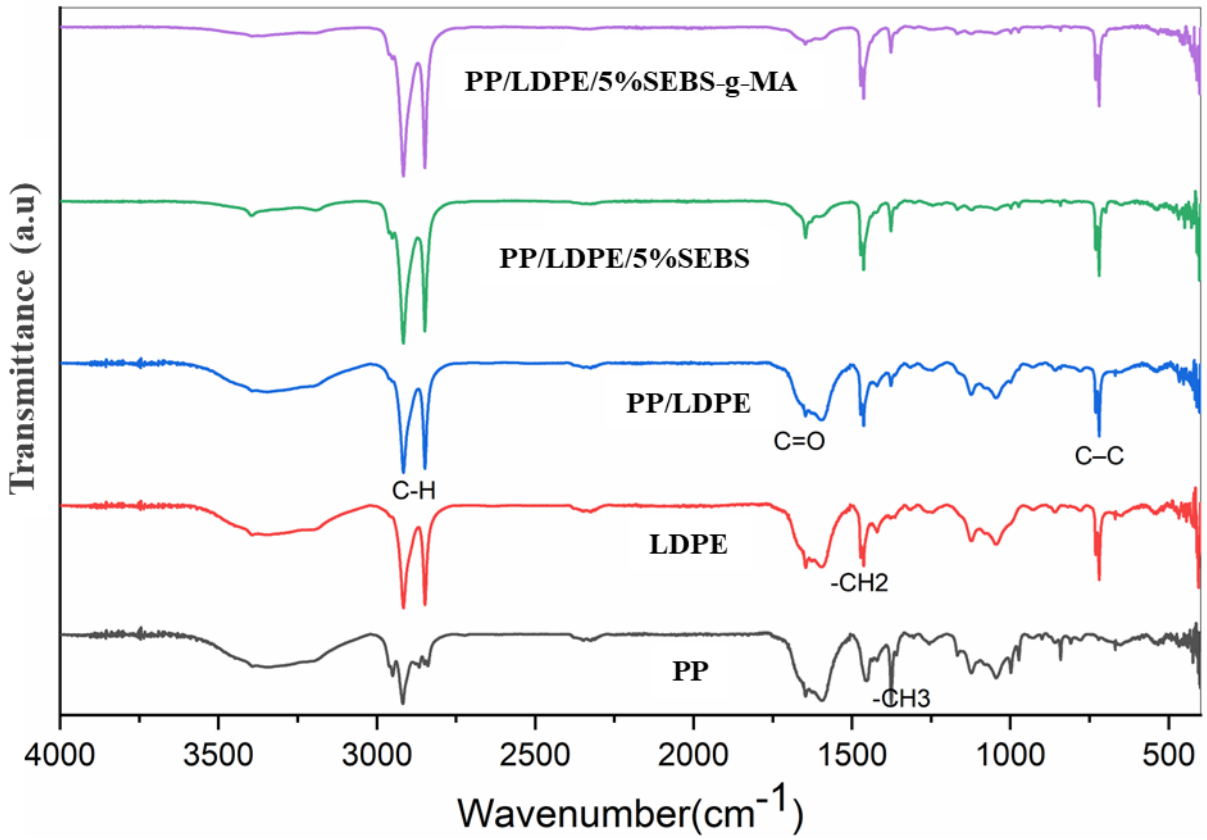

Figure V.1. FTIR spectroscopy of PP, LDPE, their blends without and with compatibilizers.

FTIR was used to analyze the functional groups present in PP/LDPE blends without and with the compatibilizer SEBS (styrene-ethylene/butylene-styrene) and SEBS-g-MA (SEBS grafted with maleic anhydride). **Figure V.1** shows the main chemical bonds detected by FTIR spectroscopy of the blends studied. PP and LDPE show characteristic peaks for specific C-H stretch (2918 cm^{-1} and 2839 cm^{-1}) (PP) and C-H (2918 cm^{-1} and 2847 cm^{-1}) (LDPE). The bending vibrations of $-CH_2$ and $-CH_3$ are 1458 cm^{-1} (PP) and 1374 cm^{-1} (PP), respectively, and that of $-CH_2$ is 1462 cm^{-1} (LDPE). The most important characteristic vibrational peak of LDPE is at 729 cm^{-1}, which is due to the vibrations of C–C bonds. As expected no disappearance of major peaks or appearance of new peaks in the FTIR spectrum of PP/LDPE blend is observed due to the lack of interaction or reaction between the two polymers [1].

In general, polyolefins are very susceptible to oxidation [2]. For PP, LDPE, and their combinations, faint and wide absorption peaks at 1650 cm^{-1} are seen. These peaks are due to

the carbonyl (C=O) group's stretching vibration. Therefore, environmental oxidation must be to blame. The absorption of the carbonyl group diminishes with the addition of the SEBS (styrene ethylene/butylene styrene) and SEBS-g-MA (SEBS grafted with maleic anhydride) compatibilizers, weakening the peak at 1650 cm^{-1}. Therefore, it can be inferred that adding the MA group to PP causes a contact between the tertiary hydrogen of PP and the carbonyl group of the MA in the SEBS-g-MA, which in turn lowers PP and LDPE oxidation in the environment [3].

V.2 Differential Scanning Calorimetry (DSC)

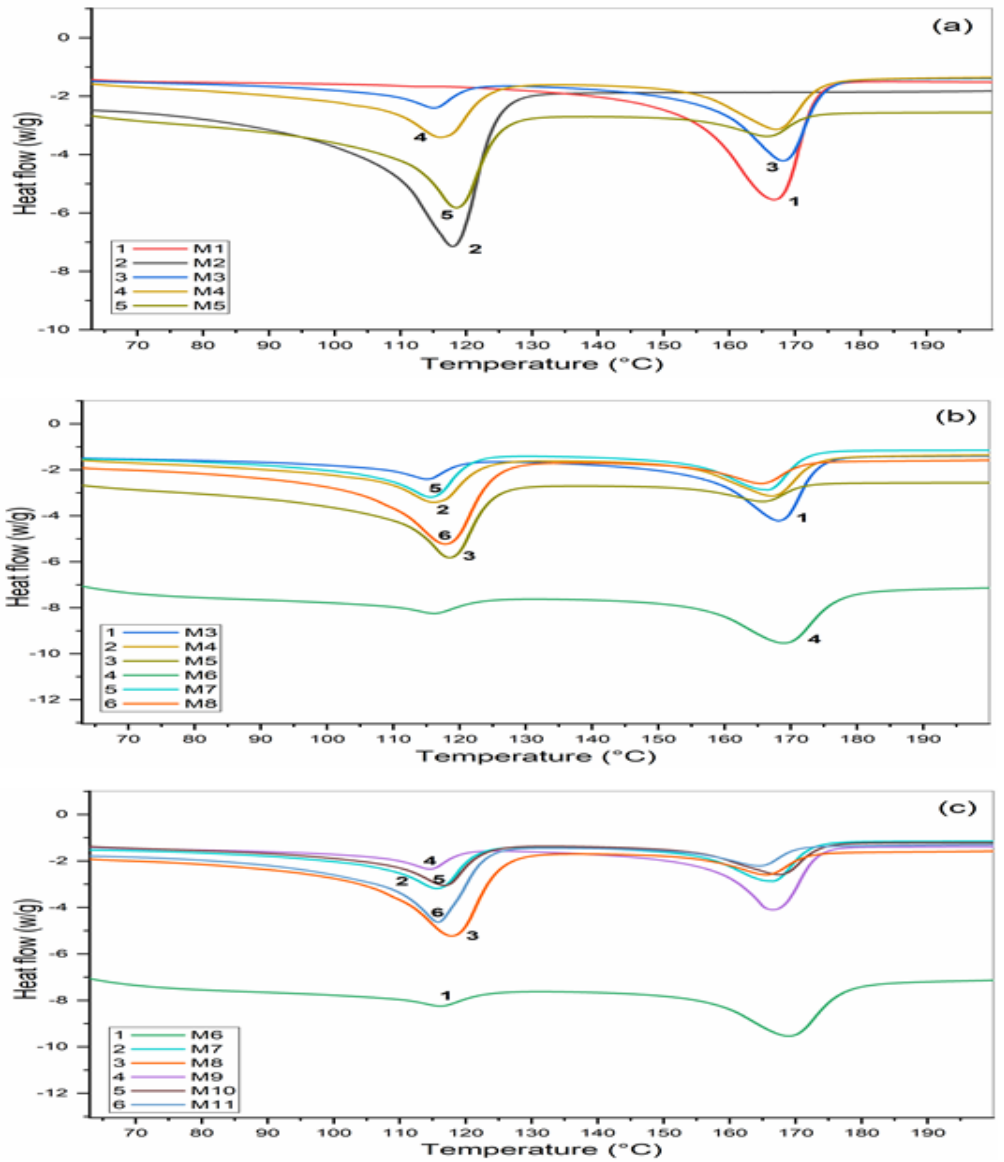

Figure V.2. DSC spectra of: (a) blends. (b) blends with SEBS. (c) blends with SEBS-g-MA.

Figure V.2 depicts the differential scanning calorimetry (DSC) thermograms of the blends, including polypropylene (PP) and low-density polyethylene (LDPE), both in the absence and the presence of the compatibilizers styrene-ethylene-butylene-styrene grafted with maleic anhydride (SEBS-g-MA) and styrene-ethylene-butylene-styrene (SEBS). **Figure V.2 (a)** demonstrates that the values of the melting temperature (T_m) of pure PP and LDPE, are 162.7°C and 112.1°C, respectively. The blends exhibit two distinct melting peaks, which correspond to the melting behaviors of PP and LDPE.

The enthalpies, calculated from DSC thermograms, of PP, LDPE, and their blends with and without compatibilizers are shown in **Figure V.2**. Also shown in **Table V.1**, are the crystallinities of PP and LDPE obtained using Eqs. (1) and (2), in the blends with and without compatibilizers, this table shows that the enthalpy of melting of PP/LDPE blends decreases with increase of LDPE content. This behavior is due to the fact that adding low-density polyethylene (LDPE) to PP leads to a decline in crystallinity.

Table V.1. DSC data of PP, LDPE, and their blends.

Material	PP Tm (°C)	LDPE Tm (°C)	PP ΔHf (J/g)	LDPE ΔHf (J/g)	PP Xc (%)	LDPE Xc (%)
M1	162.7	-	77.2	-	37	-
M2	-	112.1	-	113.2	-	46
M3	163.9	112.3	59.1	8.8	35	15
M4	161.9	112.3	39.1	41.3	37	28
M5	164.5	112.6	12.5	78.9	30	34
M6	161.6	111.2	60.2	9.4	36	16
M7	163.3	112.8	34.5	36.1	33	25
M8	163.7	111.8	12.0	79.6	29	34
M9	164.3	112.1	57.9	9.6	35	16
M10	162.2	111.9	37.1	42.6	35	29
M11	163.8	112.5	11.4	74.9	27	32

Table V.1 illustrates the impact of blending on crystallinity. The decrease in the melting enthalpy of PP is observed when the concentration of LDPE is increased. This behavior is ascribed to the decrease in the amount of PP in the blend. However, when incorporating 20 weight percent of LDPE into PP, a marginal increase in the crystallinity of PP is noted. The presence of PP in LDPE blends reduces the enthalpy of fusion of LDPE, thereby leading to a

drop in the crystallinity of LDPE. Nevertheless, incorporating 20 weight percent polypropylene (PP) into low-density polyethylene (LDPE) results in a marginal enhancement of LDPE's crystallinity. The observed phenomenon may be attributed to the presence of this low content of PP enhances the nucleation of LDPE, resulting in increased crystallinity [4]. Incorporating 5%-SEBS-g-MA into the PP20/LDPE blend results in a marginal reduction in the crystallinity of both PP and LDPE. The estimated lowest crystallinity of polypropylene (PP) in the blends was determined to be 27%. This value was obtained for a blend composition consisting of 17.5% PP, 77,5% low-density polyethylene (LDPE), and 5% of a maleic anhydride-grafted styrene-ethylene-butylene-styrene (SEBS-g-MA) copolymer.

V.3 Thermogravimetric Analysis (TGA)

The TGA curves for PP, LDPE, and PP/LDPE blends without and with SEBS and SEBS-g-MA reveal various degradation patterns in **Figure V.3**. **Table V.2** gives an overview of the specimens' decomposition temperatures. Given that PP's T5% and T50% values are lower, LDPE is more thermally stable than PP. When compared to LDPE, every second tertiary carbon in the main chain of PP is more vulnerable to attack, which accounts for its inferior thermal stability [5]. The amount of LDPE enhances the thermal stability of PP, although the temperatures of the mix are comparable to those of pure polymers. This finding suggests that the addition of the more thermally stable LDPE weight percentage will increase the thermal stability of PP. SEBS is more thermally unstable than PP and LDPE. The addition of MA groups to the SEBS chains is said to reduce the thermal stability of SEBS-g-MA in comparison to pure SEBS. In contrast to **Figure V.3(a)** and **V.3(b)**, **Figure V.3(C)** in the 20PP/80LDPE combination produced the greatest outcomes for us. Compared to the blends, the incorporation of SBES was reduced marginally. Unlike SEBS-g-MA, which marginally rises in comparison to SEBS.

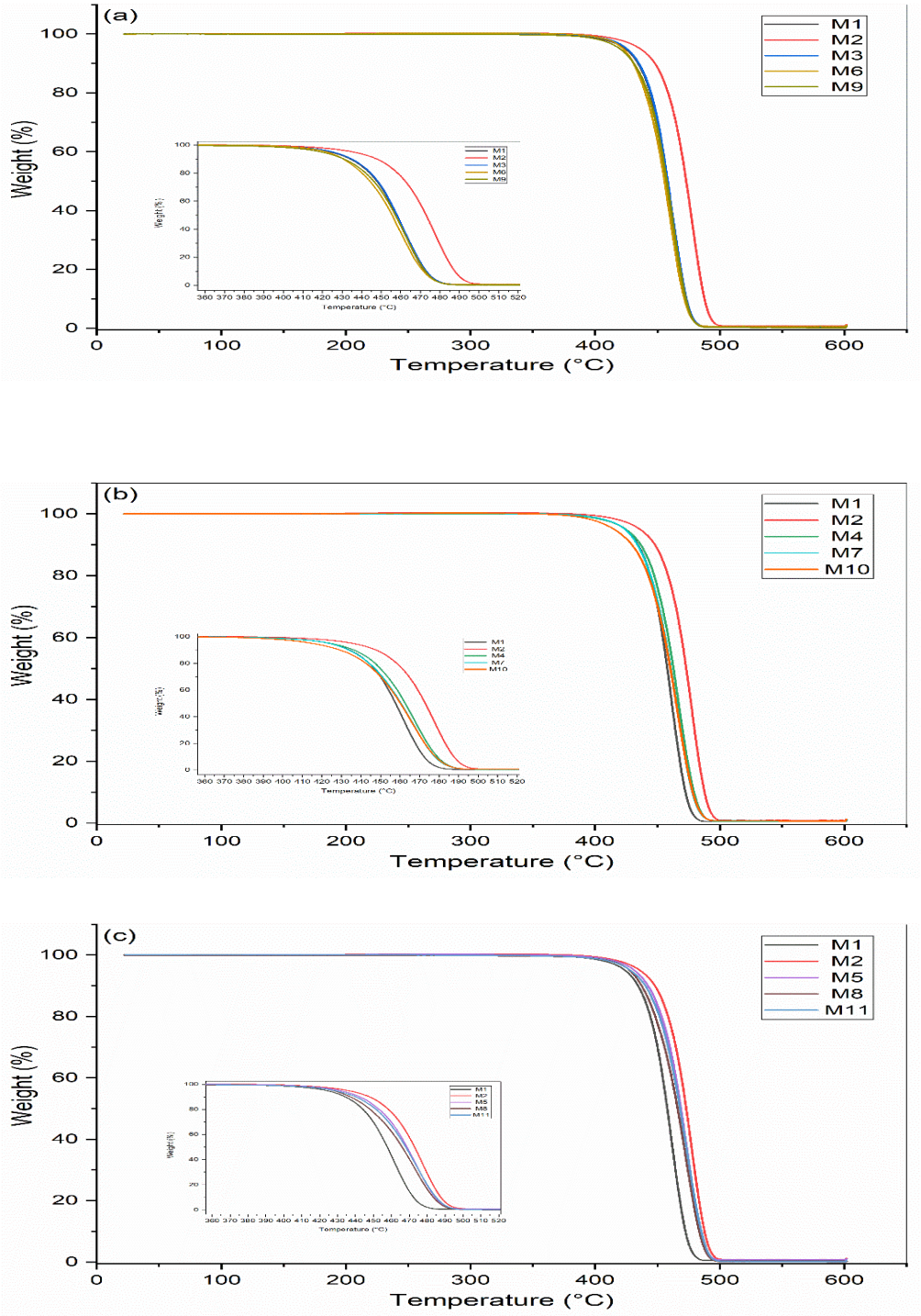

Figure V.3. ATG thermograms of PP, LDPE, and PP/LDPE blends without and with SEBS and SEBS-g-MA. (a) 80PP/20LDPE, (b) 50PP/50LDPE, (c) 20PP/80LDPE.

Table V.2. TGA data of virgin PP, LDPE and their blends.

Samples	T5%(°C)	T50%(°C)
M1	424.01	457.75
M2	436.05	472.98
M3	425.44	458.01
M4	424.65	462.78
M5	431.45	468.74
M6	422.26	455.63
M7	423.94	460.26
M8	427.58	466.06
M9	419.61	457.25
M10	415.38	460.15
M11	428.45	468.05

V.4 X-ray diffraction (XRD)

Figure V.4 shows X-ray diffraction patterns for LDPE, PP, and their mixes in terms of intensity 2θ measured in the 2θ range from 10 to 40. PP presents five diffraction picks, which correspond to the α-form typical of PP. The 2θ grating with the corresponding crystal lattices is 14.35° (110), 17.12° (040), 18.85° (130), 21.45° (111) and 22.15° (041) [6]. The characteristic peaks for LDPE are 21.7° (110) and 23.9° (200) [2]. Most of the peaks in the PP/LDPE blends (M3, M4, M5) have identical crystal lattices to PP. With the integration of SEBS and SEBS-g-MA generally, a modest rise in the intensity of the 14.35° (110) peak was seen in **Figure V.4(a)**. Due to a reduced proportion of SEBS and SEBS-g-MA, the integration has little effect on the LDPE/PP binary blend's crystal structure.

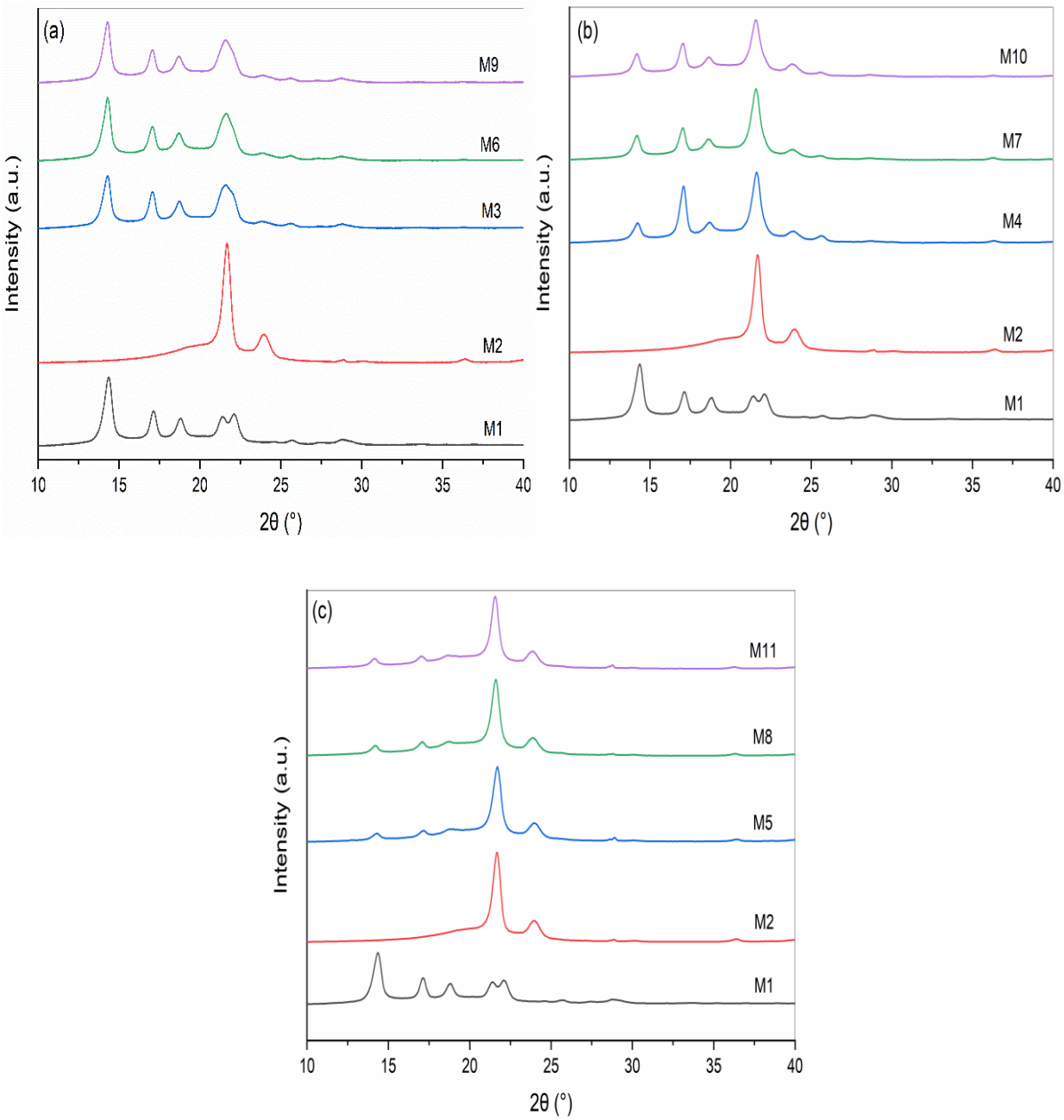

Figure V.4. X-ray diffraction (XRD) curve of PP, LDPE, and their blends.

V.5 Scanning electron microscopy (SEM) analysis

Figure **V.5**, **V.6**, and **V.7** show scanning electron microscopies (SEM) which can provide information on the morphology and interfacial adhesion of PP/LDPE blends with SEBS (styrene-ethylene/butylene-styrene) and SEBS-g-MA (SEBS grafted with maleic anhydride) as compatibilizers.

The PP and LDPE components exhibit a coarse morphology and phase separation in the SEM images of the PP and LDPE blends without compatibilizers in **Figure V.5**. Due to the high interfacial tension that exists between the blends, there is poor interfacial adhesion between

the phases, which results in the creation of voids and the detachment of the dispersed particles, which confirms poor adhesion at the interface between the homopolymers [7].

SEM micrographs may indicate enhanced interfacial adhesion between the PP and LDPE phases with the addition of SEBS (**Figure V.6**), as well as a more uniform distribution of the blend's constituent parts. By serving as a link between the PP and LDPE phases, the SEBS compatibilizer reduces the size of the scattered phase domains and produces a finer morphology. It is possible to further enhance the blend's shape and interfacial adhesion when SEBS-g-MA is added as a compatibilizer (**Figure V.7**). Due to the interaction between the PP and LDPE matrix and the maleic anhydride of SEBS-g-MA, the components may be distributed even more uniformly and the interfacial adhesion may be improved.

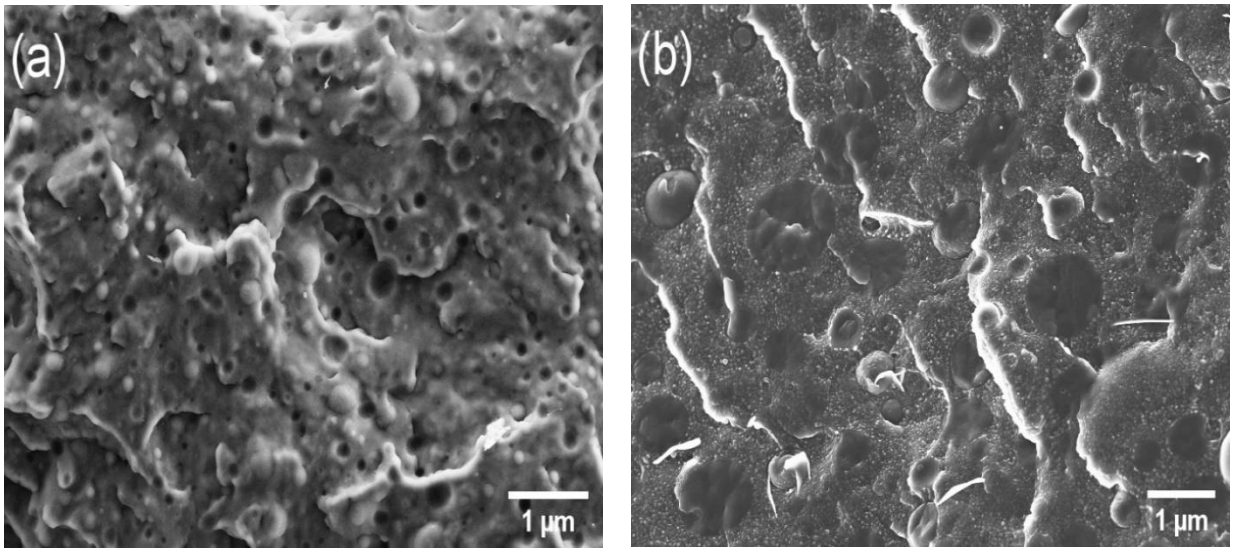

Figure V.5. Scanning electron microscope (SEM) images of PP/LDPE blends: (a) M3 (PP80/LDPE20), (b) M5 (PP20/LDPE80).

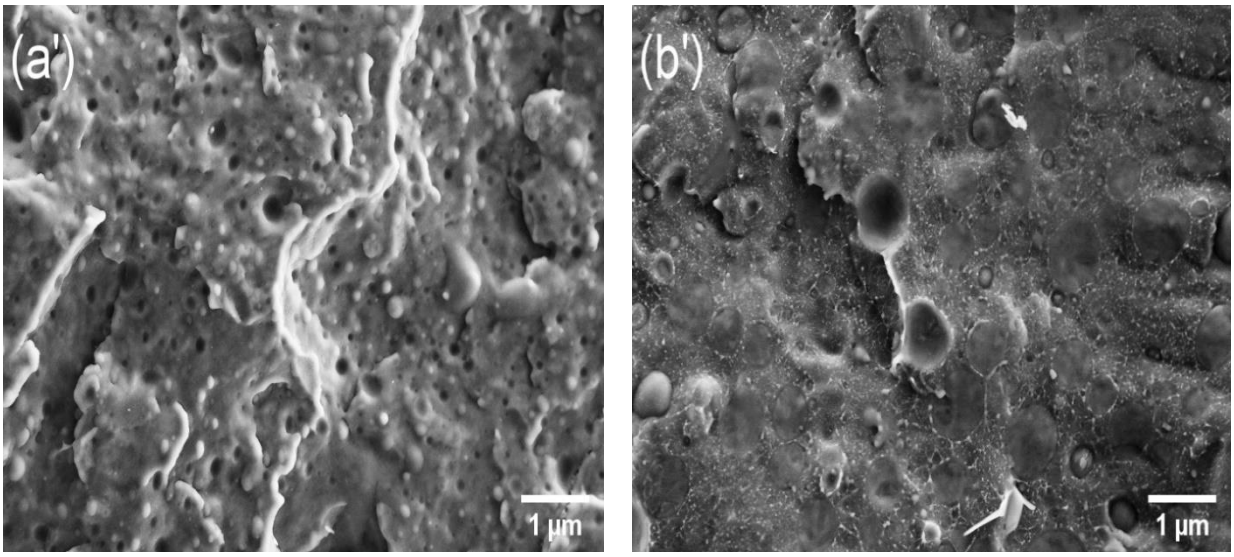

Figure V.6. Scanning electron microscope (SEM) images of PP/LDPE blends with 5% SEBS: (a') M6 (PP80/LDPE20/SEBS), (b') M8 (PP20/LDPE80/SEBS).

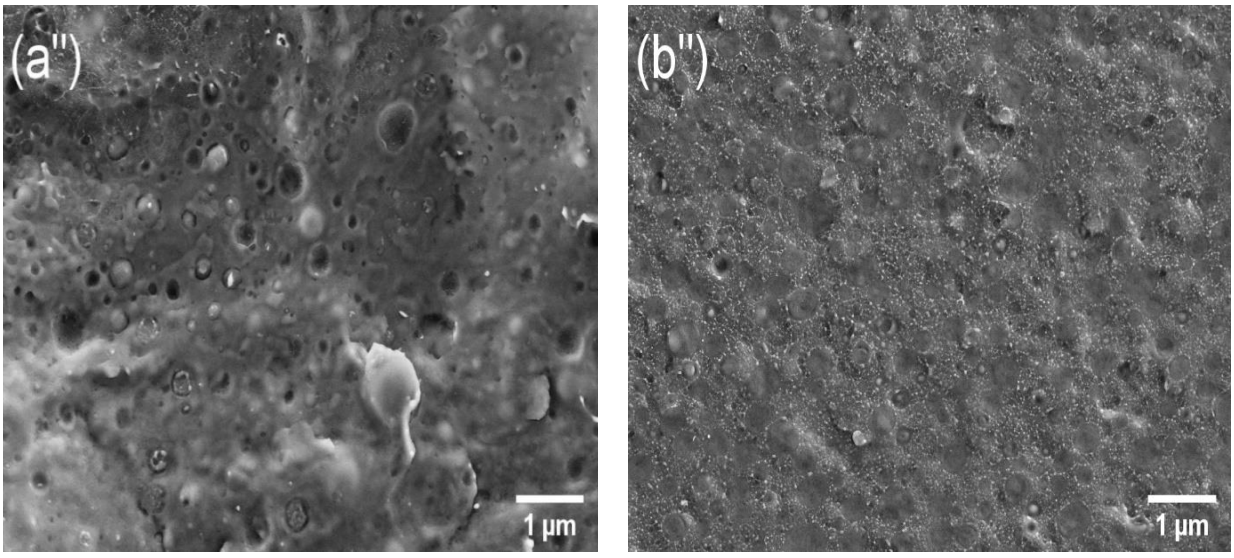

Figure V.7. Scanning electron microscope (SEM) images of PP/LDPE blends with 5% SEBS-g-MA: (a'') M9 (PP80/LDPE20/SEBS-g-MA), (b'') M11 (PP20/LDPE80/SEBS-g-MA).

V.6 Mechanical Properties

The strength at break, elongation at break, and Young's modulus are shown as a function of the compound compositions in **Figures V.8**, **V.9**, and **V.10**, respectively. The effects usually associated with impact modification are reduced elastic modulus and tensile strength and increased elongation at break [8]. Copolymers are compatible with thermoplastics and thus are frequently used for impact modification and improvement in stress–crack resistance [9]. **Figure V.8**. illustrates the tensile strength of LDPE/PP without and with the incorporation of

SEBS and SEBS-g-MA. The addition of LDPE to PP reduces the tensile strength value, so that the tensile strength of the PP/LDPE blends were between the values of the pure homopolymers. The addition of SEBS, and SEBS-g-MA to the PP/LDPE blends reduces the tensile strength values by 20 to 33%. This suggests that the tensile strength of compatibilized blends is determined not only by the interfacial adhesion, but also by the matrix strength, which is strongly affected by the amount of compatibilization [10].

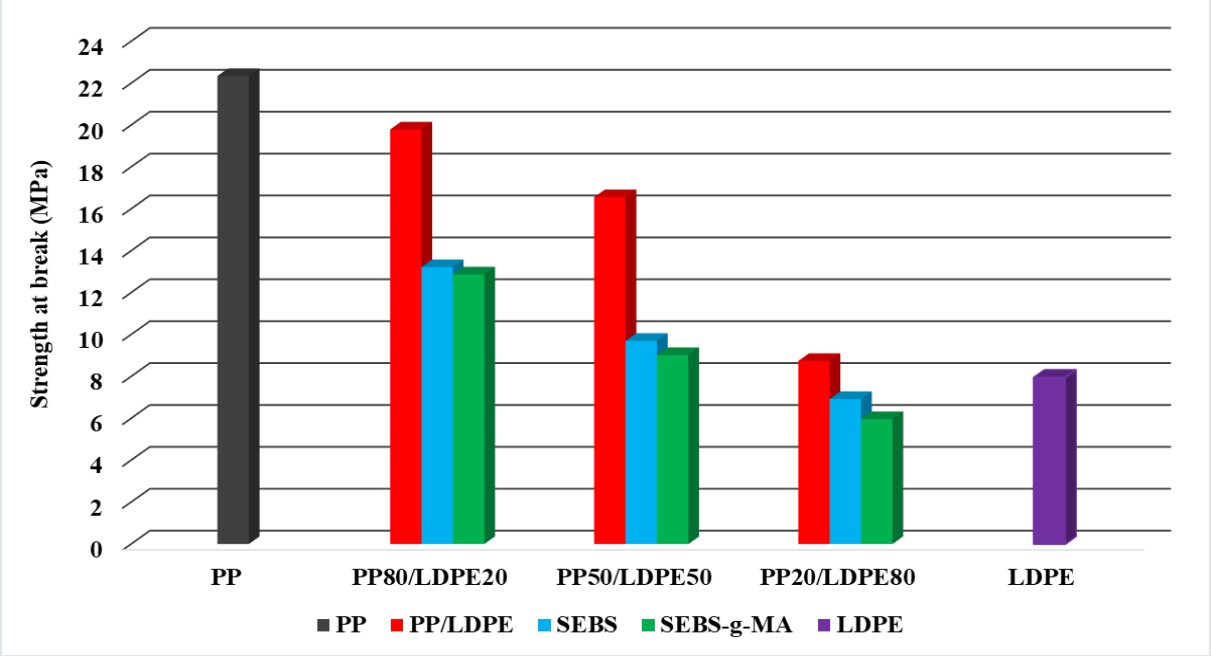

Figure V.8. strength at break of PP/LDPE, and their blends.

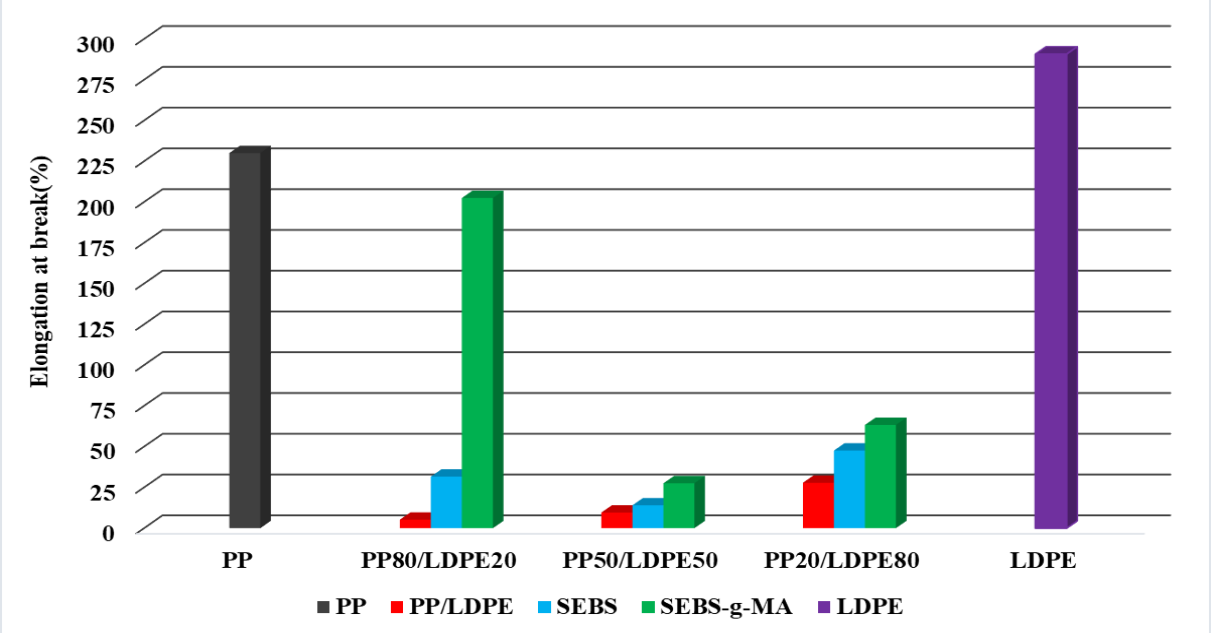

Figure V.9. Elongation at break of PP/LDPE, and their blends.

The elongation at break for the blends is shown in **Figure V.9**. The PP/LDPE 80/20, 50/50 and 80/20 blends have lower elongation at break than the pure polymers. The result of very low elongation at break in the 50/50 blend is most probably a consequence of low interfacial adhesion, i.e. high interfacial tension, indicating the incompatibility of the two polymers. These properties can be explained as follows. It is well established that at temperatures above the crystallization melting points of the two polymers, the LDPE and PP chains segregate into distinct micro domains, with LDPE exhibiting greater clustering [11]. The clustering of LDPE and PP is due to incompatibility between the LDPE and PP chains [12]. This unfavorable clustering increases with the number of individual polymers in the blend [13]. In all PP/LDPE blends, the addition of SEBS or SEBS-g-MA improves the values of the elongation at break from 4 to 39%. Similarly, a maximum value of elongation at break was observed in the 80/20 PP/LDPE blend with the incorporation of SEBS-g-MA at 190%.

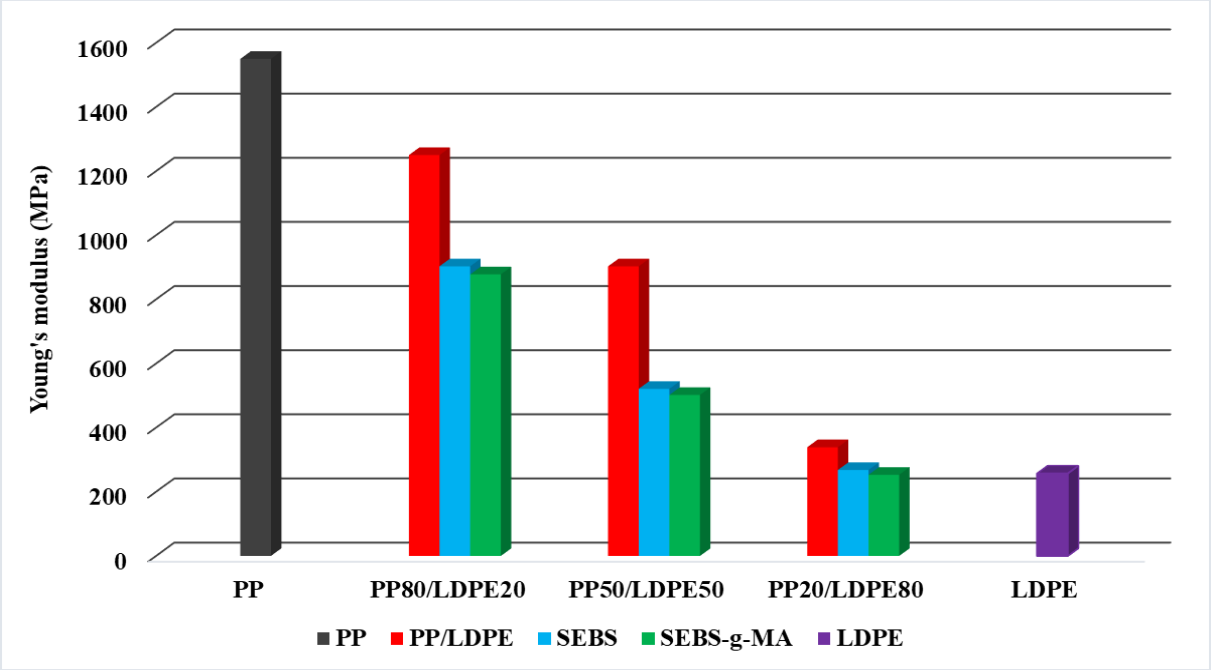

Figure V.10. Young's modulus of PP/LDPE, and their blends.

It is generally known that Young's modulus of a rigid polymer can be reduced by the addition of a soft polymer. A decrease in the Yonug's modulus of a polymer can also be caused by a decrease in crystallinity. since an increase the volume fraction of the amorphous regions in the blend [4], which are more mobile than the crystalline regions above the glass transition temperature. This result is confirmed in **Figure V.10** which shows a decrease with the addition of LDPE from 1150 to 329 MPa. Therefore, LDPE provides flexibility to PP. The

addition of SEBS and SEBS-g-MA decreases the Young's modulus values by 22 to 270 MPa, which substantially improves the flexibility of PP/LDPE blends.

V.7 Environmental Stress Cracking Resistance (ESCR)

This test consists in determining the susceptibility to develop a crack under the conditions of the test, by identifying the moment at which 50% of the samples present visible ruptures. The failure times of the different samples are depcited in **Table V.3**. Samples M4, M5, M7, M8, and M10 failed by introducing the specimens into the "U" shaped holder, as indicated by **Figure IV.2,** we found that small cracks develop on both sides parallel to the notch and lead eventually to catastrophic failure.

Table V.3. ESCR in terms of failure time of the various blend compositions.

Formulation	ESCR (h)
M1	864
M2	5
M3	770
M4	Failed
M5	Failed
M6	600
M7	Failed
M8	Failed
M9	> 1000
M10	Failed
M11	6

The specimens M3, M6, and M9 with an increase in ESCR 770h, 600h, and > 1000h respectively compared to M11 = (6h) may be due to the high impact resistance and high ESCR of the Polypropylene phase 864h, a by M9 which gave good results with incorporation of SEBS-g-MA which plays the role a compatibilizing agent.

V.8 Scanning Electron Microscopy After ESCR Tests

Scanning electron microscopy (SEM) was applied to study the morphology of LDPE/PP blends, **Figure V.12** and **V.13** show the morphology of samples M3 and M6 before and after the incorporation of IGEPAL CA 630 which resulted in visible breaks in the ESCR.

The SEM micrographs in **Figure V.12** clearly indicate that the LDPE/PP blends (M3, M6) have a two-phase morphology showing the immiscibility of the LDPE and PP used, in the compositional range studied. In combination with the DSC results, it can be concluded that the difference in the crystallization rates of LDPE and PP, leads to multiple melting peaks and phase separation in the SEM pictures. Once the ESCR test was completed, the failed samples were collected for further analysis of the crack surface by SEM.

Figure V.13 shows the fracture surface of the failed samples to obtain the morphology of the crack surfaces. Samples M3 and M6 have high ESCR resistance, which observed that the size of fibrillation inside the crack surface seems large due to the effect of IGEPAL CA 630 on the treatment zone during crack propagation. Thus, the main controlling factor of the ESCR property in blends is the fibrillation, i.e., the density of the bond chains [14].

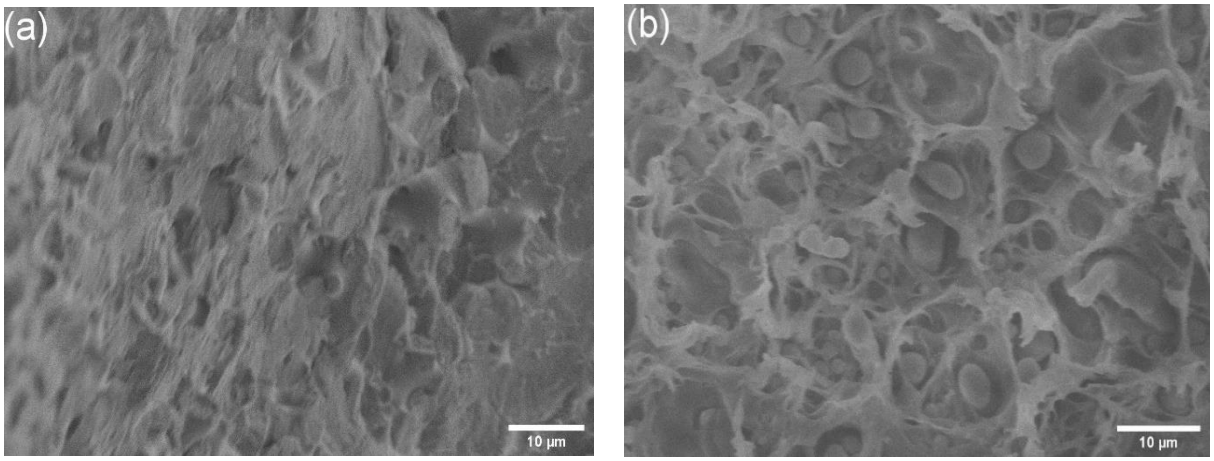

Figure V.12. SEM micrographs of the PP/LDPE blends: a: M3 (PP80/LDPE20), b: M6 (PP80/LDPE20/SEBS).

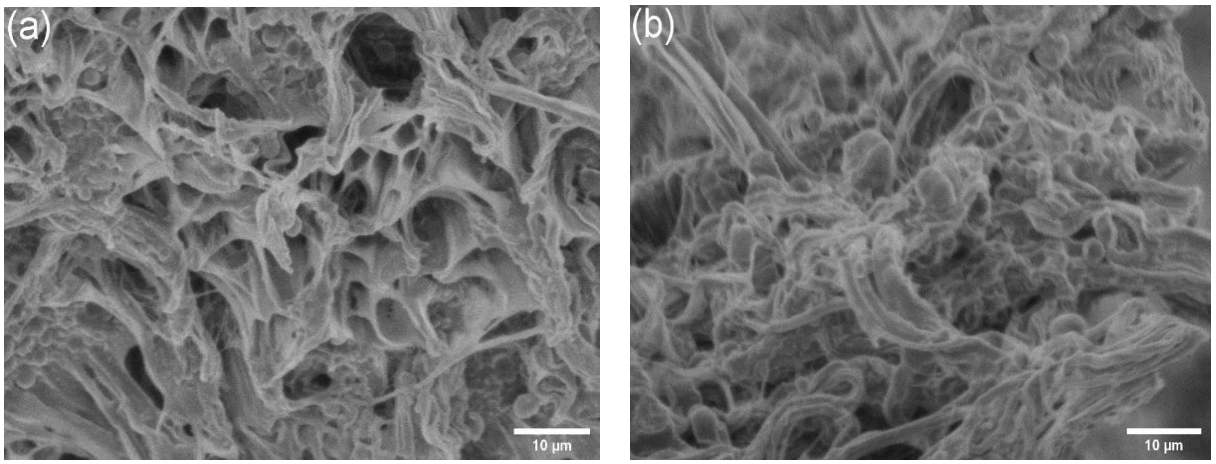

Figure V.13. SEM micrographs of the crack surfaces of the failed samples. (a: M3, b: M6,).

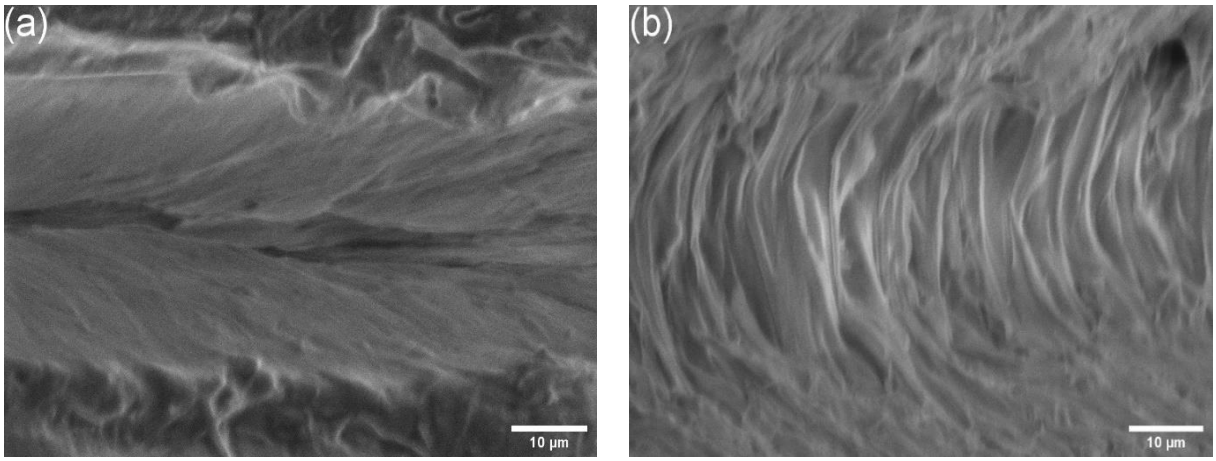

Figure V.14. SEM micrographs of the region parallel to the crack direction at different hours (a: 0h, b: 1000h,) for the sample M9.

Figure V.14 (a, b) is a high magnification image of the region parallel to the crack direction at different times (0h, 1000h) for sample M9. One notes from these micrographs the difference between a and b which results from the incorporation of IGEPAL forming a large void that the material was not stretched enough to cause failure. Furthermore, M9 surprisingly did not show any failure during the ESCR test at 50°C. Under external stress, stress concentration and stress enhancement by superposition of local stress fields are formed between the particles [15]. We can conclude that the incorporation of SEBS-g-MA decreased the local stress fields, which act as an accounting agent.

References

[1] Dikobe D.G, Luyt A.S. Investigation of the morphology and properties of the polypropylene/low-density polyethylene/wood powder and the maleic anhydride grafted polypropylene/low-density polyethylene/wood powder polymer blend composites, J. Compos. Mater, 2017.

[2] Borovanska I, Dobreva T, Benavente R, Djoumaliisky S, Kotzev G. Quality assessment of recycled and modified LDPE/PP blends. J. Elastomers Plast, 2012.

[3] Al-Juhani A.A, Suleiman M.A. Study of the Effect of EPDM Structure on the Compatibility of PP/LDPE Blends. Arab. J. Sci. Eng, 2012.

[4] Mofokeng TG, Ojijo V, Ray SS. The Influence of Blend Ratio on the Morphology, Mechanical, Thermal, and Rheological Properties of PP/LDPE Blends. Macromol Mater Eng, 2016.

[5] Mofokeng T.G, Ray S.S, Ojijo V. Structure–property relationship in PP/LDPE blend composites: The role of nanoclay localization. J. Appl. Polym. Sci, 2018.

[6] Nishino T, Matsumoto T, Nakamae K. Surface structure of isotactic polypropylene by X-ray diffraction, Polym. Eng. Sci, 2000.

[7] Penava N.V, Rek V, Houra I.F. Effect of EPDM as a compatibilizer on mechanical properties and morphology of PP/LDPE blends. J. Elastomers Plast, 2013.

[8] Khait K. Advanced recycling technology for unsorted plastic waste. J Vinyl Addit Technol, 1996.

[9] Chanda M, Roy SK. Plastics Technology Handbook. CRC Press, 2006.

[10] Chen B. Compatibilization effects of block copolymers in high density polyethylene/syndiotactic polystyrene blends. Polymer (Guildf), 2002.

[11] Choi P, Blom HP, Kavassalis TA, Rudin A, Immiscibility of poly(ethylene) and poly(propylene): A molecular dynamics study. Macromolecules, 1995.

[12] Rajasekaran JJ, Curro JG, Honeycutt JD. Theory for the Phase Behavior of Polyolefin Blends: Application to the Polyethylene/Isotactic Polypropylene Blend. Macromolecules, 1995.

[13] Jose S, Aprem A., Francis B, et al. Phase morphology, crystallisation behaviour and mechanical properties of isotactic polypropylene/high density polyethylene blends. Eur Polym J, 2004.

[14] Rose LJ, Channell AD, Frye CJ, Capaccio G. Slow crack growth in polyethylene: A novel predictive model based on the creep of craze fibrils. J Appl Polym Sci, 1994.

[15] Borisova B, Kressler J. Environmental Stress-Cracking Resistance of LDPE/EVA Blends. Macromol Mater Eng, 2003.

General Conclusions

General conclusion

Several analytical techniques were used to examine the compatibilizer addition of SEBS (styrene-ethylene/butylene-styrene) and SEBS-g-MA (SEBS grafted with maleic anhydride) to PP/LDPE blends. The compatibilizers SEBS and SEBS-g-MA enhanced the morphology and interfacial adhesion of PP/LDPE blends, according to SEM studies. The compatibilizers' effectiveness on the PP/LDPE blends was validated by FTIR testing. The addition of SEBS and SEBS-g-MA reduces the absorption of the carbonyl group. This lowers the peak's elevation by 1650 cm-1. Overall, using FTIR, TGA, XRD, and SEM approaches in combination allows for a full knowledge of the chemical, thermal, and morphological properties of the blends and may aid in the progression of innovative polymeric materials with properties tailored to certain applications.

The molecular interaction between PP, LDPE, and SEBS-g-MA was studied. According to DFT analysis, which contends that the compatibilizer agent serves as an electron donor for PP and LDPE, the inclusion of SEBS-g-MA increases the interaction energies between PP and LDPE. This conclusion is consistent with MDS results.

Environmental stress cracking is a major concern when designing products exposed to chemical environments. The ESC resistance of LDPE and PP are different. Although PP is more resistant to ESC than LDPE, the ESC resistance of the blend is affected by the incorporation of LDPE microdomains in PP. The blend cracks and develops microvoids in external stress due to stress concentration. This study investigated the impact of (IGEPAL CA 630) on the environmental stress cracking resistance of polypropylene and low-density polyethylene blends with varying weight fractions, both with and without the addition of compatibilizers (SEBS and SEBS-g-MA). The research found that while PP inherently possesses better ESC resistance than LDPE, increasing the PP content improves the time to failure in the ESCR test.

Furthermore, incorporating SEBS-g-MA into the blend significantly enhances the flexibility and ESCR performance of PP/LDPE blends with specific weight fractions. The compatibilizer SEBS-g-MA has the potential to make PP/LDPE useful in many applications where the material is subjected to significant environmental stress.

Perspectives

Perspectives

Several research aspects need deep investigation for future research. In this regard, the following additional investigations could, therefore, be recommended:

Experimental and theoretical study of the effect of environmental stress cracking with other active tension and aggressive milieus with the change of polymers according to use for industrial applications (storage of concentrated solutions).

***ABSTRACT**:*
This thesis investigates the impact of SEBS and SEBS-g-MA as compatibilizers for polypropylene (PP) and low-density polyethylene (LDPE) blends, along with the influence of IGEPAL CA 630 on environmental stress crack resistance (ESCR). The study involves theoretical calculations using molecular dynamics, and experimental analyses such as X-ray diffraction, differential scanning calorimetry, thermogravimetry, and scanning electron microscopy. The addition of SEBS and SEBS-g-MA enhances the morphological and interfacial adhesion of the blends, reducing carbonyl group absorption and improving rupture time in ESCR tests. Molecular dynamics simulations and density functional theory confirm the compatibilizing effects of SEBS and SEBS-g-MA. The inclusion of SEBS-g-MA particularly enhances flexibility and ESCR performance in PP/LDPE blends with specific weight fractions, suggesting that compatibilizers can enhance the properties of these blends in various applications.

***Keywords** : Polyolefin blends, compatibilization, MD simulation, Environmental Stress Crack Resistance.*

***RÉSUMÉ** :*

Cette thèse étudie l'impact du SEBS et du SEBS-g-MA en tant que compatibilisants pour les mélanges de polypropylène (PP) et de polyéthylène basse densité (LDPE), ainsi que l'influence de l'IGEPAL CA 630 sur la résistance à la fissuration sous contrainte dans l'environnement (ESCR). L'étude comprend des calculs théoriques utilisant la dynamique moléculaire et des analyses expérimentales telles que la diffraction des rayons X, la calorimétrie différentielle à balayage, la thermogravimétrie et la microscopie électronique à balayage. L'ajout de SEBS et de SEBS-g-MA améliore l'adhésion morphologique et interfaciale des mélanges, réduisant l'absorption du groupe carbonyle et améliorant le temps de rupture dans les tests ESCR. Les simulations de dynamique moléculaire et la théorie de la fonctionnelle de la densité confirment les effets de compatibilité du SEBS et du SEBS-g-MA. L'inclusion du SEBS-g-MA améliore particulièrement la flexibilité et la performance ESCR dans les mélanges PP/LDPE avec des fractions de poids spécifiques, ce qui suggère que les compatibilisants peuvent améliorer les propriétés de ces mélanges dans diverses applications.

***Mots-clés :** Mélanges de polyoléfines, compatibilisation, Dynamique moléculaire simulation, résistance à la fissuration sous contrainte environnementale.*

ملخص :

تدرس هذه الأطروحة تأثير SEBS وSEBS-g-MA كمتوافقين لخليط البولي بروبيلين (PP) والبولي إيثيلين منخفض الكثافة (LDPE)، بالإضافة إلى تأثير IGEPAL CA 630 على قوة التكسير بالإجهاد البيئي (ESCR). تتضمن الدراسة حسابات نظرية باستخدام الديناميكيات الجزيئية والتحليلات التجريبية مثل حيود الأشعة السينية، وقياس السعرات الحرارية بالمسح التفاضلي، وقياس الجاذبية الحرارية، والمجهر الإلكتروني الماسح. تعمل إضافة SEBS وSEBS-g-MA على تحسين الالتصاق المورفولوجي والسطحي للخلطات، مما يقلل من امتصاص مجموعة الكربونيل ويحسن وقت الاختراق في اختبارات ESCR. تؤكد عمليات محاكاة الديناميكيات الجزيئية ونظرية الكثافة الوظيفية تأثيرات التوافق بين SEBS وSEBS-g-MA. يؤدي إدراج SEBS-g-MA بشكل خاص إلى تحسين المرونة وأداء الحقوق الاقتصادية والاجتماعية والثقافية في خلطات PP/LDPE بأجزاء وزن محددة، مما يشير إلى أن المتوافقات يمكنها تحسين خصائص هذه الخلطات في تطبيقات مختلفة.

الكلمات المفتاحية : مخاليط البولي أوليفين، التوافق، محاكاة الديناميكية الجزيئية، مقاومة التشقق تحت الضغوط البيئية